Modulation of neural activity in human visual cortex during saccade programming

Inaugural-Dissertation zur Erlangung der Doktorwürde

der Philosophischen Fakultät II (Psychologie, Pädagogik und Sportwissenschaft)

der Universität Regensburg

vorgelegt von

Ignacio Vallines García

aus Madrid

Regensburg 2007

Erstgutachter: **Prof. Dr. rer. nat. Mark W. Greenlee**

Zweitgutachter: **Prof. Dr. med. Klaus W. Lange**

Obergutachter: **Prof. Dr. rer. nat. Marianne Hammerl**

Contents

List of Figures

List of Tables

Abbreviations

ACC Anterior Cingulate Cortex

ADC Analog-to-Digital Converter

BA Brodmann Area

BOLD Blood Oxygen Level Dependent

CEF Cingulate Eye Field

CPU Central Processing Unit

CRT Cathode Ray Tube

dHb deoxygenated Haemoglobin

D-ILA Digital Direct Drive Image Light Amplifier

DLPC Dorso-Lateral Prefrontal Cortex

EPI Echo Planar Imaging

ERP Event-Related Potential

FEF Frontal Eye Fields

fMRI functional Magnetic Resonance Imaging

FWHM Full Width Half Maximum

G Gabor-only condition

GLM General Linear Model

Hb Haemoglobin. Oxigenated haemoglobin.

HRF Hemodynamic Response Function

HDR Haemodynamic Response

iPAT integrated Paralell Acquisition technique

IPS Intra Parietal Sulcus

IR Infra Red

ISI Inter-Stimulus Interval

LCD Liquid Crystal Display

LED Light Emmiting Diode

LFPs Local Field Potentials

LGN Lateral Geniculate Nucleus

LIP Lateral Intra Parietal

MPRAGE Magnetization Prepared RApid Gradient Echo

MR Magnetic Resonance

MST Medial Superior Temporal

MT Middle Temporal

NIRS Near Infrared Spectroscopy

PEF Parietal Eye Fields

PPC Posterior Parietal Cortex

RF Receptive Field

ROI Region Of Interest

RT Reaction Time

S Saccade-only condition

SC Superior Colliculus

SEF Suplementary Eye Fields

SG Self Guided

SNR Signal to Noise Ratio

SOA Stimulus Onset Asynchrony

SP Self Paced

SPL Superior Parietal Lobule

REM Rapid Eye Movement

SPM Statistical Parametric Mapping

TE Time to Echo

TMS Transcranial Magnetic Stimulation

TR Time to Repeat

V1 primary visual cortex, Striate cortex

V2 extrastriate cortex

VG Visually Guided

VSG Visual Stimulus Generator

1 Introduction

Almost every living organism is sensitive to light, and humans depend on vision more than on any other sense. Over a third of our brain total volume is devoted to process the vast amount of visual information delivered by the retinas. Light receptors have evolved differently in various species to attend to the needs of different ecological niches. Nocturnal species and those living in the depths of the ocean have developed big receptor organs in order to be able to capture the tiny amounts of light present in their environments. Some invertebrates have light-sensitive cells distributed through their bodies and certain amphibians poses photo-receptors directly onto the encephalon. In all of them, visual perception depends on the way the brain processes the basic information delivered by the receptors about the spatial distribution of light sources with different wavelengths. In mammals, the sense of vision is provided by two identical organs called the eyes. Ruminants have their eyes placed laterally to increase peripheral vision and be able to detect danger coming from any direction, whereas predators have them frontally placed to improve depth perception and facilitate distance calculations. Primate eyes are sensitive to a wide range of luminance levels, have retinal receptors that respond specifically to certain parts of the spectrum allowing for colour vision, and are capable of moving very rapidly to bring relevant parts of the visual scene onto the dense mosaic of cone photo receptors located in the fovea, where acuity is maximal.

Despite the importance of the eyes, it is in the brain where our visual world is constructed, to the point for instance, that we can elicit visual experience without light receptors (e.g. induced phosphenes in primary visual cortex by using Transcranial Magnetic Stimulation) whereas cortical damage can result in permanent blindness while hav-

ing perfectly functioning eyes. The exploration of the visual world is thus the result of intense flow of sensory information from the eyes to the brain, the filtering and processing of this information, and the generation of motor commands to change gaze to the next position from which the next bit of visual information will be obtained.

Because of its functional relevance and anatomy, no other measurable behavior is as closely linked to the brain as eye movements. Despite this fact, eye movements and vision have been traditionally studied as independent systems, assuming their connection but ignoring to which extent they are integrated into each other. This dissertation examines the close functional relationship between saccadic eye movements and the function of the primary visual cortex.

1.1 Saccadic eye movements

Even though vision research has been based on the image-forming eye for at least 400 years and despite the invaluable work of pioneers like Purkinje, Listing, Helmholtz, Donders and Hering during the early nineteenth century, the term saccade was not introduced until 1879 by the French ophthalmologist Lois-Émile Javal while describing experiments conducted in his laboratory by his collaborator Lamar. While testing a mechano-acoustic transducer, Lamar heard noises corresponding to the discontinuous movements of the eyes during reading and noted that the number of saccades per line of text remained constant unaffected by differences in viewing distance. In 1916, the American psychologist Raymond Dodge suggested that the French term 'saccade' (jerky, spasmodic) should be used for describing the rapid movements of the eyes that occur while reading, and introduced photographic methods that enabled the characterization of their dynamics with great accuracy (from Wade, Tatler & Heller, 2003). In his very influential classification published in 1902, Dodge had already distinguished saccades (referred at the time as Type I movements), pursuit, vestibular, vergence and reactive-compensatory eye movements (nystagmus). Saccades are used to quickly relocate the eyes from one position of gaze to another, thereby bringing objects of interest onto the fovea, where the receptor den-

sity and consequently the spatial resolution is maximal. Humans make an average of three saccadic eye movements per second (Bridgeman, Heijden & Velichkovsky, 1994; Leigh & Zee, 1991; Schiller & Tehovnik, 2005). Saccades are characterized by showing a constant relationship between their amplitude and peak velocity, which can reach up to 900°/s. This constant linear relationship has been termed the main sequence (Becker, 1989; Bollen et al., 1993), and experiences a progressive peak velocity saturation at amplitudes above 20°. Another important feature of saccades is their ballistic nature. Even the biggest saccade can be executed in less than 100 ms, which is less than the response time of the primary visual system to retinal stimulation (Regan, 1989), therefore impeding the brain to make use of any visual feedback during the movement. Under these circumstances accuracy must rely solely on internal monitoring of neural signals, and trajectories cannot be modified during the movement. This leads often to small degrees of saccadic hypometria (especially when a larger eye movement is generated) that is compensated by small corrective saccades (Kowler, Anderson, Dosher & Blaser, 1995) which bring the target to the precise center of the fovea, that subtends only about three degrees of the visual field (Findlay, Walker & Kentridge, 1995). Because of this ballistic nature, the coordinate information for the saccadic target must be readily available before the eye movement begins, in order for the system to successfully integrate it into a motor command that cannot be corrected "on the fly".

1.2 The neuroanatomy of saccades

There are several reasons why eye movements are considered an excellent source of information for both clinical and scientific studies. One remarkable advantage is that eye movements are restricted to rotation in three planes. This facilitates precise measurement, thus allowing for quantitative analysis. Motion in these three planes is achieved by means of three pairs of antagonist muscles called lateral, medial, superior and inferior recti, as well as the superior and inferior oblique. The abducens nucleus (VIth cranial nerve) contains lateral rectus motoneurons that move the eye horizontally away from the

nose, while the trochlear nucleus (IVth cranial nerve) contains superior oblique motoneurons that rotate the eye. The oculomotor nucleus (IIIrd cranial nerve) contains superior and inferior rectus motoneurons that move the eye vertically, medial rectus motoneurons that move it horizontally towards the nose, and inferior oblique motoneurons that rotate the eye. Neural circuits located in the dorso-medial part of the pons at the level of the abducens nucleus are ultimately responsible for providing the patterns of activity in lateral and medial rectus motoneurons that serve the generation of a rapid eye movement (Figure 1.1, left). This region is called paramedian pontine reticular formation (Sparks, Barton, Gandhi & Nelson, 2002).

Another subcortical structure located at the dorsal extent of the brainstem and directly related to the execution of saccadic eye movements is the Superior Colliculus (SC). Its multilayer structure is topographically organized and contains a representation of the visual space; the upper layer receives visual input from the retina and responds to visual stimuli while the intermediate/deep layers contain build-up/burst neurons that discharge prior to eye movements (Munoz & Wurtz, 1995; Wurtz & Goldberg, 1972). Neuron populations in deeper layers of the SC are involved in the execution of saccades and are ordered in a map by their preferred saccade metrics. Their firing behavior appears to encode the direction, amplitude and velocity of the eye movement (C. Lee, Rohrer & Sparks, 1988). The SC is considered the central gateway to the brainstem nuclei controlling the eye muscles (Sparks, 1988) and, even though it was thought that cortical signals for the generation of saccades were conveyed entirely through the SC, it has been demonstrated that under certain circumstances monkeys are still able to make fairly accurate visually guided saccades after SC removal (Keating & Gooley, 1988; Schiller, True & Conway, 1980).

The cerebellum is also involved in the generation of saccades. Via the pontine nuclei, major projections from the subcortical oculomotor centers reach the cerebellum, from which eye movements can also be elicited by electrical stimulation (Fujikado & Noda, 1987). In humans, Kornhuber (1973) observed that patients with cerebellar atrophy execute large angular-distance gaze shifts by executing fast series of short saccades instead

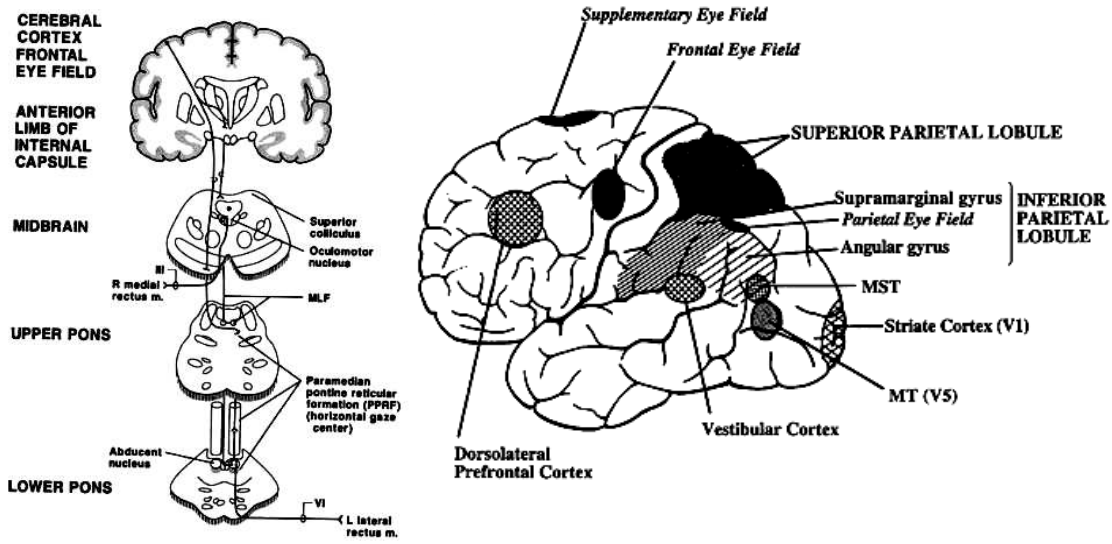

Figure 1.1: Cortical and subcortical structures that contribute to the generation of saccadic eye movements (from Leigh & Kennard, 2004).

of single large movements followed by a small corrective saccade. In cats, the cerebellum receives input from the extra-ocular muscles (Fuchs & Kornhuber, 1969), and complete cerebelloctomy in trained monkeys creates an enduring saccadic pulse dysmetria (Optican & Robinson, 1980). The cerebellum appears to be important for the control of saccadic accuracy, dynamics and trajectory, and possibly in correcting for position-dependent changes in the mechanical properties of the eye muscles and orbital tissues. According to a model proposed by Quaia and colleagues (1999), during the execution of a saccade, the cerebellum integrates the efference copy of the drive signal that feeds the ocular muscles (Figure 1.2). This efference copy provides the only extraretinal signal about eye position that is available without delay and can, therefore, be used by the system to recompute the location of the objects in the visual space after the saccadic target is reached.

At the cortical level, visual information about a target coming from the retina via the Lateral Geniculate Nucleus (LGN) is relayed from the visual cortex to both the SC and parietal areas such as the Lateral Intra Parietal (LIP) cortex, which are known to contain multiple representations of visual space (Colby, Duhamel & Goldberg, 1996). Neurons in these areas are both visually responsive and active in relation to saccades, and seem to be involved in coordinating eye movements and visuo-spatial attention (Bisley & Gold-

berg, 2003; Wardak, Olivier & Duhamel, 2002). LIP projects to the SC (Pare & Wurtz, 2001) and the Frontal Eye Fields (FEF), located at the lateral-superior precentral sulcus (Bruce & Goldberg, 1985), and there are excitatory and inhibitory SC-FEF pathways that run through the basal ganglia and the caudate nucleus (Hikosaka & Wurtz, 1983; Munoz & Everling, 2004; Sommer & Wurtz, 2000). The FEF is classically thought of as a premotoric center involved in selecting targets for eye movements. The neighboring Suplementary Eye Fields (SEF)[1] (Schlag & Schlag-Rey, 1987) receive input from parietal and the Dorso-Lateral Prefrontal Cortex (DLPC), (Luppino, Rozzi, Calzavara & Matelli, 2003) and seem to be responsible for complex motor programming such as those needed to saccade to a sequence of targets (Isoda & Tanji, 2002) or in antisaccade tasks (Amador, Schlag-Rey & Schlag, 2004). After unilateral FEF and SEF damage, monkeys can perform accurate saccades towards the intact side but showed great difficulties in saccading to sets of two target sequences presented in the contralateral hemifield (Schiller & Chou, 1998; Schiller & Chou, 2000).

Saccades can be elicited by electrically stimulating most of these cortical areas. The needed voltage, as well as the different latencies and trajectories, have proven very useful at unveiling their particular role in saccadic generation. While stimulating the monkey LIP area produces saccades only rarely, FEF stimulation consistently elicits saccades even at very low currents. Amplitude and direction for these saccades depend on the subregion stimulated in each of these areas (Robinson & Fuchs, 1969). Saccadic eye movements can also be electrically stimulated from primary visual cortex (V1) and extrastriate cortex (V2), to the point that suprathreshold stimulation in the absence of any targets elicits saccades that shift the center of gaze into the receptive field location of the stimulated neuron (Tehovnik, Slocum & Schiller, 2003). After ablation of the SC, saccades still can be elicited from the FEF and the SEF but not from visual areas (Keating, Gooley, Pratt & Kelsey, 1983; Schiller, 1977; Tehovnik, Lee & Schiller, 1994). Ablation of both the SC and the FEF eliminates all visually guided saccades (Schiller et al., 1980). According to this evidence, and despite classical models of saccadic generation that ex-

[1] Also known as the medial eye fields.

cluded the involvement of visual areas (Moschovakis, Scudder & Highstein, 1996; Munoz, Dorris, Pare & Everling, 2000; Wurtz & Goldberg, 1989), Schiller and colleagues postulate that there are two major streams for the generation of visually guided saccadic eye movements: the anterior stream, in which the FEF and the SEF have direct connections to the brainstem oculomotor centers, and the posterior stream, in which parietal and visual areas gain access to the brainstem through the SC (Schiller & Tehovnik, 2001). A schematic representation of the sub-cortical and cortical structures involved in the execution of saccades is depicted in Figure 1.1.

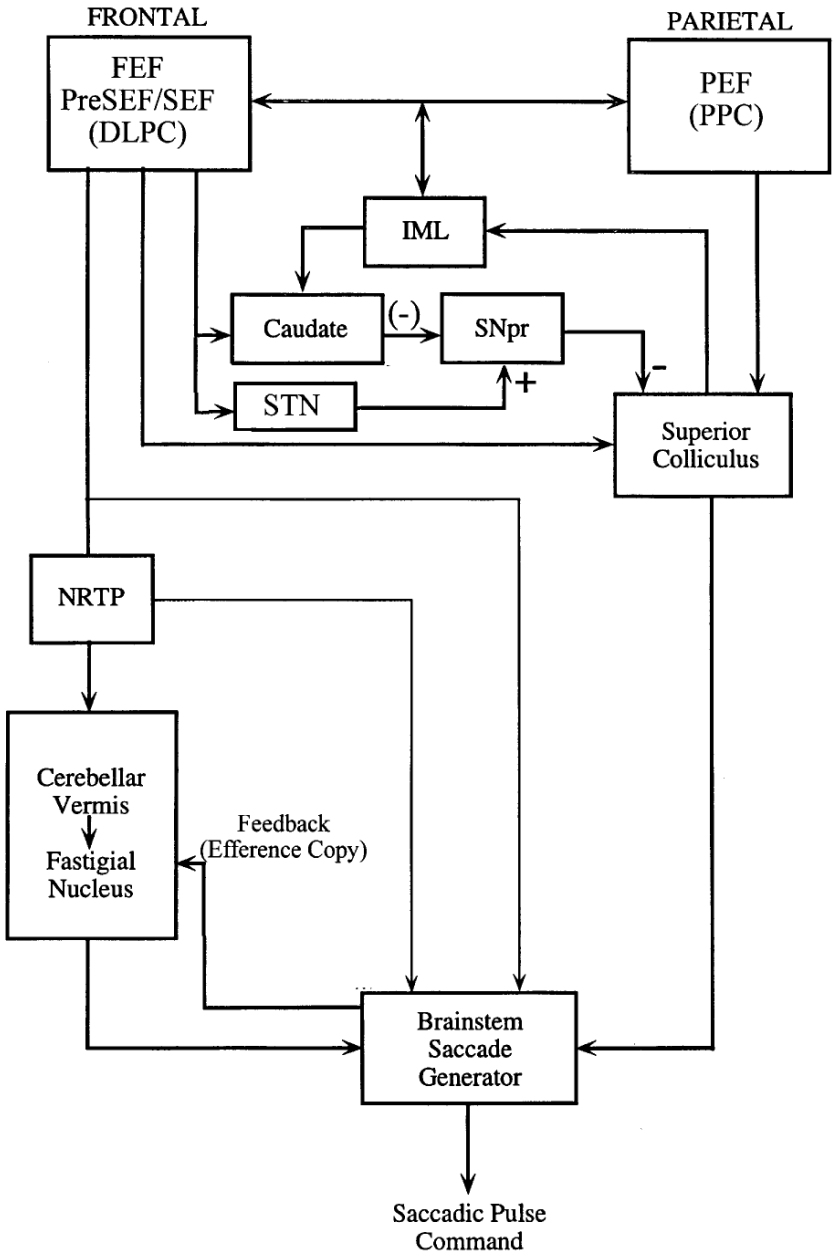

Figure 1.2: A classical block diagram illustrating the major structures that project to the brainstem saccade generator (from Leigh & Zee, 1991), involving cortical centers along the anterior/frontal (FEF, SEF, DLPC) and the posterior/parietal stream (PEF, PPC) and subcortical structures (NRTP, nucleus reticularis tegmenti pontis; IML, intramedullary lamina of the thalamus; riMLF, rostral interstitial nucleus of the medial longitudinal fasciculus; SNpr, substantia nigra pars reticulata; STN, subthalamic nucleus; Cerebellar vermis; Caudate nucleus; SC). In this complex model, the absence of visual areas is remarkable.

1.3 Saccadic latencies

Saccadic latency is defined as the time interval between the onset of a visual target and the onset of a saccadic eye movement towards this target. Because everything must be ready before sending the motor command to the premotor burst neurons in the oculomotor, trochlear and abducens nuclei, saccadic latency must reflect visual processing, target selection and motor programming. Latencies are dependent on stimulus properties such as luminance and the nature of the cognitive task[2], and increase with saccadic amplitude so that the average latency to a 5° saccade is around 200 ms; to 40° saccade about 250 ms (Bartz, 1962; Saslow, 1967). When a sequence of saccades is programmed (more than one target in presented), initiation of a 6° first-saccade increases to 230 ms (Wheeless, Boynton & Cohen, 1966), and top-down processes arising from specific task instructions can dramatically reduce saccadic latencies to about 150 ms for a 14° horizontal movement (Trottier & Pratt, 2005). Based on the complexity of the processes underlying oculomotor behavior, several types of saccades can be differentiated. As mentioned before, quick phases of vestibular nystagmus during passive rotation in darkness represent the most rudimentary form of saccades. Hard-wired reflexive saccades[3] are triggered in response to the sudden onset of a salient stimulus, whereas antisaccades involve executing a saccade with the same amplitude but the opposite direction. Previous disengagement of attention by including a gap between the disappearance of the fixational dot and the appearance of the target can elicit very short latency movements called express saccades (Schiller, Sandell & Maunsell, 1987). Voluntary saccades are performed on command triggered by cues, and memory guided saccades are those targeting a spatial location stored in visual memory.

Saccadic reaction periods can be divided into, at least, three separate processes (Becker & Jurgens, 1979; Fischer & Boch, 1983; Fischer, Gezeck & Huber, 1995): The disengagement of attention from a previously attended target, the localization of a new target in the visual space, and the specification of the desired coordinates of the saccade and

[2]For example such as in reflexive versus voluntary saccades.
[3]Also known as prosaccades.

the use of these coordinates by the brain stem oculomotor region to generate the eye movement. It has been proposed that the disengagement and redeployment of attention could be controlled by a saliency map provided by V1 (Itti & Koch, 2001; T. S. Lee, Yang, Romero & Mumford, 2002; Li & Lin, 2002), computing the spatial location of the target involves probably V1, V2 and the Frontal Eye Fields (FEF) in both of which a precise topographic representation has been demonstrated (DeYoe et al., 1996; Robinson & Fuchs, 1969).

1.4 The primary visual cortex

Retinal information provided by the eyes and qualitatively optimized by saccadic eye movements travels through the optic nerve and decussates at the optic chiasm. From that point, some fibers project directly to the superficial layers of the SC (D. L. Robinson & McClurkin, 1989), while the rest travel through the lateral geniculate nucleus as the optic radiations into the primary visual (striate) cortex at V1: the first stage of cortical processing in the visual system.

V1 is localized in the occipital pole of the brain along the calcarine fissure, and is cytoarchitectonically organized in six layers and alternating columns of neurons exhibiting dominant input from either eye (Hubel & Wiesel, 1972). Each cell in the visual cortex has a Receptive Field (RF), a discrete area in space relative to the fovea where the presentation or removal of a visual stimulus will cause activation of that neuron. The V1 receptive fields of layer IV cells are roughly circular, and have a constant location and size (Hubel & Wiesel, 1968; Schiller, Finlay & Volman, 1976). The spatial distribution of the ganglion cells within the retina is preserved by the spatial organization of the neurons in the LGN (Erwin, Baker, Busen & Malpeli, 1999), in what is known as retinotopic organization. The signals in V1 are also retinotopically organized, which means that there is a point-to-point spatial relation between a visual stimulus projected on the retina and its topographic representation in V1, as depicted in Figure 1.3.

While physiological and anatomical techniques have long been able to demonstrate the

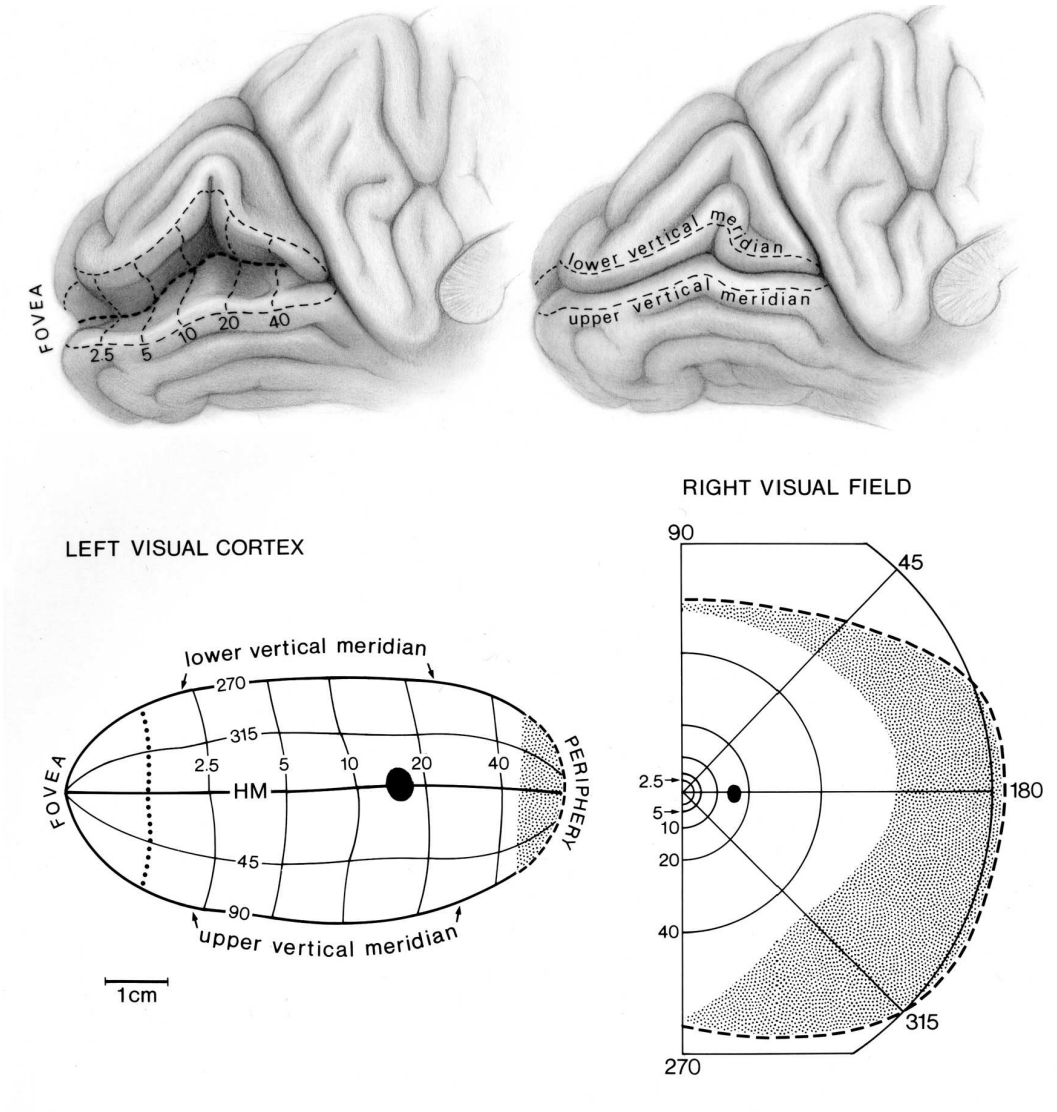

Figure 1.3: Retinotopic organization of the primary visual cortex in the occipital lobe and along the calcarine fissure (from Horton & Hoyt, 1991): There is a point-to-point correspondence between the location of any visual stimulus presented on the retina and its encoding location in the visual cortex. The upper drawing shows the fissure opened, with the eccentricity marked in degrees. Each visual hemifield is represented in the contralateral hemisphere. The upper visual field is represented ventrally whereas the lower visual field is represented dorsally. The lower graph depicts a flat representation of the coordinate map (in degrees) contained in V1. Central vision (about 5 degrees of eccentricity) is represented by almost half of the cortical extent of V1 while the visual periphery is represented by a much smaller area. The amount of cortex devoted to encoding a part of the retina is not determined by its size but by its spatial resolution, in what has been coined as "cortical magnification".

topographic organization of the monkey striate cortex (Schaefer, 1888; Van Essen, Newsome, Maunsell & Bixby, 1986), recent functional Magnetic Resonance Imaging (fMRI) studies have succeeded at producing retinotopic maps with sufficient detail to segment cytoarchitectonically distinct cortical visual areas (Cheng, Waggoner & Tanaka, 2001; Engel, Glover & Wandell, 1997; Tootell et al., 1998), and even the LGN (Chen, Zhu, Thulborn & Ugurbil, 1999; Schneider, Richter & Kastner, 2004). V1 has direct feedforward connections to areas V2, V3, V5, Middle Temporal (MT), and the FEF (Fitzpatrick, Usrey, Schofield & Einstein, 1994; Maunsell & Van Essen, 1983; Ungerleider & Desimone, 1986), receives feedback projections from V2, V3, V5, MT, Medial Superior Temporal (MST), FEF, LIP and inferotemporal cortex (Shipp & Zeki, 1989; Suzuki, Saleem & Tanaka, 2000; Ungerleider & Desimone, 1986), and has direct feedback projection to the SC, LGN, pulvinar, and pons (Fries, 1990; Graham, 1982; Gutierrez & Cusick, 1997). In fact, the eye movements that can be evoked electrically from V1 by applying low-currents are abolished after SC lesions (Schiller, 1977), suggesting that V1 can directly gain access to the brainstem saccade generator via the SC.

1.5 BOLD imaging

The results of the investigation on the molecular structure of hemoglobin by Pauling (1936), together with the discovery of magnetic resonance by Purcell (1945), the introduction of magnetic field gradients by Lauterbur (1973) and the development of fast Echo Planar Imaging (EPI) methods by Mansfield (1977), provided Seiji Ogawa and colleagues (1990) with the necessary grounds to use Magnetic Resonance (MR) for examining brain physiology in the late 1980's.

Blood Oxygen Level Dependent (BOLD) imaging has since then experienced a fast development, and has become one of the most widely used techniques for studying human brain function. MR signal (T_2 weighted) results from the time-differences in which hydrogen-protons begin to lose phase coherence after switching off a strong electromagnetic pulse responsible for bringing them from precessing along the longitudinal plane

(parallel to the main MR magnetic field) to the transversal plane (perpendicular to the main MR field). While Haemoglobin (Hb) is diamagnetic (it has no unpaired electrons and almost zero magnetic moment), deoxygenated Haemoglobin (dHb) is paramagnetic (it has both unpaired electrons and a significant magnetic moment) and has a magnetic susceptibility which is about 20% greater than fully oxygenated blood (Huettel, Song & McCarthy, 2004). Different concentrations of dHb resulting from the metabolic demands of neural activity induce local susceptibility artifacts that distort the homogeneity of the main magnetic field, thus accelerating spin dephasing times. These differences can be interpreted to reconstruct spatially extended BOLD signal changes into a so-called T_2^* weighted image.

Because the BOLD signal is an indirect way of estimating neural activity, it is closely linked to the very slow vascular dynamics and has a very low Signal to Noise Ratio (SNR). As a consequence, it has taken some time until skepticism about the nature and usefulness of the signal could be mostly eradicated. In 1992, Blamire and colleagues observed for the first time local intensity image changes in the visual cortex of a normal human brain during visual stimulation that could be used for functional imaging. Almost a decade later, Logothetis, Pauls, Augath, Trinath and Oeltermann (2001) compared Local Field Potentials (LFPs) to single- and multi-unit spiking activity with highly spatio-temporally resolved BOLD fMRI responses from the monkey visual cortex by using a 4.7 T MR scanner. Their results clearly show the existence of a strong correlation between BOLD signal and neural activity and suggest that the BOLD contrast mechanism reflects best the input and intracortical processing of a given area rather than its spiking output. BOLD signal is tightly linked to the Haemodynamic Response (HDR) and rises shortly after stimulation onset, reaches a peak amplitude after about 5 s and reaches back baseline levels after a prolonged undershoot some 13 s after the stimulation offset. These slow dynamics impose some temporal limitations that can be partially overcome by the experimental design and the analysis technique, as demonstrated in the last two studies of this dissertation (Chapters 4 and 5).

1.6 Measuring eye movements in a MR environment

The accurate estimation of the eye position within the strong magnetic field of an MR scanner has been a challenge since the beginning of fMRI research. In order to comply with the safety regulations and preserve image quality, all equipment inside in the gantry[4] of the scanner must neither contain any ferromagnetic parts, nor introduce any distorting electrical currents inside the magnetic field. Most commercially available eye-trackers are video based, and their video cameras both have ferromagnetic parts and need low electrical currents for functioning. Within the frame of this dissertation work, a recently introduced Infra Red (IR) limbus[5] reflexion technique for the measurement of eye movements during fMRI experiments (Kimmig, Greenlee, Huethe & Mergner, 1999) was further developed. The "MR-Eyetracker" was initially designed and prototyped by Dr Hubert Kimmig, Professor Mark W. Greenlee, and Dipl. Ing. Frank Huete in conjunction with Cambridge Research Systems, and it is based on back-measuring the reflected infrared light that is tele-projected onto the eye by means of long fiber optics (Figure 1.5). This configuration allows for the electronics to be remotely located outside the Faraday chamber that protects the sensitive MR receiver coils from external interferences. The system measures the differential reflectance between the boundary of the sclera and the iris. The output of this device is an analog full-scale $\pm 5\,\mathrm{V}$ signal per channel (x and y), and is equipped with a digital gain control and an offset correction circuit. For eye movements on the cardinal axes and within the $\pm 20^\circ$ range, the output voltage is a linear function of eye rotation and can be converted to a spatial resolution of about 0.1°.

A software platform was written in Delphi-Pascal to control the visual stimulation, the button response acquisition, the eye movement recordings and the MR triggering system. This platform (Figure 1.4) makes use of a Visual Stimulus Generator (VSG) system (model VSG2/5) with an ultra-high 15 bit output resolution per color channel, a 50 MHz graphics processor, twenty digital input/output (I/O) digital and six 12 bit analog channels. Its I/O buffered system was used to read and store the digital MR

[4] Opening or tunnel in a MRI scanner through which the table carrying the patient is fed.
[5] The margin between the cornea and the sclera.

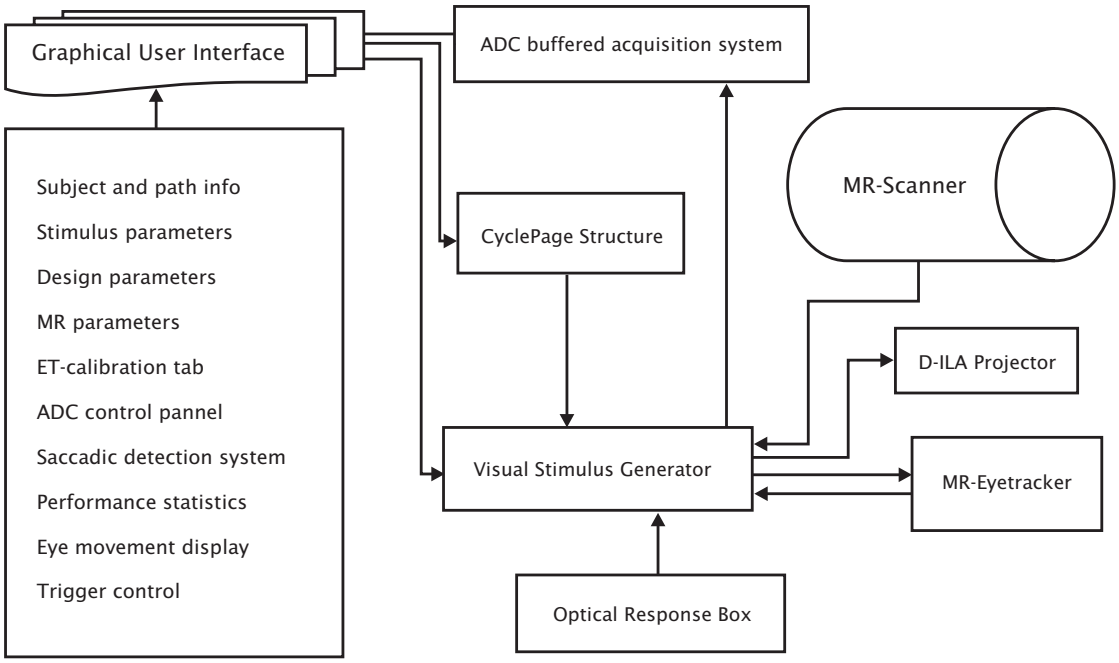

Figure 1.4: Software-hardware setup arquitecture ilustrating how the visual stimulator-LCD projector, the response devices, the eye-tracker and the MR scanner were tightly integrated and controlled by a single piece of software especially developed for the studies presented in this dissertation. The system is capable of recording and interpret signals from the MR scanner, the visual stimulus generator, the MR eye tracker and the optical response box. Behavioral performance is computed on the fly during the experiment, and the code incorporates calibration routines, offset correction, and a saccadic detection algorithm. At the same time, visual stimulation is generated by the software, loaded into a cycle page structure and then launched to the VSG for real-time stimulus presentation via a gamma-calibrated high performance D-ILA projector.

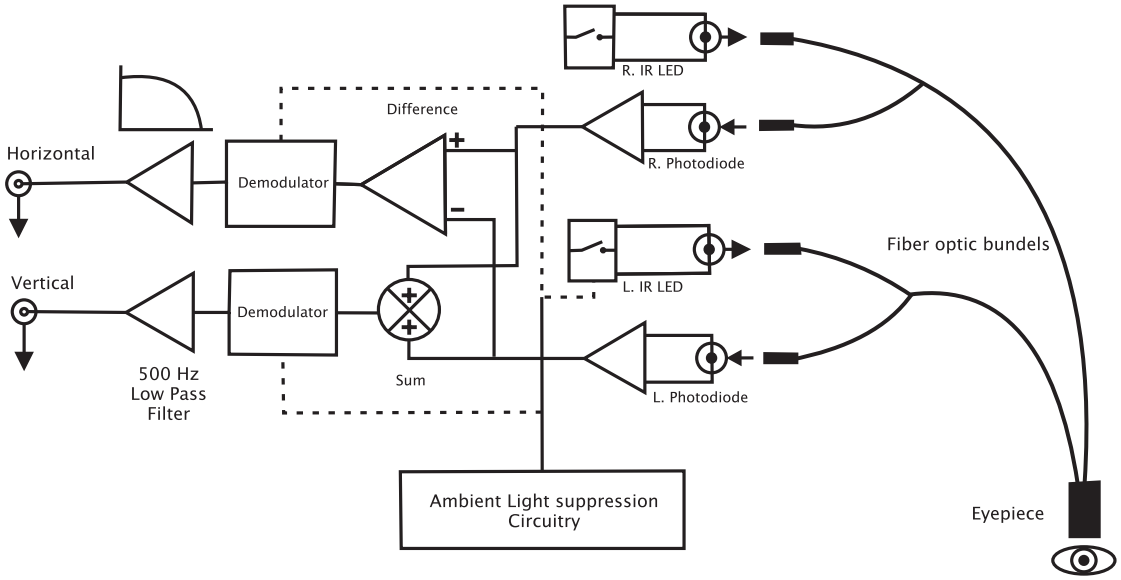

Figure 1.5: Simplified block diagram of the MR-tracker circuitry. The fibers from each fiber optic bundle are split into two. One half is coupled to an LED for transmission of the infrared light, the other half to a photo-diode for capture of the IR light reflected back from the eye. At the eyepiece, fibers from both halves are uniformly interleaved. The two LEDs are switched on and off at 10 kHz. The signal current resulting from the reflected light is converted to a voltage and buffered. The sum and difference of the signals from each side of the eye is derived. The difference is proportional to the horizontal eye position, and the sum of the signal is proportional to the vertical position. Subtracting the signal when illumination is off from the signal when illumination is on demodulates the chopped signals, compensating for ambient infrared illumination (adapted from CRS).

triggers, the VSG videopage-change digital triggers, and to sample the MR-eyetracker analog channels at 1 kHz, as well as to control the switching of LEDs. At the same time, the software implemented routines to create and load the stimulation videopages into a cyclepage structure that, once launched, runs with real time accuracy by using an on-board Central Processing Unit (CPU), independent of Windows pre-emptive multitasking system. Eye movement calibration was achieved by presenting dots at various known eccentricities, recording their Analog-to-Digital Converter (ADC) values and, using a least-squares procedure, to find the best fitting parameters for a polynomial function that was later used to convert the signal in degrees of visual angle. An on-line saccadic detection algorithm used for latency-prediction was also implemented and used for the experiment described in Chapter 5.

Lastly, but of great importance for the studies described in this work, are the inter-individual differences in oculomotor performance and ocular anatomy. Because of the difficulties in measuring eye movements during fMRI sessions and due to cost factors beyond our control, we did not attempt to extract random population samples and were forced to select participants based on strict performance parameters that were always tested before the actual fMRI sessions took place. The selection criteria were based on a reduced set of parameters such as easily accessible ocular anatomy, stable fixation and low saccadic intrusion levels, moderate blink rate, motivation, and average-to-small cranial diameter to facilitate the allocation of the MR-tracker eye-piece inside the radio-frequency coil.

1.7 Statistical parametric mapping

Statistical Parametric Mapping (SPM) refers to the construction and assessment of spatially extended statistical processes used to test hypotheses about regionally specific effects in functional imaging data. Most of the analysis of the data presented through this dissertation is based on this idea, as implemented in the software package SPM, (Functional Imaging Laboratory, UCL, London, http://www.fil.ion.ucl.ac.uk/spm/, Friston, Frith, Frackowiak & Turner, 1995). SPM is specifically designed for the analysis of brain

imaging data sequences as those obtained during BOLD imaging. After a series of pre-processing steps (e. g., motion and time correction, spatial smoothing, trend removal, spatial normalization), time series resulting from repeated measurements are extracted from each voxel[6] and tested against a parametric statistical model that makes use of the General Linear Model (GLM) to describe the data in terms of experimental effects, confounding effects, and residual variability. Predictive models of BOLD signal variations are constructed by convolving the onset of the modeled events with a canonical Hemodynamic Response Function (HRF) whose shape results from the difference of two gamma functions and that account for an initial dip with and onset delay, a signal peak and a slow undershoot. The full form of the canonical HRF, as used for most of the fMRI analyses done within this work is defined by the following expression

$$f(t) = \frac{m(x)}{\max\left[\frac{(t-d(x))^{p(x)-1}e^{\lambda t}}{\int_0^\infty t^{p(x)-1}e^{\lambda}dt}\right]} \times \left(\frac{(t-d(x))^{p(x)-1}e^{-\lambda t}}{\int_0^\infty t^{p(x)-1}e^{-\lambda}dt} - \frac{1}{6} \times \frac{(t-d(x))^{15}e^{-\lambda t}}{\int_0^\infty t^{15}d^{\lambda}dt}\right)$$

where m is the stimulus magnitude, p is the modified shape of the difference between two gamma functions, d is the offset parameter, t is the time following the stimulus onset, x is the position in the stimulus sequence, and λ is a constant scaling parameter equal to the Time to Repeat (TR) divided by the sampling resolution. The first term is a scaling parameter for the magnitude of the response and the second term describes the gamma function for the positive BOLD response (Wager, Vazquez, Hernandez & Noll, 2005).

Classical statistical inference is later used to test hypotheses that are expressed in terms of GLM parameters of the form

$$y = \beta_1 + \beta_2 x + \varepsilon$$

where y is the measured signal at a given point in time, β_1 is a constant value that determines the baseline signal level, β_2 defines the contribution of each component of the design matrix to the value of y (estimated so as to minimize the error by using least sums of squares), and ε is the error or difference between the observed data x and that

[6] The three dimensional equivalent to a pixel which corresponds to the smallest element measured in a functional brain image.

predicted by the model x. Extended in time the GLM can be represented in matrix form as a multivariate general linear model

$$\begin{pmatrix} y_1 \\ y_j \\ : \\ y_J \end{pmatrix} = \begin{pmatrix} \beta_1 \\ \beta_1 \\ : \\ \beta_1 \end{pmatrix} + \begin{pmatrix} x_{11} & x_{1l} & x_{1L} \\ x_{j1} & x_{jl} & x_{jL} \\ : & : & : \\ x_{J1} & x_{Jl} & x_{JL} \end{pmatrix} \times \begin{pmatrix} \beta_{21} \\ \beta_{2l} \\ : \\ \beta_{2L} \end{pmatrix} + \begin{pmatrix} \varepsilon_1 \\ \varepsilon_l \\ : \\ \varepsilon_L \end{pmatrix}$$

where j is time and l are the explanatory variables or regressors. After estimating the parameters for each voxel, statistical testing (mostly t-tests and F-tests) is performed on the parameter values. The result of this testing is coded into statistic images or maps where voxel values contain the resulting statistic value that are (under the null hypothesis) distributed according to a known probability density function. A threshold is then used to overlay onto an anatomical MR image, only those voxels that reach a pre-determined statistical significance level, conforming the statistical parametric maps (SPMs).

1.8 Imaging of the saccadic system in humans

Functional Magnetic Resonance Imaging based on fast EPI of the BOLD signal has recently developed into one of the most widely used techniques for the study of brain function. Because of the tight linkage between eye movements and visual cognition, the possibility of studying the human visual system in combination with oculomotor measurements in a non-invasive manner has created a great deal of enthusiasm among vision researchers during the very last years. In the early studies, most areas known to be related to the control and execution of eye movements in primates could be localized in the human brain confirming many similarities with non-human primates and revealing some important anatomical differences. fMRI studies have delimited the location of the FEF mainly to the intersection between the precentral sulcus and the superior frontal sulcus (Paus, 1996; Rosano et al., 2002) demonstrating that the human FEF is located in Brodmann Area (BA) 6, unlike the monkey FEF which is located in the posterior

part of BA 8 (Petit, Clark, Ingeholm & Haxby, 1997). The FEF is involved in the preparation and triggering of all intentional saccades (Pierrot-Deseilligny, Milea & Muri, 2004) and a recent fMRI study shows that set-related activity in this area correlates with saccadic latencies (Connolly, Goodale, Goltz & Munoz, 2005). Human SEF has been localized on the medial surface of the superior frontal gyrus, in the upper part of the paracentral sulcus (Grosbras, Lobel, Moortele, LeBihan & Berthoz, 1999), and a Transcranial Magnetic Stimulation (TMS) experiment (Tobler & Muri, 2002) has been able to replicate electrode work in monkeys that shows the involvement of the SEF in the coding of complex temporally ordered sequences of saccades (Isoda & Tanji, 2002). The posterior part of the Anterior Cingulate Cortex (ACC) has been shown to be involved in saccadic control (Paus, Petrides, Evans & Meyer, 1993). Its role seems to be restricted to the execution of intentional saccades but not in reflexive saccadic control (Gaymard, Ploner, Rivaud, Vermersch & Pierrot-Deseilligny, 1998). It has been proposed that this Cingulate Eye Field (CEF), located at the border between Brodmann areas 23 and 24, could, via an intentional motivational process, prepare all the frontal ocular motor areas involved in intentional saccade control to act in the forthcoming motor behavior (Pierrot-Deseilligny et al., 2004).

Experimental paradigms involving the maintenance of complex task such as instructions, decisional processes, saccadic inhibition or spatial memory, recursively engage the DLPC, located in BA 46 and the adjacent BA 9 (Leung, Gore & Goldman-Rakic, 2002; Sakai, Rowe & Passingham, 2002). The Intra Parietal Sulcus (IPS) in the Posterior Parietal Cortex (PPC) is considered to be the Parietal Eye Fields (PEF) equivalent to the monkey LIP. The IPS separates the Superior Parietal Lobule (SPL) located medially around BA 7 (Perry & Zeki, 2000), from the inferior parietal lobule that comprises BA 40 (Pierrot-Deseilligny et al., 2004). Also matching single unit work on primates, parietal areas are active in imaging studies not only during the execution of saccades but also during covert shifts of spatial attention (Posner, 1980), evidencing that attentional and oculomotor processes are tightly integrated at the neural level (Gitelman et al., 1999; Nobre, Gitelman, Dias & Mesulam, 2000; Perry & Zeki, 2000). Also consistent with

animal data, activated areas related to visually guided saccades have been observed in the cerebellar vermis (declive and folium) and in both hemispheres (mainly the superior semilunar lobule) of the cerebellum (Hayakawa, Nakajima, Takagi, Fukuhara & Abe, 2002).

Quantitative aspects of cortical activity related to saccadic eye movements have been also studied with fMRI showing a positive correlation between saccadic frequency and the amplitude of the hemodynamic response in areas V1, V5/V5A, BA 19, SPL, precuneus, FEF and SEF (Kimmig et al., 2001).

1.9 Aims of this work

The premise on which this dissertation starts is that vision can only be understood as a dynamic interplay between oculomotor and visual systems, in what has been coined as "active vision" (Findlay & Gilchrist, 2003). In the following work, we argue that these two systems first meet at the primary visual cortex (V1) and provide evidence of how V1 is tightly integrated with the oculomotor machinery. For this purpose, we took advantage of the rapid advances in fMRI techniques (for a review, see Nobre et al., 2004), and extended its experimental capabilities by further developing a method (Kimmig et al., 1999) to record saccades with high spatial and temporal resolution during fMRI measurements. Being able to determine the position of the eyes allowed us to measure the influence of eye movements on the visual representation of stimuli in the retinotopically organized primary visual cortex (Engel et al., 1997; Tootell et al., 1998).

In the first study of this work (Chapter 2) we localize the network driving eye movements by comparing visually guided, self-generated, and self-paced saccades while determining whether V1 plays an active role in the execution of saccadic eye movements when completely deprived from visual input, and we look at how retinotopically defined areas are activated based solely upon saccadic activity. These experiments are further developed in the second study (Chapter 3) by segregating areas involved in saccadic and attention control by comparing self-generated and covert shifts of attention during ab-

solute darkness in a mixed fMRI design (Amaro & Barker, 2006) that allowed sorting events according to saccade direction, to search for a topographic cortical organization.

The experiment in the third study (Chapter 4) pushes fMRI temporal resolution to the limit by demonstrating that extremely brief stimulus presentation times in the millisecond scale can be precisely resolved under strict experimental control, opening the possibility of studying very fast processes, which is the subject of the last study (Chapter 5) on saccadic suppression.

The last part of this dissertation (Chapter 5) builds on knowledge obtained by the previous studies by combining retinotopy, psychophysical, oculomotor, behavioral and imaging methods to show for the first time in humans the existence of an active saccadic suppression mechanism that reduces visual sensitivity immediately before a saccade, demonstrating that neural activity in human primary visual cortex is modulated during saccade programming (the title of this dissertation work). This could be achieved only after developing a system for measuring eye movements within in the MR scanner in cooperation with Freiburg Neuroscientific Technologies and Cambridge Research Systems.

Parts of this dissertation have been presented at international conferences and published as conferences procedures or abstracts (Vallines et al., 2002; Vallines, Bodis-Wollner, Oezyurt, Rutschmann & Greenlee, 2003; Vallines & Greenlee, 2004, 2005a, 2005b), and the last study (Chapter 5) has been recently published as a research article in the Journal of Neuroscience (Vallines & Greenlee, 2006).

2 The non-visual role of V1 in oculo-motor control

Summary

Recent physiological evidence indicates that primary visual areas might not only passively contain a retinotopic representation of visual input, but also play an active role in the execution of saccadic eye movements. It has been proposed that the primary visual cortex (V1) provides the spatial information essential to compute saccadic vectors even in the absence of visual stimulation. This study uses functional magnetic resonance imaging and high resolution eye tracking to determine whether V1 is active while subjects execute sequences of exogenously and endogenously triggered saccades while completely deprived of visual stimulation. An increase of activation was observed in both the posterior and the anterior streams for endogenous compared to the exogenous condition. In our data, the visual cortex responds actively not only in the presence of visual targets but also during the execution of saccades in the absence of visual input. These results are consistent with the hypothesis that visual areas provide coordinate information used for saccadic vector computations. It is proposed that non-visual signals generated in V1 could be fed directly into the parietal areas and the frontal eye fields for the preparation of the motor command, while visual information would be forwarded to higher visual areas before being used for saccade preparation.

2.1 Introduction

Saccadic eye movements are the behavioral result of a highly complex system that relies on a widely distributed network of cortical structures. This network involves centers located in the frontal lobe, the parietal lobe and parts of the cingular cortex. Surprisingly, while the frontal and parietal cortical mechanisms that ensure visual stability and continuity associated with saccades have been the object of intense research (Merriam, Genovese & Colby, 2003; Mort et al., 2003; Petit et al., 1996; Schiller et al., 1987; Skoyles, 1997), visual areas of the occipital cortex have been systematically ignored based on the assumption that the occipital cortex is solely responsible for providing information about the location and spatial structure of visual stimuli (Everling & Fischer, 1998; Li & Lin, 2002; Petit et al., 1996; Schall & Thompson, 1999; Segraves & Goldberg, 1987).

There is now accumulated evidence that challenges the classical conception of V1 as being a passive one-way station between the retina and the higher order areas of the brain (Bodis-Wollner et al., 1997; Bodis-Wollner, Bucher & Seelos, 1999; Leopold & Logothetis, 1998; Sylvester, Haynes & Rees, 2005; Sylvester & Rees, 2006; Tehovnik, Slocum, Carvey & Schiller, 2005). Gandhi, Heeger and Boynton (1999) demonstrated that attending to a stimulus caused a consistent and systematic change in V1 brain activity, suggesting that it was tightly linked to higher cognitive processes, to the point that performance in a visual detection task can be predicted from the amplitude of the response in primary visual cortex (Ress, Backus & Heeger, 2000). Further developing these ideas, a recent fMRI study by Haynes and Rees (2005) shows how there is enough information present in the response patterns measured at specific early visual areas (V1 to V3) to allow highly precise reconstruction of conscious perception from brain signals alone. Bodis-Wollner and colleagues (1997) have proposed that there could be at least two, not mutually exclusive intrinsic roles of V1 when saccades are executed. One is to prepare an eye movement vector to a target; the second is to rescale the visual map in preparation for the location of a new center of regard.

2.1.1 Electrophysiological evidence

Electrophysiological studies in primates have shown that low intensity electrical stimulation of V1 and V2 elicit saccades whose vectors are constant and independent of the initial eye position within the orbit (Schiller, 1972, 1977; Schiller & Chou, 1998). Schiller (2001) proposes that these areas are likely to carry a vector code. According to this view, V1 would compute a retinal error signal between the center of gaze and the location of the receptive field activated by the target; saccades would serve to null this error. The idea of a topographic organization of V1 in primates was first suggested by Schaefer (1888), who found that electrical stimulation of V1 evoked contralateral eye movements and that stimulation above the calcarine sulcus produced downward eye movements, whereas stimulation below the sulcus generates upward movements. Replications of these results in a variety of primates (Tehovnik et al., 2005) have demonstrated that electrical stimulation of V1 evokes saccadic eye movements that terminate in the center of the visual receptive field of the stimulated cell (McIlwain, 1988; Schall, 1995; Schiller, 1972, 1977; Schiller & Tehovnik, 2001; Tehovnik, Slocum & Schiller, 2002), with the shortest saccadic latencies (about 50 ms) obtained when the deepest layers of V1 were stimulated, at about 2 mm below the cortical surface (Tehovnik et al., 2003). Based on reported evidence of direct projections between V1 and the brain stem saccadic generator via the superior colliculus (Schiller, 1977), it has been suggested that the output layer of V1 could directly carry the saccade signal to the brain stem. Electrical stimulation applied to the occipital cortex of the intensity used in monkey research, induces humans to report the appearance of phosphenes in their visual field (Penfield & Perot, 1963). In an attempt to segregate the sensory event from the motor event, Berg and colleagues (2002) trained a monkey to generate memory-guided saccades to locations in the visual fields activated by V1 stimulation, but whether electrically induced saccades are due exclusively to the sensory effect of an induced phosphene has not yet been elucidated. Short-latency saccades as found by Schiller and colleagues (1987) are taken as evidence of a direct link between V1 and the saccadic centers. Segraves and colleagues (1987) studied the effects of unilateral V1 ablations on saccadic eye movements showing that saccades were accurate when

executed into the field ipsilateral to the lesion, but presented significant undershoots and overshoots when executed to moving stimuli presented on the field contralateral to the lesion. Smooth pursuit was also greatly impaired indicating that V1 is intimately involved in providing information about the stimulus position used in the preparation of eye movements.

The results reported in the animal and neuropsychological literature are controversial with respect to the exact nature of the non-visual role of V1 for the control of saccadic eye movements. It is clear that V1 provides information about the spatial location of objects present in the visual field, and that this information is somehow transferred to oculomotor centers to prepare saccadic motor sequences. The question remains: Where does the spatial information come from when no visual stimulus is present, when executing a voluntary eye movement within a uniform visual field or when visual input is not available?

2.1.2 Reflexive versus voluntary control

Reflexive saccades represent an immediate eye movement towards an unexpected change in the peripheral sensory environment, such as the onset of a salient visual target. The most common paradigm to elicit reflexive saccades is usually based on the sudden appearance of a visual target in the periphery to which a saccade must be performed. Saccadic latencies can be significantly reduced if the disengagement of attention is facilitated by prior visual offset at the fixation location (Reuter-Lorenz, Hughes & Fendrich, 1991), to the point that an extremely fast sub-population of saccades referred to as express-saccades and with latencies of around 100 ms (70 ms in monkeys) can be observed (Fischer, 1986) when a time gap is introduced between the fixation offset and the target onset. In contrast, voluntary saccades require a greater cognitive effort, involving decisions regarding where and when to move the eyes. These decisions translate into latency increases of about 100 ms for voluntary anti- and symbolically cued saccades compared to the latencies of reflexive saccades (Walker, Walker, Husain & Kennard, 2000). Anti-saccades are known to have longer latencies, more variable amplitudes and

lower peak velocities than reflexive saccades (Everling & Fischer, 1998), but as in delayed and memory guided tasks, also involve the suppression of the reflexive saccadic response to the cueing visual stimulus. No cue-interpretation or inhibition processes are present in reflexive saccades and therefore, in these cases it is not possible to identify whether latency differences actually come from extra time required by these processes, or from cognitive manipulations of the spatial parameters required by voluntary saccades. However, Walker and colleagues (2000) could show that at least a portion of this latency difference persists even after obviating the need to attend to and process direction from the cue, suggesting that different neural processes might be sub-serving the production of reflexive and voluntary saccades. As evidenced by electrophysiology and lesion studies in both primates and humans (Bruce & Goldberg, 1985), reflexive saccades are thought to strongly rely on PPC (Gaymard et al., 1998) whereas the FEF seems to play a major role in the generation of voluntary saccades. Supporting these ideas, it has been shown that the FEF contains neurons that fire maximally during visual search when a target, lying in their receptive field, is selected for a saccade (Schall, 1995).

2.1.3 Previous fMRI studies

Previous functional imaging studies have examined reflexive saccades (Kimmig et al., 2001; Muri, Iba-Zizen, Derosier, Cabanis & Pierrot-Deseilligny, 1996; Nobre et al., 2000; Petit et al., 1997) and voluntary saccades (Bodis-Wollner et al., 1997; Corbetta & Shulman, 1998; Law, Svarer, Rostrup & Paulson, 1998; Oezyurt, Rutschmann, Vallines & Greenlee, 2002, 2004; Paus et al., 1993; Perry & Zeki, 2000; Petit et al., 1996) but only one study has directly compared both saccade types searching for specific differences (Mort et al., 2003). Mort and colleagues found greater regional activity in FEF and IPS by arrow-cued voluntary saccades compared to reflexive saccades which, in turn, elicited more activity in the angular gyrus and the inferior parietal cortex. Again in this case, activity triggered by the voluntary saccades included the processing of the cue which was absent in the reflexive condition. Apart from this, only Kimmig and colleagues (2001) were able to accurately measure saccadic eye movements during MR imaging sessions by

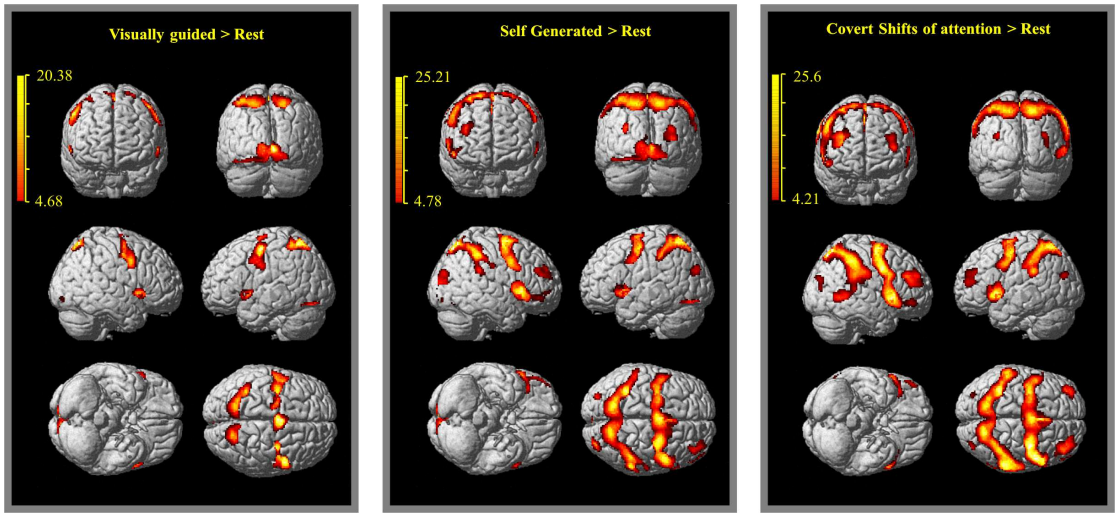

Figure 2.1: Reflexive and self generated saccades engage the same cortical areas than covert shifts of attention with the exception of visual cortex (Vallines et al., 2003). Visually guided (VG) saccades selectively engaged FEF and SEF (BA 6), the parietal eye field (BA 7), lateral parietal (BA 40) and visual areas V1 and V2 (BA 17, 18). Self generated eye movements (SG) activated the same areas as VG, but the activity extended along the inferior parietal sulcus and the intraparietal sulcus. Also the frontal operculum (BA 47) and a focalized area on the prefrontal cortex (BA 46) were recruited by SG saccades. Covert shifts of attention elicited greater frontal and parietal activity and engaged the same areas as SG, with the exception of the visual areas.

using an MR-eye tracker based on infrared light reflection (Kimmig et al., 1999). This method was further developed during pilot experiments (Vallines et al., 2003) that led to this dissertation work (see Section 1.6 and Figure 2.1).

2.1.4 Saccades in the absence of visual stimulation

A few imaging studies have recognized the potential of looking at areas activated by saccadic activity in the absence of visual stimulation (Bodis-Wollner et al., 1997; Law et al., 1998; Paus, Marrett, Worsley & Evans, 1995; Petit et al., 1996; Sylvester et al., 2005; Sylvester & Rees, 2006; Wenzel et al., 2000) to try to segregate the oculomotor from the visual processes. During these experiments, subjects executed self-paced or auditory cued saccades while no visual stimulation was present, and most of them found

saccade-related signal changes also in primary visual cortex (Bodis-Wollner et al., 1997; Paus et al., 1995; Sylvester et al., 2005; Wenzel et al., 2000). In an fMRI study, Wenzel and colleagues (2000) measured a bilateral signal intensity decrease at the occipital pole during the performance of acoustically triggered saccades at 2 Hz and observed, by using Near Infrared Spectroscopy (NIRS), that the increase in deoxygenated hemoglobin and the decrease of oxygenated hemoglobin was dependent on the frequency of the saccades. Bodis-Wollner and colleagues (1997) could measure BOLD signal changes in V1 triggered by saccadic eye movements executed in the dark but not during imagined saccades, and Sylvester and colleagues (2005) found that saccades modulated V1 BOLD signal levels elicited by ganzfeld flicker stimulation, even though some residual signal could also be measured in the absence of visual stimulation (replicated in Sylvester & Rees, 2006).

2.1.5 Purpose of this study

The purpose of this study is to investigate to whether V1 plays a role in the execution of saccades in the complete absence of visual information. Reflexive saccades to a visual target presented in a reference-less visual space (visually guided, VG) are compared to voluntary saccades (self guided, SG) executed in complete darkness but triggered by the extinction of a fixation reference, and to blocks of Self Paced (SP) saccades for which subjects were completely deprived of visual information. In our experiment, we explicitly avoid the use of cues that could complicate the interpretation of the imaging results, we unambiguously define "absence of visual stimulation" as the absolute lack of visual experience even after long periods of dark adaptation, and we accurately measure eye movements during the actual scanning sessions with high temporal and spatial resolution by using an IR-based eye tracker specifically designed for the MR environment. We hypothesize that, apart from selective activation differences in motor and higher cortical areas, activity in a purely visual V1 should be related to the amount of visual information to be processed. Stronger activation is expected in the Visually Guided (VG) condition for which the position of the target has to be transferred to motor areas for the preparation of the saccade compared to Self Guided (SG), in which only the offset

of the fixation can be visually interpreted. Saccades executed in the absence of visual input should elicit no activity in an area purely devoted to vision.

2.2 Methods

2.2.1 Subjects

Seven healthy right-handed subjects (age range 22-43, 4 female) with normal visual acuity participated voluntarily and received a monetary compensation for successfully taking part in the experiment. The experimental protocol was designed and implemented in accordance with the ethical standards of the 1964 Declaration of Helsinki (Rickham, 1964) and all participants gave written informed consent prior to the fMRI measurement. Subjects went through two training sessions in the psychophysics laboratory before performing the task in the MR scanner. During these sessions, the task was carefully explained to the subjects, who completed several hundred test-trials during which fixation stability and eye movement quality were assessed. Due to the difficulties involved in measuring eye movements within the strong magnetic field produced by MR scanners, only subjects with excellent oculo-motor performance were selected for this study (Section 1.6).

2.2.2 Stimulation and experimental design

Visual stimulation consisted in an array of three horizontally arranged red LEDs mounted on the back of a black foam-board and placed 20° apart. LED control was achieved by using three analogue output channels of a VSG2/5 visual stimulator (Cambridge Research Systems, Ltd.) that were radiofrequency filtered to avoid the introduction of perturbing signals in the scanner room. To minimize residual environment illumination, the light emitted by the LEDs was seen by the subjects through punctured holes (of about 0.03° of visual angle, see Figure 2.2) on the outer layer of the foam board. The inside of the gantry, the MR-chamber's window and all monitors and light emitting displays were covered with darkening material until the scanner room was in absolute darkness, which was defined as subjects not being able to report any visual experience after adaptation

periods of over 30 min. Three experimental conditions were sequentially measured in a block design (Amaro & Barker, 2006), alternating blocks of saccadic activity with rest periods (Figure 2.3). In the first experimental condition (VG) subjects executed a saccadic eye movement to a LED in the periphery, randomly switched on either to the left or the right simultaneously with the extinction of the central LED. Subjects were trained to maintain their gaze on the target as long as it was present (1 s) before executing a return saccade to the center LED whenever switched back on. The timing of the events followed a standard step procedure (Leigh & Zee, 1991), with a mean saccadic frequency of 0.56 Hz. In the second condition (SG), no saccadic target was presented, and subjects were trained to execute a saccade to the left or to the right of the central LED after it was switched off. In the third condition (SP), blocks of rest in which subjects had to fixate the central LED, were alternated with blocks in which no visual stimulation was presented (Figure 2.3). During these blocks in complete darkness, subjects were trained to perform saccadic eye movements of similar frequency and amplitude as in the first condition. Blocks lasted 40 s and each fMRI measurement contained 6 cycles of rest/task. LED real-time control, eye movement calibration and recording, and the acquisition and management of the triggers delivered by the MR scanner and the VSG, were controlled by software especially written for this experiment in Delphi Pascal using the VSG 6 library (Section 1.6).

2.2.3 Retinotopy of visual areas

Retinotopic maps were obtained for four subjects by using visual stimulation consisting of a rotating flickering (8 Hz) dartboard wedge of 45° following a standard procedure carefully described by Warnking and colleagues (2002). The wedge was presented during 5 s in each of the 16 positions (22.5° apart), two clockwise and two counter-clockwise runs. BOLD signal changes were modeled independently by convolving the onset of each of the wedge positions with a canonical HRF (Section 1.7). A GLM-based analysis was performed and T contrast vectors were defined to create maps of voxels that significantly responded selectively to one wedge position but not to the others. After segmenting the gray-white matter boundary, using 3 mm gray matter reconstruction algorithm, inflating,

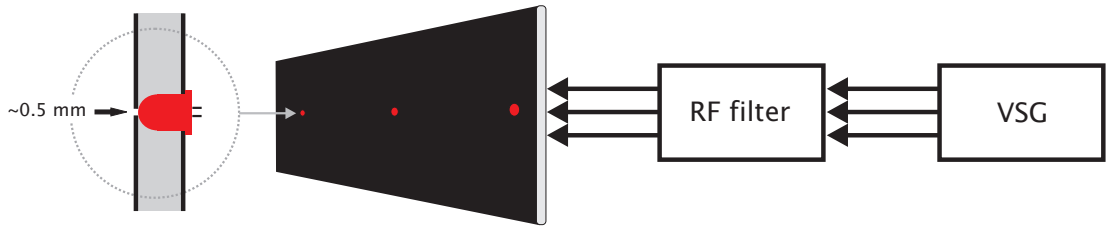

Figure 2.2: An array of three LEDs was use throughout the experiment to minimize residual and scattered light. The LEDs were RF-filtered, mounted on a black foam and could be visible only through a pinhole subtending about 0.03° of visual angle.

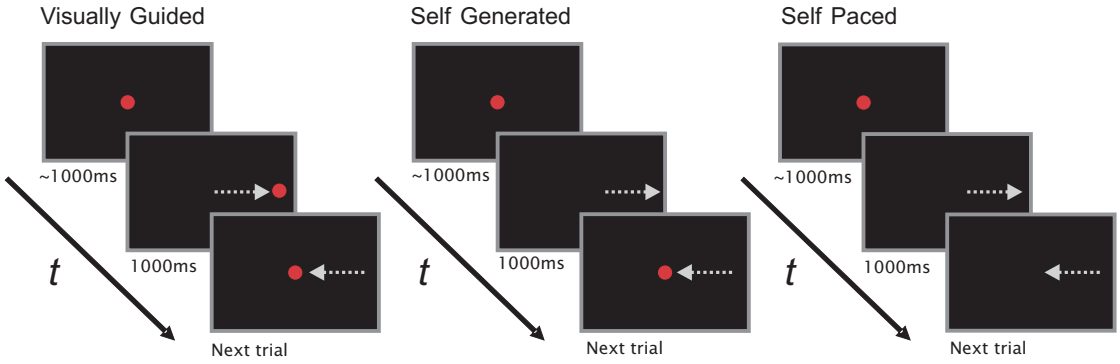

Figure 2.3: Description of the three experimental conditions: In the visually-guided (VG) condition (left), subjects were trained to execute a saccade to a red target appearing step-wise in the periphery. In the self-guided condition (SG, center), the disappearance of the fixation dot cued the subject to execute a saccade to a self determined position along the horizontal axis. During the self-paced (SP) condition (right), subjects had to perform previously learned sequences of horizontal saccades in a complete absence of visual stimulation.

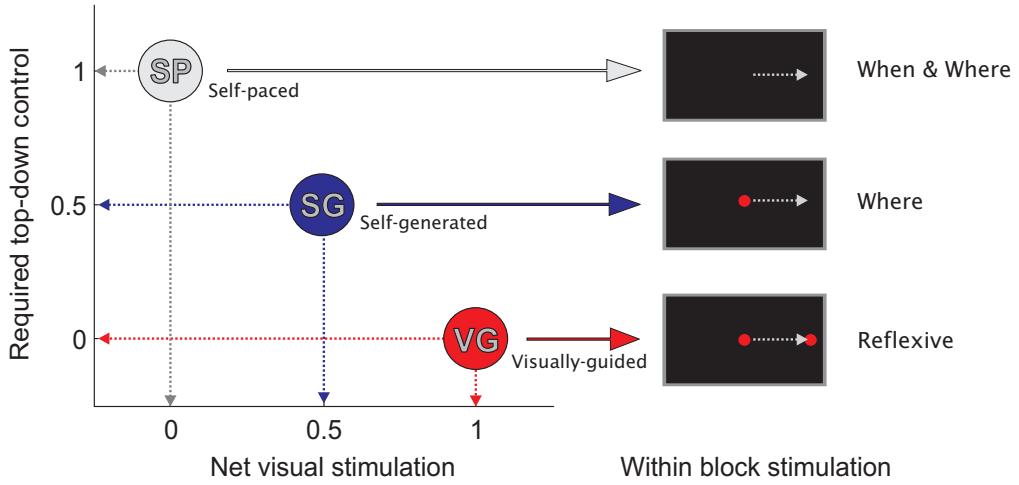

Figure 2.4: Because of the sluggish nature of the BOLD signal, the three blocked conditions create a gradient of net visual input versus the required amount of top-down control to perform the task.

cutting and correcting for spherical deformations by using Brain Voyager (Brain Innovation B.V., Maastrich, The Netherlands), functional data were overlaid onto flattened cortex (Van Essen, Drury, Joshi & Miller, 1998) to search for a topographical relation between the direction and amplitude of the saccades and the patterns of activation.

2.2.4 Eye movement recording

Eye movements were recorded by using a fiber-optic, infrared limbus reflection device (MR-Eyetracker, Cambridge Research Systems, Ltd.) with an optimal spatial resolution of 0.2° of visual angle. The system is linear within 3% for horizontal eye displacements of ±20 deg and velocity can be derived by on-line differentiation of the eye position signal. Position signals of the left eye were sampled at 1 kHz directly on the VSG card by using a buffering technique built into the experimental software developed for the purpose, and stored in a laboratory computer for off-line analysis (Section 1.6). Calibration of the eye position signal was performed prior to and after each run. For calibration, subjects made saccades from the central fixation point to targets at predefined locations within a range of ±10°. Eye movement analysis was performed with the help of an in-house developed software (DeSouza, 2000), which yielded accurate estimates of latency, duration, peak

velocity and amplitude of each saccade.

2.2.5 Imaging methods

Each of the three imaging sessions through which each subject underwent contained alternating 10 volume (40 s) blocks of rest and a single condition (120 scans per session). Functional images were acquired using a Maxwell-corrected T_2^* weighted echo-planar MRI sequence (36 transversal contiguous slices; TR = 4 s; Time to Echo (TE) = 54 ms; flip angle = 90°; voxel size 3x3x3 mm; field of view = 192 mm; matrix size = 64×64 bins) on 1.5 T Siemens Sonata Maestro equipped with a 40 mT ultra-fast gradient system. Volumes were transversally oriented and covered the whole brain and the upper half of the cerebellum. For identification of anatomical landmarks and to aid co-registration and normalization a high resolution, T_1-weighted structural image TR = 9.7 ms; TE = 4 ms; flip angle = 12°; voxel size = 1 mm^3) was acquired for each subject. Data preprocessing and analysis were computed on a high-performance Linux workstation. The functional images were corrected for head motion, co-registered with the structural image, normalized into standard stereotaxic space (Montréal Neurological Institute, McGill University, MNI. Quebec, Canada), spatially smoothed by using a Gaussian kernel with a full width at the half-maximum FWHM = 8 mm), and analyzed using the MATLAB plattform (The Mathworks, Natick, Massachusetts, USA) running SPM2 software (Section 1.7). Temporal bandpass filtering (Low-Pass: Gaussian 4 s, High-Pass: 0.375 cycles/°) was applied during block-design fixed-effects (Amaro & Barker, 2006) GLM-based analysis (box car convolved with canonical hemodynamic response function as modeling waveform). Voxel clusters in which T > 5, $p_{\text{corr}} < 0.001$ and cluster size k > 20 were defined as significant. Clusters of activity in V1 were delimited as regions of interest (ROI) by using the toolbox Marsbar (Brett, Anton, Valabregue & Poline, 2002). Time signals extracted from voxels belonging to these clusters were averaged and the resulting series were re-tested by using the same original SPM design.

2.3 Results

Saccades recorded during the imaging sessions show a linear relationship between their amplitude and their peak velocity (Figure 2.5). Visually guided saccades (global mean = 215 ms; sd = 65 ms) showed significantly (F = 9.68; $p > 0.001$) shorter latencies and higher peak velocities than voluntary saccades (global mean = 236 ms; sd = 82 ms) and presented wider distributions (Figure 2.5). Despite not being identical, due to the training sessions SG and SP saccades are of a comparable size to that of VG saccades as revealed by visual inspection of the eye traces.

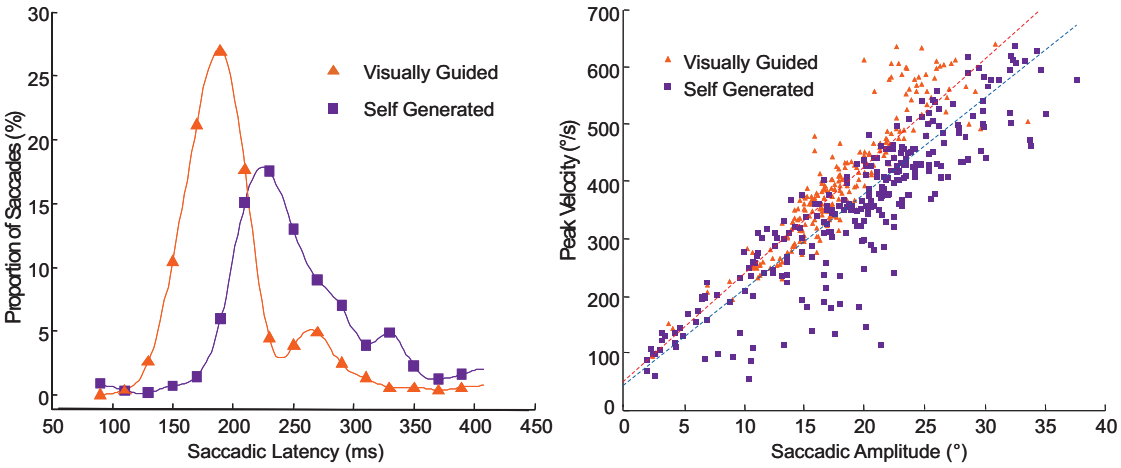

Figure 2.5: Saccadic latency distributions for visually guided and the self generated saccades are plotted to the left. Visually guided saccades (red line-triangles) show shorter latencies and narrower distributions, whereas programming the execution of self guided saccades (blue line, squares) takes longer time and the latency variability is greater. Non-reflexive saccades require some extra preparatory effort that reflects not only in the latencies but also in the cortical response pattern of areas involved in saccadic execution. The relation between saccadic amplitude and velocity is determined by a linear relation in what is known as the main sequence. Plotted to the right, it can be observed how as the amplitude increases the maximum peak velocity reached by the saccade becomes higher. The slope for the voluntary (endogenously generated) saccades is gentler than for the visually guided (exogenously triggered) saccades, indicating slower movements. Depicted are not only saccades to the target but also over- and undershoots, as well as corrective saccades.

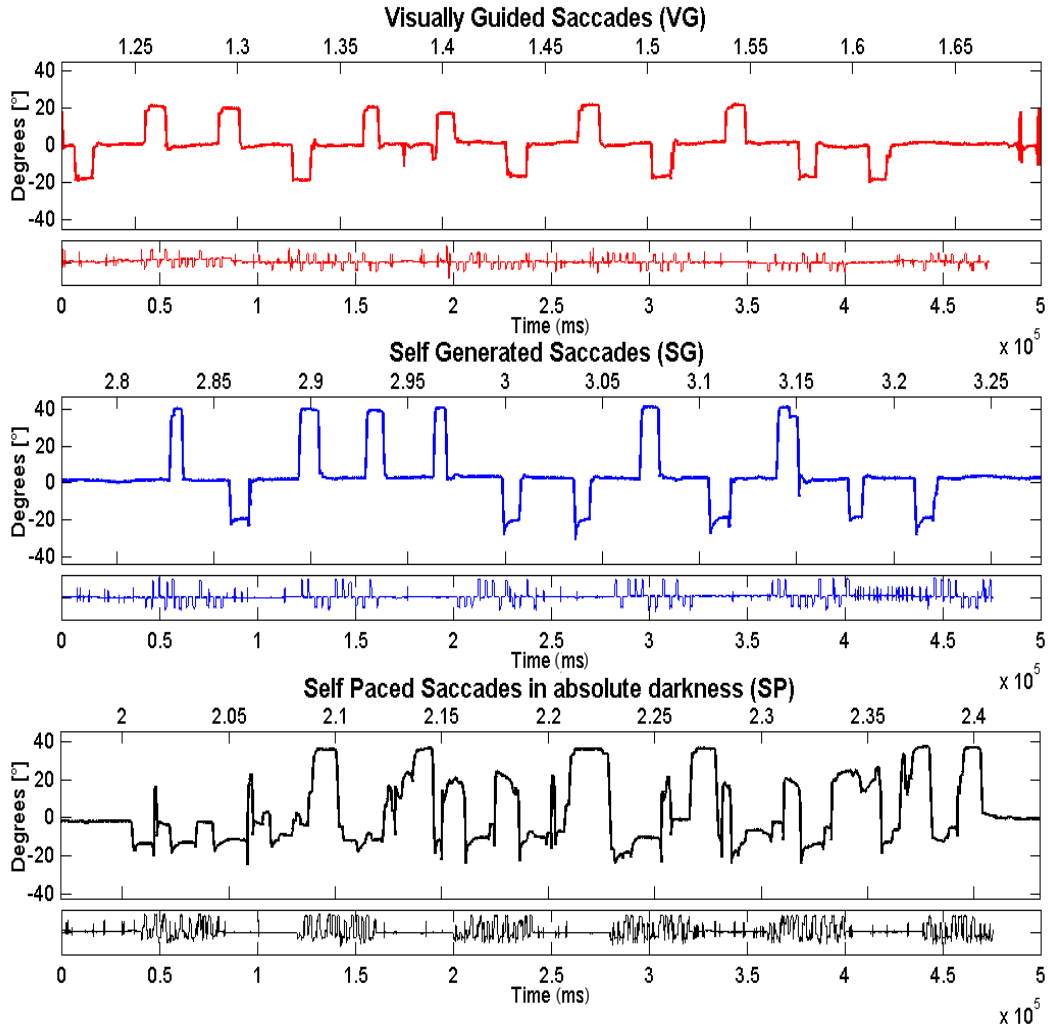

Figure 2.6: In the eye movement traces collected during the MR session of the second experiment it can be observed that VG saccades (red) are very symmetrical and show stable fixations. in contrast, SG saccades are asymmetrical, have unstable fixations and present drifts (blue). Self paced (SP, black) saccades performed during blocks of uninterrupted absolute darkness are very irregular, have great amplitude variability and fixations are extremely unstable. The panner under the traces shows the eye movement recording during the whole MRI measurement evidencing the blocked nature of the design.

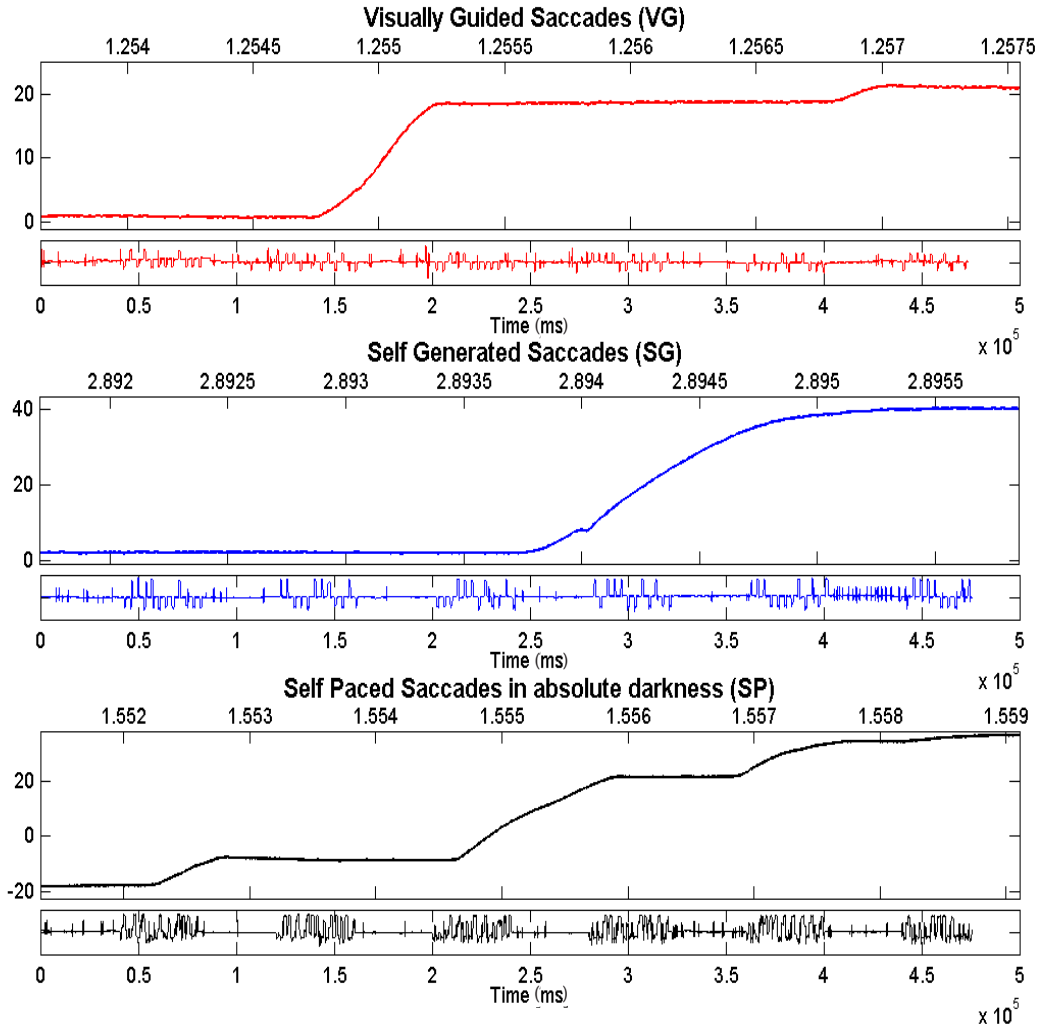

Figure 2.7: On the top graph, a typical visually guided reflexive saccade can be observed (red). VG saccades are characterized by shorter latencies, higher peak velocities and are often followed by a corrective saccade. In the middle graph (blue), a typical self generated endogenous saccade is plotted. SG saccades have longer latencies, reach lower peak velocities than VG saccades and need over 100 ms before their fixations stabilize. At the bottom, a typical self paced saccade (black) is depicted. SP saccades characterize by broken trajectories and very unstable fixations.

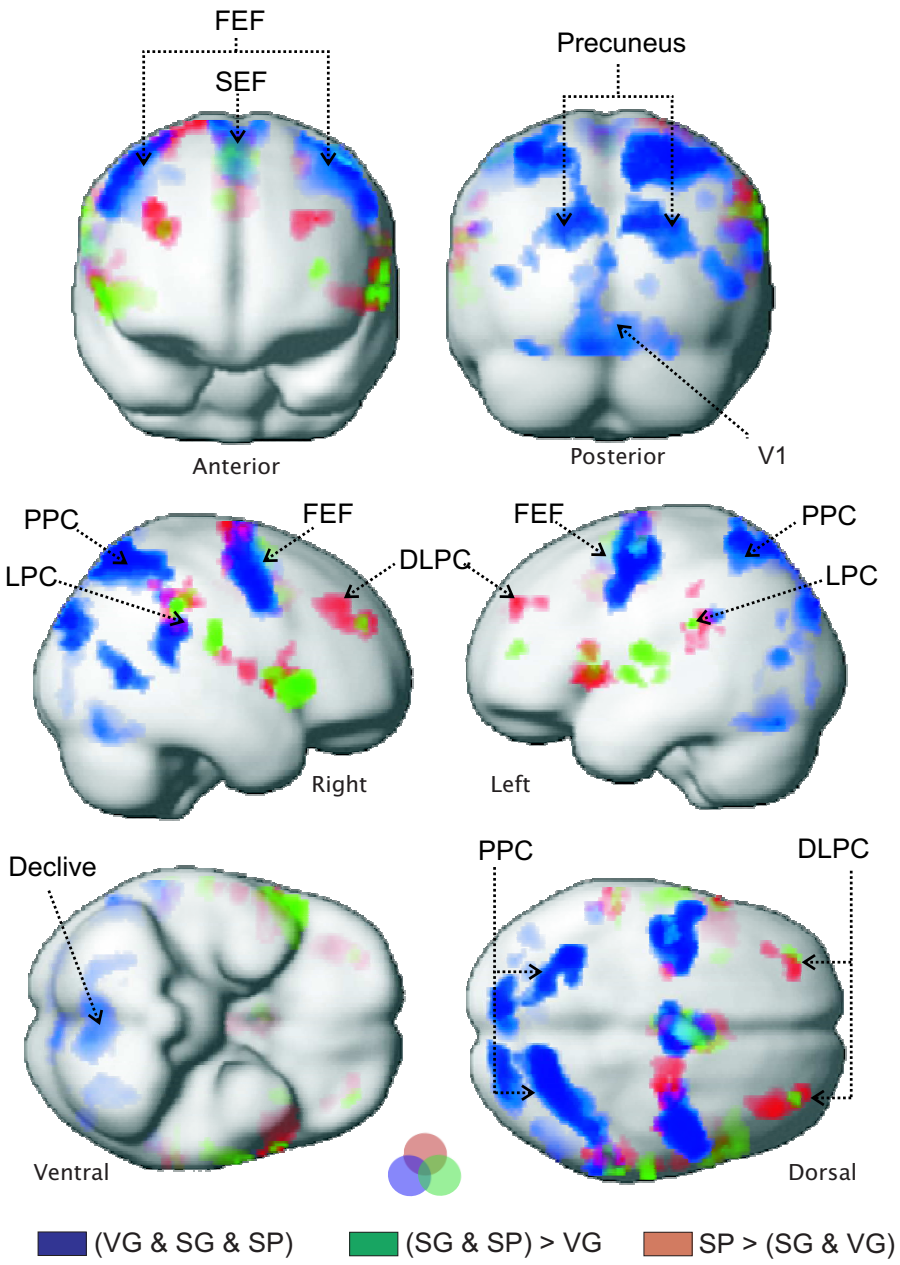

Figure 2.8: Common and specific cortical areas engaged by visually guided, self generated and self paced eye movements overlaid on a MNI standard averaged-brain template. All types of saccades engage the frontal, supplementary and parietal eye fields, as well as primary visual cortex. Non-reflexive conditions (SG and SP) bilaterally activate regions in the dorsolateral prefrontal cortex, evidencing their top-down nature.

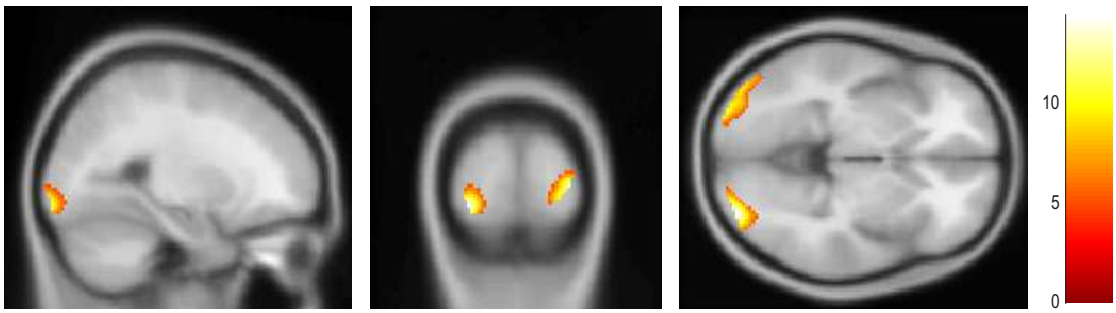

Figure 2.9: Conditions in which there was limited visual input available (VG and SG) show a significant signal increase in secondary visual areas V2 and V3 (BA 18 and 19), either related to up-stream processing of the visual information or to feedback signals being sent to V1 ($T > 5$; $p_{corr} < 0.001$; $k > 50$). ROI analysis in both clusters (MNI cluster center coordinates x = -30, y = -94, z = -10 and x = 34, y = -90, z = -4) revealed a positive relationship between net visual input and signal strength (VG > SP: $T = 11.74$, $p < 0.0001$ and $T = 12.62$, $p < 0.0001$; VG > SG: $T = 1.53$, $p = 0.06$ and $T = 3.71$, $p = 0.0001$; SG > SP: $T = 9.99$, $p < 0.0001$ and $T = 8.89$, $p < 0.0001$).

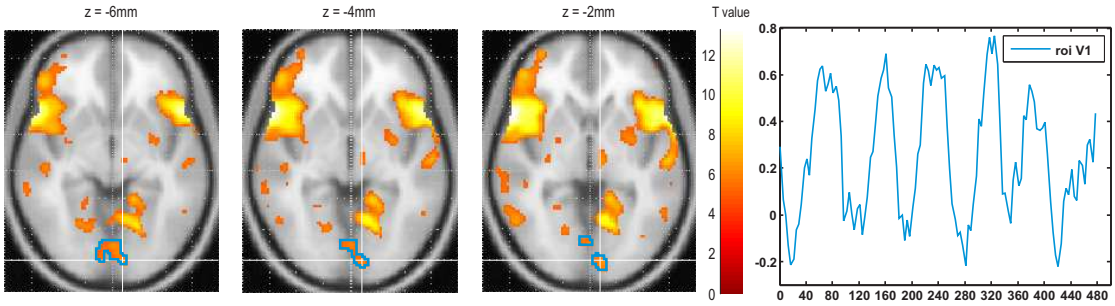

Figure 2.10: V1 activity during the execution of self paced saccades in absolute darkness (cluster center MNI coordinates x = -10, y = -96 and z = 4). Plotted to the left is the result from averaging the signals extracted from all the voxels belonging to the V1 cluster (marked in cyan). The nature of the block design is clearly reflected by the periodicity of the signal fluctuation (ROI analysis; $T = 7.12$; $p < 0.0001$).

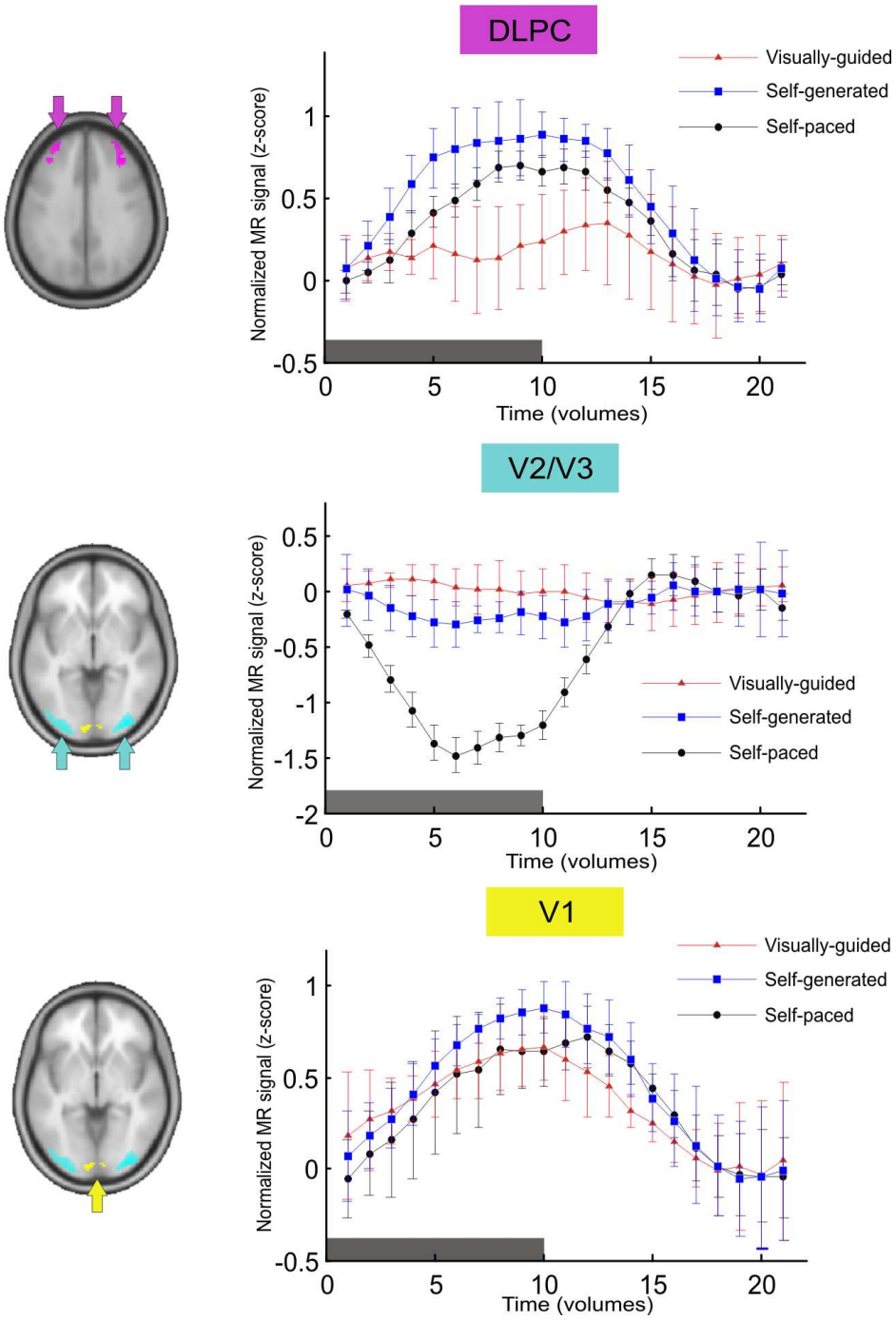

Figure 2.11: Time-course average signals extracted from the ROIs (gray areas represent the blocked saccadic activity periods). The DLPC is actively engaged by voluntary saccades but not by reflexive saccades. Extrastriate areas V2/V3 experience a pronounced decrease of activity after removal of visual input during SP blocks. Surprisingly, and despite the classical conception of V1 as being a pure visual area, bilateral areas of the primary 'visual' cortex are equally active during all three conditions, including during the generation of saccades in the absence of any visual stimulation.

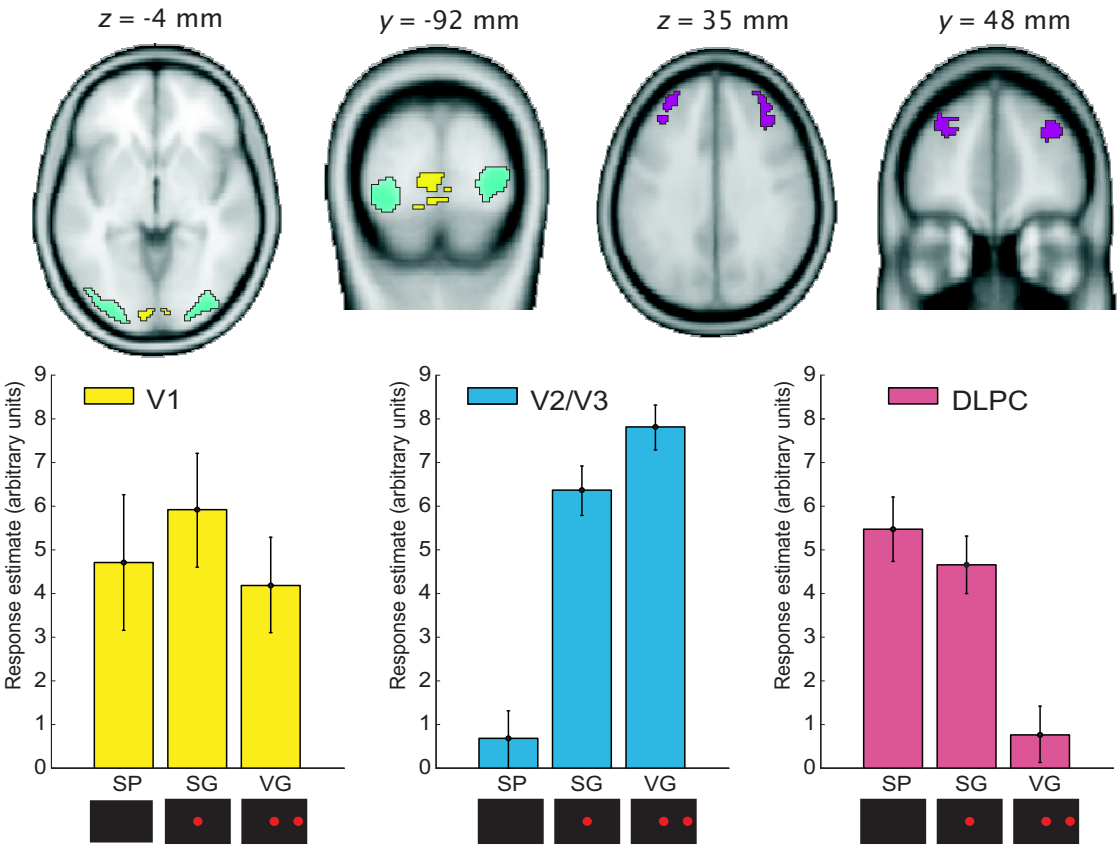

Figure 2.12: Contrast estimates and 90% confidence intervals for a ROI analysis of clusters in the DLPC (magenta left bar plot), extrastriate areas (cyan central bar plot), and a cluster in V1 (yellow right bar plot) for all three conditions SP, SG and VG. While there is a significant decrease in the amplitude of the signal in prefrontal frontal areas that correlate with the amount of top-down control (SG > VG: $T = 6.91$, $p < 0.001$; SP > SG: $T = 1.36$, $p = 0.08$; SP > VG: $T = 7.82$, $p < 0.0001$), and a strong positive correlation between the amount of visual input and the signal-change amplitude in extrastriate areas, there is no monotonic relation between the net amount of visual stimulation available and the signal changes in V1 (SG > SP: $T = 2.37$, $p = 0.009$; SP > VG: $T = 3.09$, $p = 0.001$; SG > VG: $T = 5.73$, $p = 0.0001$). All three conditions though (including the SP condition) elicited significant signal changes in V1 with respect to baseline levels measured during the fixation periods (VG: $T = 5.30$, $p < 0.0001$; SG: $T = 12.51$, $p < 0.0001$; SP: $T = 8.61$, $p = 0.0001$).

Table 2.1: Brain areas significantly activated concurrently during all three conditions (VG+SG+SP).

	Left hemisphere					Right hemisphere				
Contrast: SG + VG + SP	x	y	z	**Voxels**	**T (max)**	x	y	z	**Voxels**	**T (max)**
Striate cortex (V1)	-8	-90	-10	174	6.25	12	-78	6	18	5.58
Precentral Gyrus (FEF)	-42	-10	54	1136	10.69	48	-2	50	1029	8.89
Medial Frontal Gyrus (SEF)	-2	2	56	373	9.75	2	-6	66	392	10.06
IntraParietal Sulcus (IPS)	-34	-58	62	913	8.98	22	-66	66	1350	10.21
Cuneus/Precuneus	-12	-88	34	92	8.57	14	-90	32	451	8.01
Middle Temporal Gyrus (MT)	-44	-76	10	70	6.68	54	-62	6	290	8.18
Cerebellar Declive	-8	-74	-22	432	11.05	8	-72	-20	491	9.08

MNI coordinates for clusters (T > 5; k > 20) surviving correction for multiple comparisons at the voxel-level (p<0.001).

Table 2.2: Brain areas significantly more active during conditions in which visual stimulation was available compared to self-paced saccades executed in complete darkness (VG+SG>SP).

	Left hemisphere					Right hemisphere				
Contrast: VG + SG > SP	x	y	z	**Voxels**	**T (max)**	x	y	z	**Voxels**	**T (max)**
Extrastriate Cortex (V2, V3)	-30	-94	-10	426	14.03	34	-90	-4	439	14.30

MNI coordinates for clusters (T > 5; k > 20) surviving correction for multiple comparisons at the voxel-level (p<0.001).

Table 2.3: Brain areas significantly more active during the execution of self paced saccades compared to SG and VG in which limited visual stimulation was available (SP>VG+SG).

	Left hemisphere					Right hemisphere				
Contrast: SP > VG + SG	x	y	z	**Voxels**	**T (max)**	x	y	z	**Voxels**	**T (max)**
Medial Frontal Gyrus (SEF)	-4	-14	48	198	5.98	2	-2	62	204	7.23
Middle Frontal Gyrus (DLPC)	-34	48	14	50	6.09	32	50	30	20	5.59
Cingulate Gyrus (CEF)	-2	5	44	20	5.06	8	8	42	99	6.49
Inferior Parietal Sulcus	-60	-34	24	23	5.5	68	-36	38	71	5.7
Inferior Frontal Gyrus						54	22	0	367	6.99
Superior Temporal Gyrus	-62	-10	12	108	6.83					

MNI coordinates for clusters (T > 5; k > 20) surviving correction for multiple comparisons at the voxel-level (p<0.001).

Table 2.4: Brain areas significantly more active during the execution of non-reflexive voluntary saccades (SP+SG>VG).

	Left hemisphere					Right hemisphere				
Contrast: SP + SG > VG	x	y	z	**Voxels**	**T (max)**	x	y	z	**Voxels**	**T (max)**
Medial Frontal Gyrus (SEF)	-2	-8	54	645	7.62	4	8	42	751	8.84
Precentral Gyrus (FEF)	-44	-10	58	65	6.37	48	-16	58	77	5.92
Middle Frontal Gyrus (DLPC)	-28	48	34	101	5.96	32	50	30	7.17	354
Frontotemporal Cortex (FTC)	-58	12	0	515	7.28	58	10	2	833	7.8
Inferior Parietal Sulcus	-60	-38	26	202	6.94	60	-40	38	399	7.12

MNI coordinates for clusters (T > 5; k > 20) surviving correction for multiple comparisons at the voxel-level (p<0.001).

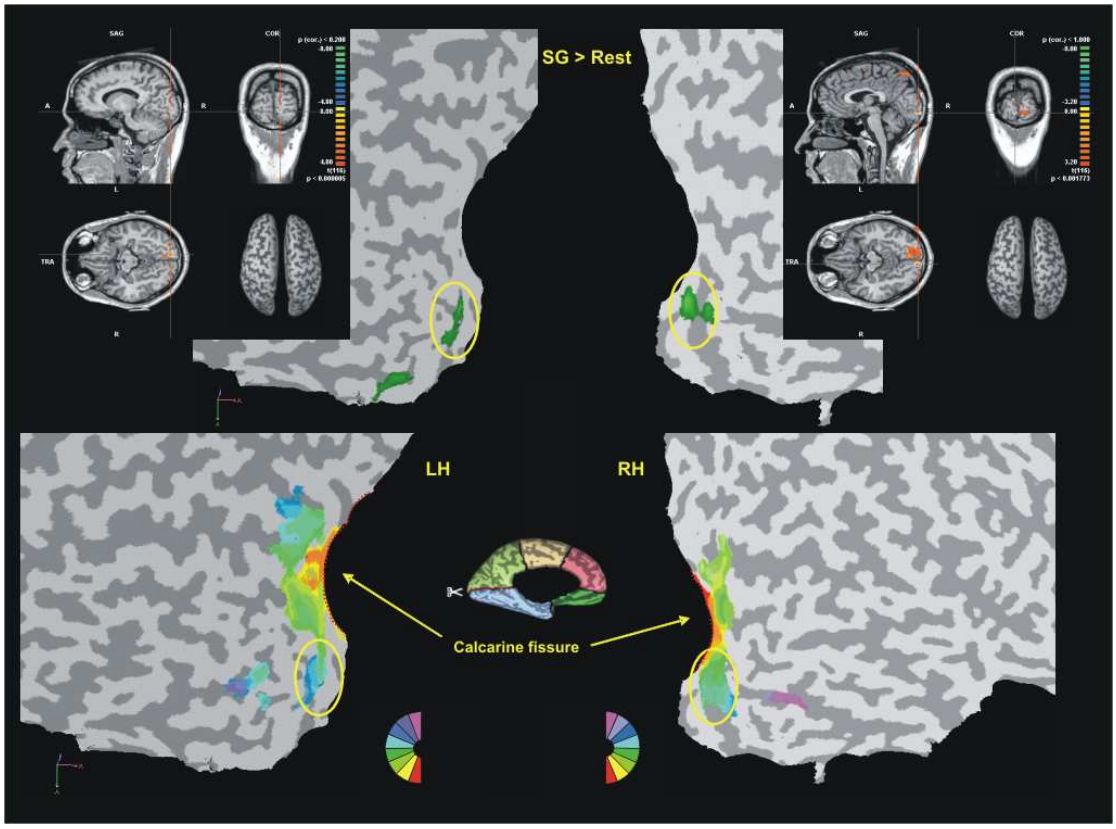

Figure 2.13: Primary visual cortex activity elicited by self guided saccades overlayed onto a retinotopic flat map from one participant. A cut along the calcarine sulcus (dotted red line) allows to display the activity maps onto unfolded 2D cortical surface. On the top images, activity clusters in V1 during the execution of saccades is mapped onto flattened cortex. In the lower panels, the result of the retinotopic mapping (Section 2.2.3) shows that the clusters of activity during horizontal SG saccades correspond to cortical areas retinotopically encoding the horizontal visual meridian, providing supporting evidence for the active involvement of V1 in the execution of non-visually guided saccades (the rainbow scale encodes the orientation of the stimulating wedge).

Concurrently in all three conditions, we found significant bilateral activations ($T > 5$, $p_{corr} < 0.001$, $k > 20$) in the FEF (BA 6), SEF (medial superior frontal gyrus, BA 6), CEF (cingulate cortex, BA 23, 24), parietal areas (BA 7, 30, 39, 40), medial temporal

(BA 37), primary visual areas (BA 17) and the declive of the cerebellum (Figure 2.1 and Table 2.1). SP and SG saccades are associated with significantly greater activity than VG saccades in the FEF, SEF, CEF (BA 24), inferior parietal lobe (BA 40), selectively engaged large bilateral areas along the superior temporal gyrus (BA 22, 24, 42), the inferior frontal gyrus (BA 44, 45, 47), and DLPC areas along the middle and superior frontal gyrus (BA 9, 10, 46) (Figure 2.8 and Table 2.4). The amplitude of the response in the DLPC was proportional to the amount of voluntary control (significantly higher in SP than in SG; $T > 5.5$; $p_{corr} < 0.001$). VG and SG bilaterally engaged extrastriate visual areas (BA 18, 19) (Figure 2.9 and Table 2.2) that were statistically silent during the execution of SP saccades. Responses amplitude in these areas was significantly higher during the VG compared to the SG condition, even though this difference was not significant at a corrected level ($T > 3.59$; $p < 0.001$). SP saccades, compared to SG and VG saccades, engaged more strongly the anterior cingulate gyrus (BA 24), the SEF (BA 6), and areas around the frontal operculum (BA 42, 43, 44) and the medial-superior frontal gyrus (BA 10). V1 activation patterns overlaid onto flattened cortex were constrained to the horizontal meridian of the visual field, as obtain during the retinotopic measures performed in four of the subjects (Figure 2.13).

2.4 Discussion

While reflexive Visually Guided (VG) saccades are executed based on a bottom-up process in which an external stimulus elicits a response, during the Self Guided (SG) and Self Paced (SP) conditions, top-down control is required to initiate an eye movement to a spatial position that has to be self determined. Whereas only pure visually guided saccades are present in the VG blocks, voluntary saccades performed in complete darkness to an eccentric location mix with visually guided re-centering saccades to the reappearing fixation diode in the SG condition, and only voluntary saccades in complete absence of visual stimulation are contained in SP blocks. Within this arrangement, we take advantage of the sluggishness of the BOLD response in which signals from different events

contained in a block summate in a roughly linear way (Huettel et al., 2004; Wager et al., 2005) to create an across-condition gradient of visual input and top-down control from VG to SG (Figure 2.4) leading to a completely lack of visual stimulation and pure top-down saccadic control in the SP condition in which both "when" and "where" to execute a saccade are self determined. The magnitude of this top-down cognitive effort is clearly reflected by a saccadic latency increase observed for SG saccades (Figure 2.5), that parallels a widespread increase of cortical activation along the anterior and the posterior saccade centers, as well as selective bilateral prefrontal activity that is absent during the execution of reflexive saccades (Figure 2.8).

Prefrontal cortex is thought to serve the guidance or inhibition of future responses that require temporal integration of events for purposeful actions. Supporting this idea, Pierrot-Deseillingny and colleagues (2003) studied a group of patients with DLPC lesion and observed a significant impairment for the execution of antisaccades, memory guided saccades and predictive saccades performed before the onset of the stimulation (all of them non-visually triggered voluntary saccades). In our data, the strong signal changes in prefrontal cortex during SG and SP saccades (Figures 2.8 and 2.12) denote that they are executed fully (during the SP condition) or partially (during the SG condition) under voluntary top-down (non-reflexive) control. Increased activation levels in lateral parietal areas during the SG and SP condition might be related to higher demands imposed by non-reflexive control of spatial attention that must be voluntarily shifted in the direction of the saccade (Corbetta, Kincade, Ollinger, McAvoy & Shulman, 2000). During VG saccades these areas could be relieved by an automatic mechanism of attention-capture, solely based on stimulus saliency (Itti & Koch, 2000).

Because SG and SP saccades were executed in the complete absence of visual stimulation, no spatial references are available to the system and saccadic vectors must be calculated based on some type of internal spatial representation that must be retrieved for the programming of a ballistic saccadic eye movement. Candidates for containing and providing this information are those areas engaged by these type of tasks in which a clear topographic organization has been stated, such as PPC (Schluppeck, Glimcher &

Heeger, 2005; Schluppeck, Curtis, Glimcher & Heeger, 2006; Sereno, Pitzalis & Martinez, 2001) and V1 (Engel et al., 1997; Van Essen et al., 1986). In our data, even though both areas are active during all three conditions, BOLD signal changes in parietal areas are much greater during the SG and the SP condition compared to the VG condition, while V1 remains at a similar activation level (Figure 2.12). This last result was unexpected since no significant differences between SG and SP were found for the signal amplitudes in V1 despite the differences in the amount of visual stimulation.

Recent work from Tehovnik, Slocum and Schiller (2002) shows that microstimulation of the lower layers of V1 evokes saccadic eye movements that terminate in the receptive field location of the activated neuron, while stimulation of the upper layers disrupts visual signals from the retina in its route to higher cortical areas. In our data, higher cortical visual areas BA 18 and BA 19 are only active when retinal information has been made available through V1 during the VG and the SG conditions. Unlike in V1, the amplitude of the BOLD signal changes in these secondary areas is proportional to the amount of visual information to be processed. Accordingly, activity levels triggered by the processing of the extinction of the fixation plus the immediate onset of the peripheral target in the VG condition are significantly higher than those elicited by the termination of fixation alone in the SG (Figure 2.9). As suggested by Logothetis and colleagues (2001), such extrastriate activations could reflect the up-stream processing of the feed-forward visual signals provided by V1.

The fMRI results presented in this study are compatible with the notion that V1 activity occurs either before, during or after a saccade. Corollary discharge from the frontal oculomotor centers may reach the visual cortex, even in the dark, but evidence for an intrinsic role of V1 in saccade generation comes from microelectrode stimulation studies in the cat (McIlwain, 1988) and the monkey (Tehovnik et al., 2002). Perisaccadic fMRI activity in the presence of visual targets may thus reflect either facilitatory or inhibitory, incoming or outgoing saccade related signals in human cortex.

While the dorsal layers of the SC are "visual" and contain a representation of the visual field, the more ventral layers contain a motor map (in polar coordinates) from which eye

movements can be elicited by using electrostimulation (Schiller, 1972). Although there are connections between both the ventral and the dorsal layers (Moschovakis et al., 1996), activity in the ventral layers seems to be more important for the execution of eye movements, to the point that visually induced stimulation of the dorsal layers does not necessarily lead to movement activity in the ventral layers, whereas movement activity in the ventral layers occurs without visual activity in the dorsal layers by applying low voltage currents (Leigh & Zee, 1991). Both V1 and extrastriate areas have projections to the ventral layers of the SC. These ventral layers, in turn, project to the brain stem from where the motor command for saccades is sent to the eye muscles through the cranial nerves. It has even been proposed (Fischer et al., 1995) that short latency express saccades could be originated within a loop consisting exclusively of V1 and the SC, yet only for visually guided saccades. In our study, the observed activation of V1 during the VG and SG conditions might therefore not only reflect visual processing of the target, but also the processes involved in neural computations underlying accurate saccade metrics, which takes place even in the absence of visual stimulation (as in SP). In fact, the localization of V1 activity along the horizontal visual meridian during the execution of horizontal self paced saccades, as shown by the retinotopic mapping, seems to strongly support this idea (Figure 2.13). As one possibility, we suggest that the role of V1 in perisaccadic activity is to provide coordinate information to other cortices (as the SC) even in the absence of visual input. Once an eccentric spatial location has been selected by other cortices to become the target of next saccade, a sequence of neural events might lead to the suppression of current processing to facilitate the remapping of spatial representation (Nakamura & Colby, 2002). The part of visual cortex that encodes the properties of a visual target at the selected location will usually fall within the foveal region after the saccade. Such fast switching of perisaccadic visual processing might be best reflected in the high-frequency gamma range of EEG. Indeed, it has been shown (Bodis-Wollner et al., 2002) that occipital gamma range frequency bursts occur following saccade onset and prior to each new fixation, even when saccades are performed in the dark or in the absence of visual targets. All this evidence strongly suggests a dynamic

interplay between the visual and oculomotor areas in the processing and targeting of objects in the real world, and compels us to reexamine the role of human striate cortex in visually guided behavior.

Although it is traditionally assumed that the role of V1 in saccade programming is coupled to the processing of the location and elementary features of visual targets, the present results indicate that this cannot be the sole reason for the activity registered in V1, since perisaccadic activity can still be measured in primary visual cortex when all visual input is removed. Together with those of earlier studies (Bodis-Wollner et al., 1997; Sylvester et al., 2005), these results provide converging evidence that V1 is specifically activated when saccades are executed and should therefore be incorporated into the structures that conform the cortical network responsible for saccades.

3 Perisaccadic V1 activity and attentional enhancement effects

Summary

Attention maximizes the efficiency of the visual system by weighting the relevance of the different objects in the visual field for the purpose of target selection. Although it has been recently demonstrated that attending to a visual stimulus enhances the responsiveness of the V1 neurons that retinotopically encode its corresponding spatial location, it has never been tested whether this modulation also occurs in the absence of visual input. Saccadic eye movements are always preceded by a shift of spatial attention to the location of the target, therefore, the perisaccadic V1 modulation observed during saccades in the dark (Chapter 2) could also be due to an attentional enhancement effect rather than to saccades per se. Recently developed eye-tracking techniques allow us to approach this question in an fMRI hybrid design study where trained subjects were asked to generate self-guided saccades and to perform voluntary covert shifts of attention in the absence of visual stimulation. Despite differences in spread and intensity, covert shifts of attention elicited the same activation pattern as self-guided saccades, including the activation of parietal areas, the frontal and the supplementary eye fields, and a complete absence of activity in visual areas. These results show that visual input is a requisite for attentional enhancement in V1, implying that shifts in visuo-spatial attention cannot be the cause of perisaccadic V1 activity and strengthening the idea of primary visual cortex playing an essential role for saccadic eye movements.

3.1 Introduction

Attention denotes the allocation of limited processing resources to some stimuli or task at the expense of others. Accurate saccades require shifts of perceptual attention to the target. These shifts of attention might serve a variety of purposes unrelated to saccadic control, such as to evaluate whether a particular eccentric target is a suitable goal for a saccade or to get a head start on processing the next item in a sequence (Kowler et al., 1995). The sequence that precedes a simple reflexive saccadic eye movement can be decomposed into the following: the onset of a salient stimulus that engages visual attention to that spatial location, a covert shift of attention towards that stimulus and the programming and execution of a motor command to bring that location to the fovea for fine scrutiny (Schiller, 1977). The visual system seems to continuously compute saliency maps for the different objects in a scene by using both bottom-up, image-based saliency cues, and top-down, task-dependent cues (Itti & Koch, 2001). These maps are thought to guide shifts of visuo-spatial attention and may be responsible for eliciting a saccade to a certain location in the scene. Saliency maps, by definition, can only be computed based on the presence of visual information.

3.1.1 Overt versus covert attention

As opposed to overt attentional shifts, in which the eccentrical deployment of attention is immediately followed by a re-centering saccade, it is possible to dissociate the locus of attention from the line of gaze by maintaining eye fixation while attending to an object located on the periphery in what is known as covert attention (Posner, 1980). Both covert and overt shifts of visuospatial attention are controlled by a network distributed across many cortical areas that involve the precentral sulcus, intraparietal sulcus and lateral occipital cortex (Beauchamp, Petit, Ellmore, Ingeholm & Haxby, 2001; Corbetta & Shulman, 1998). These areas, which traditionally have been related to oculomotor control, show increased activity related to the rate at which the attentional shifts occur (Beauchamp et al., 2001). Covertly attending to a location facilitates stimulus detection

and discrimination, as originally demonstrated by Posner (1980) and later replicated by Rizolatti, Riggio, Dascola and Umilta (1987), who observed that the Reaction Time (RT) to the onset of a visual stimulus increased when the stimulus is presented at a location different than the attended one. An even larger increase in RT occurs when stimulus appears at a non-attended location in the opposite hemifield (Rizzolatti et al., 1987). While Moran and Desimone (1985) found that attending to a stimulus modulated the firing responses of neurons in the extrastriate cortex (V4) but not of those in V1, modern imaging techniques have demonstrated that the spatial allocation of attention alters visual signals as early as in V1 by enhancing responses to the attended stimulus and suppressing responses when attention was directed away from the receptive field encoding the visual stimulus (Gandhi et al., 1999; Smith, Singh & Greenlee, 2000; Somers, Dale, Seiffert & Tootell, 1999). Moreover, Huk and Heeger (2000) observed that in some cases this attentional modulation could be affected by the subject's cognitive state, related to the task. Pestilli and Carrasco (2005) showed that transient covert attention increases sensitivity for contrast at the target location, and proposed that transient attention helps to control the selective deployment of limited cortical computational resources by modulating signals as early as in V1.

3.1.2 Spatial attention and saccadic eye movements

Shifts of spatial attention are closely linked to the execution of saccadic eye movements. Studies using single-unit recording, fMRI, and microstimulation indicate that the same brain areas are involved in both saccades and shifts of attention, suggesting that attentional and oculomotor processes are tightly integrated at the neural level (Beauchamp et al., 2001; Corbetta & Shulman, 1998; Schall, 2004). In fact, there is strong evidence that shows how a shift of spatial attention precedes each saccade, to the point that subjects are poor at making visual discriminations just before a saccade except at the target location (Deubel & Schneider, 1996; Kowler et al., 1995). Bushnell and colleagues (1981) recognized that it is very difficult to determine whether the observed relationship between neuronal responses and eye movements was specific to the movement or more

related to the attentional mechanisms that precedes the eye movement. As stated in the previous study of this dissertation (Chapter 2), V1 seems to play an active role in the execution of saccades in the absence of visual stimulation, but it was left unclear whether this involvement is related to the execution of the saccade as such, or to the preceding shift of visuospatial attention to the target location.

In macaques, V1 neuron responses are correlated with target choice in tasks requiring monkeys to attentively trace a line to plan a saccade (Roelfsema & Spekreijse, 2001), and this local attentional enhancement in V1 is rapidly restored after the saccade is performed (Khayat, Spekreijse & Roelfsema, 2004). Roelfsema and colleagues noticed that this modulation has very long latencies that on average are over 200 ms, which is considerably longer than response latencies to stimulus onset (with latencies of about 40 ms). This evidence suggests that this modulation might be driven by feedback signals from areas outside of V1, such as V2, V4, and MT, where firing rates are elevated for attended stimuli at substantially shorter latencies (Di Russo, Martinez & Hillyard, 2003; Martinez et al., 2001; Reynolds, Pasternak & Desimone, 2000).

3.1.3 Purpose of this study

Whether attentional modulation in V1 takes place even in the absence of visual input has never been investigated, and local enhancement effects, as the ones described above, could be the origin of the signal changes that we observed in our previous experiment (Chapter 2). The goal of this study is to determine whether covert attention alone can modulate BOLD responses in V1 when no visual stimulation is available. We hypothesize that visual stimulation is a pre-requisite for any enhancement effects and therefore no differential activation in V1 should be observed while laterally shifting spatial attention in the dark. The validation of this hypothesis would strengthen the idea that the V1 signal changes observed during Self Paced (SP) saccades (Section 2.3) are truly related to providing the non-visual spatial information used to compute the motion vectors needed for a saccade, since they could not be attributed to the reallocation of attention in the absence of visual input.

3.2 Methods

3.2.1 Subjects

Sixteen left-handed subjects with normal visual acuity and normal oculomotor performance (10 female, mean age = 24, SD = 3.4) participated in the experiment after giving informed written consent. The experimental protocol was designed and implemented in accordance with the ethical standards of the 1964 Declaration of Helsinki (Rickham, 1964). Two training sessions were used to assess the quality of the eye movements and allowed subjects to get acquainted to the task. Three fMRI measurements were performed for each subject. Subjects received a monetary compensation after successful completion of all sessions.

3.2.2 Stimuli and task

A horizontal array of three contiguous LEDs inserted in a black matt foam board was used as visual stimulation. Light emitted by the diodes could only be seen through a very small hole punctured on the external coating layer of the foam board so that resulting light dots were perceived very dim and had a size of about 0.03° of visual angle (Figure 2.2). A red LED located on the center of the visual field was used for fixation and was flanked by two yellow LEDs located at only 0.2° of eccentricity. The inside of the gantry, the MR-chamber's window and all monitors and light emitting displays were covered with darkening material until the scanner room was in absolute darkness, defined as subjects being unable to report any visual experience after adaptation periods of over 30 min. The three LEDs were controlled by three RF-filtered independent digital-output channels and specific real-time software written for this experiment in Delphi-Pascal by using the VSG library V6 (Section 1.6).

In a hybrid (mixed) fMRI design, two experimental conditions were blocked in an ABBA fashion while single trials were sorted and analyzed as events (Amaro & Barker, 2006). After a fixation period of about five seconds (jittered by a random fraction of half a TR value) in which only the fixation dot was visible, one of the yellow LEDs was

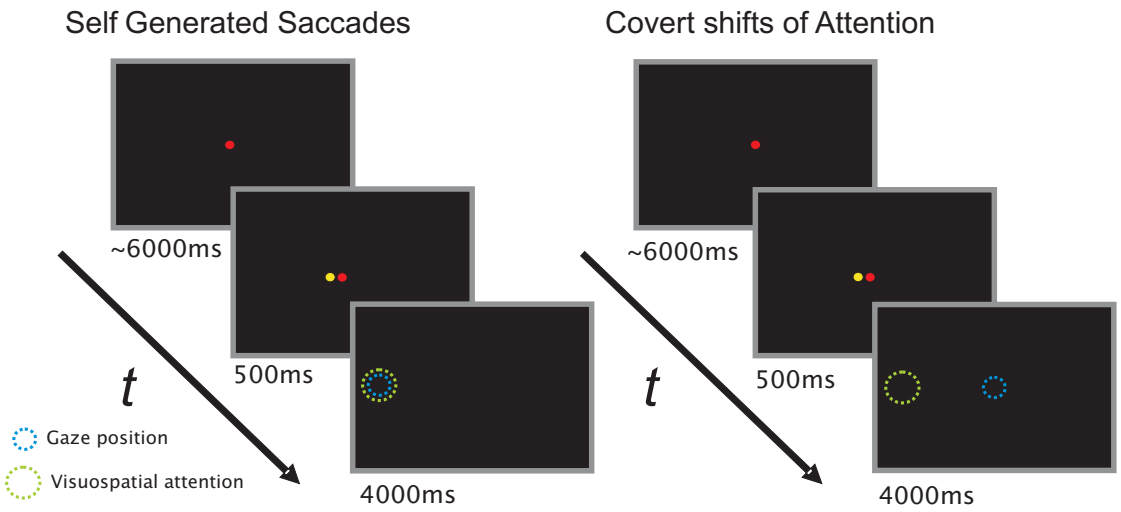

Figure 3.1: Stimulation sequence during the SG and the CA trials. After a variable fixation time, a direction cue was briefly presented either to the left or to the right of the fixation (yellow dot). The synchronous extinction of fixation and cue triggered the execution of a self guided saccade (SG, left sequence) or a covert shift of attention (CA, right sequence) to the cued direction in the absence of any visual input. This eccentric position was maintained for four seconds until the fixation was turned on again. By measuring the oculomotor behaviour, we could control that both the SG saccades and the covert shifts of attention performed during the CA trials occured in absolute darkness.

simultaneously turned on randomly either to the left or to the right of the fixation dot during 500 ms. The combination of the red and the yellow LED served as a direction cue. In the first condition subjects were trained to perform a Self Guided (SG) saccade with a previously practiced amplitude (without a visual target) immediately after the simultaneous extinction of the fixation red and the yellow LEDs. In the second condition, subjects had to maintain fixation and covertly perform a lateral shift of visuospatial attention of similar amplitude in complete darkness. Subjects were trained to maintain gaze or attentional locus for 4000 ms, after which the fixation dot reappeared triggering the return to the central red LED. The three LEDs were turned on together during three seconds to signalize subjects the block change. During the training session, subjects learned to interpret the combination of the red dot and the yellow dot appearing to the left or to the right as a cue indicating the direction of the eye movement or the covert shift of attention to be performed. Subjects were familiarized with the skill of covertly shifting of attention during a session in wich they were asked to report the value of numbers presented in peripheral vision while maintaining fixation. During each fMRI session, 20 trials of each condition where presented.

3.2.3 Eye movement recording

Eye movements were recorded using a fiber-optic, infrared limbus reflection device (MR-Eyetracker, Cambridge Research Systems, Ltd.). Eye movements were sampled at 1000 Hz directly on the VSG by using a buffering technique built into the experimental software developed for the purpose, and stored in a laboratory computer for off-line analysis (Section 1.6). Calibration of eye position was performed prior to and after each run. For calibration, subjects made saccades from the central fixation point to horizontal targets presented with an eccentricity of 20°.

3.2.4 Imaging methods

Imaging was performed on a 1.5 T Siemens Sonata Maestro (Siemens Erlangen, Germany), equipped with ultra-fast 40 mT/m gradients and a standard RF head-coil. A

T_2^* weighted Maxwell-corrected EPI sequence (TR = 3.2 s; 16 non-contiguous transversal slices; voxel size = 3x3x3 mm; distance factor 25%; flip angle = 90°; field of view = 192 mm; matrix size = 64×64 bins) was used to acquire 160 volumes containing 16 slices roughly aligned along the calcarine sulcus. Three of these 160-volume measurements were performed for each subject. After each measurement, a high-resolution (isovoxel size = 1 mm^3) Magnetization Prepared RApid Gradient Echo (MPRAGE) sequence was used to obtain one anatomical image composed of 160 sagittal slices that where latter used for the normalizing and overlaying of the functional data.

3.2.5 Data Analysis

The imaging data analysis was computed on a high-performance Linux workstation running MATLAB. Functional images were time-corrected to the central slice, realigned to the first image od the series, unwarped, normalized to a template from the Montreal Institute of Neurology (MNI152, T_1) and smoothed with a Gaussian kernel with a Full Width Half Maximum (FWHM) of 6 mm. Time series were high-pass filtered (90 s cut-off) to remove slow drifts and artifacts.

The event related analysis was performed using the standard hemodynamic response function (canonical HRF), and an event-related fixed-effects group analysis as implemented in SPM2 (Friston, Fletcher et al., 1998; Friston, Josephs, Rees & Turner, 1998). Similarly as in block-designs, the precise knowledge of the occurrence of the single events is used to set up a predictor for the accompanying blood flow changes (Section 1.7). In our case, the disappearance of the cue was used to create direction specific onset vectors for each condition (SG-left, SG-right, CA-left and CA-right), as well as for the return events to the central LED after the onset of the fixation that were convolved with the HRF in order to create eight regressors. These regressors were then used as covariates in a general linear model and applied on the time series extracted from each single voxel to derive statistical estimates of how well the observed BOLD signal change actually correlates with the predicted profiles. T-test contrast vectors were set up to test for significant differences in the amplitude of the hemodynamic response among the different experimental conditions.

3.3 Results

Eye movements could only be reliably measured for 12 of the participants. Eye movements performed during the SG condition had average amplitudes of about 30° and presented unstable fixations during the period before the execution of the return saccades. During the CA condition, small microsaccades ($< 3°$) whose direction showed a small but significant correlation ($r = 0.19$; $p > 0.001$) with the direction of the cue, were observed for most of the subjects (Figure 3.2).

Both SG and CA engaged cortical areas located in the precentral gyrus (FEF and SEF) and in the lateral intraparietal sulcus. Significantly higher activation clusters were found during the SG condition in the visual cortex (V1 and V2) and the the precuneus compared to the CA condition. During the CA trials, signal changes were significantly greater at the FEF, SEF and the lateral intraparietal cortex (Figure 3.3 and Table 3.1), as compared to the average signal amplitude estimated for the SG trials.

Table 3.1: Brain areas significantly more active during covert shifts of attention than during the execution of self guided saccades.

	Left hemisphere					**Right hemisphere**				
Contrast: CA > SG	x	y	z	**Voxels**	**T (max)**	x	y	z	**Voxels**	**T (max)**
SEF (BA6)	-4	-2	54	225	5.3	8	0	60	225	4.27
FEF (BA 6)	-26	-4	60	684	6.58	10	-10	64	539	6.01
PEF(lateral intraparietal, BA 40)	-48	-36	60	665	5.88	40	-60	48	298	5.08

MNI coordinates for clusters (T > 3.5; k > 20) surviving correction for multiple comparisons at the voxel-level (p<0.002).

Table 3.2: Brain areas significantly more active during the execution of self guided saccades than during covert shifts of attention.

	Left hemisphere					**Right hemisphere**				
Contrast: SG > CA	x	y	z	**Voxels**	**T (max)**	x	y	z	**Voxels**	**T (max)**
Striate cortex (V1)	-8	-66	14	23	4.51	2	-64	12	34	4.30
Extrastriate cortex (V2)	-24	-102	-2	11	4.05	26	-94	0	18	4.55
Precuneus	-18	-66	30	292	5.86	14	-70	30	451	5.75

MNI coordinates for clusters (T > 3.5; k > 20) surviving correction for multiple comparisons at the voxel-level (p<0.002).

Lateralized activation patterns were found for both the SG and the CA conditions. SG saccades executed to the left, elicited a strong focused activity in the contralateral extrastriate cortex (V2) on the right hemisphere, while saccades performed to the right activated the homologue areas in the left hemisphere (Figure 3.4). Identical but weaker

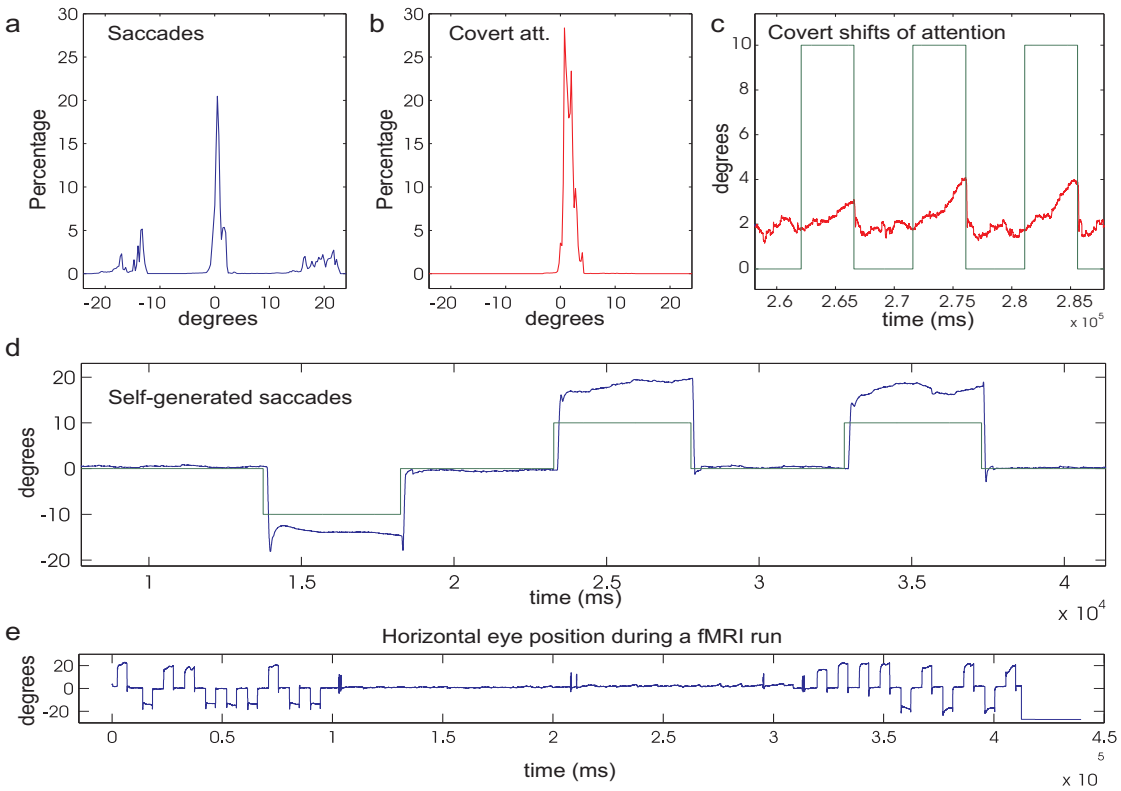

Figure 3.2: Eye movement recordings during the imaging sessions served as a control for the correct performance of the task. In the upper left plots (a and b), a histogram of the horizontal eye position reveals correct eccentrical fixations during the saccadic tast and permanent central fixation during the CA task accompained of small drifts in the direcction of the shift (c). A detail of eye movement traces during the SG condition can be seeing in the middle plot (d). The horizontal eye traces recorded during an imaging session (e) evidence the hybrid "blocked-events" structure of the measurement: SG-CA-CA-SG. Measurements with unstable fixations or a high degree of saccadic intrusion during the CA condition were excluded from the analysis.

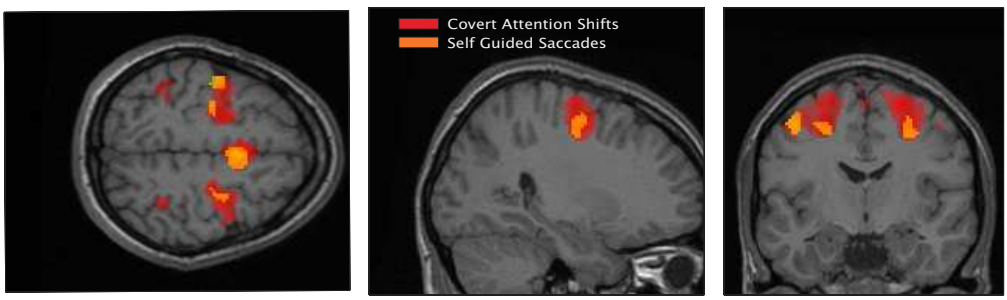

Figure 3.3: Activity patterns elicited by the execution of covert shifts of attention (red) and self guided saccades (orange) ($T > 5$, $p < 0.0001$, $k > 20$). Covert shifts of attention engaged more actively the FEF and the PEF, both reflected in increased cluster extent and larger signal amplitude.

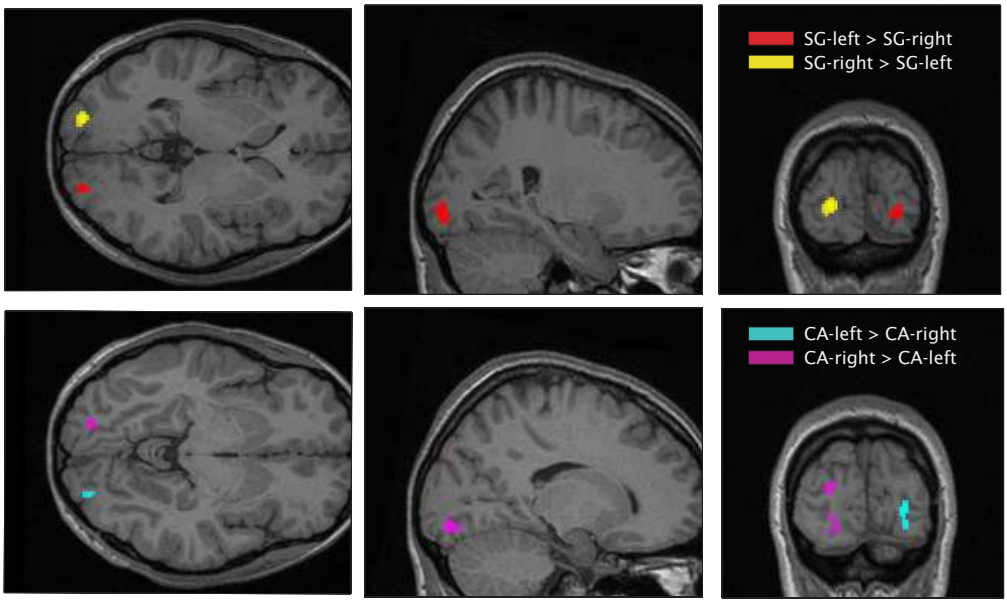

Figure 3.4: Contralateral activity in extrastriate areas engaged by SG saccades (upper row) and CA shifts (lower row) ($T > 5$, $p_{corr} < 0.0001$, $k > 20$).

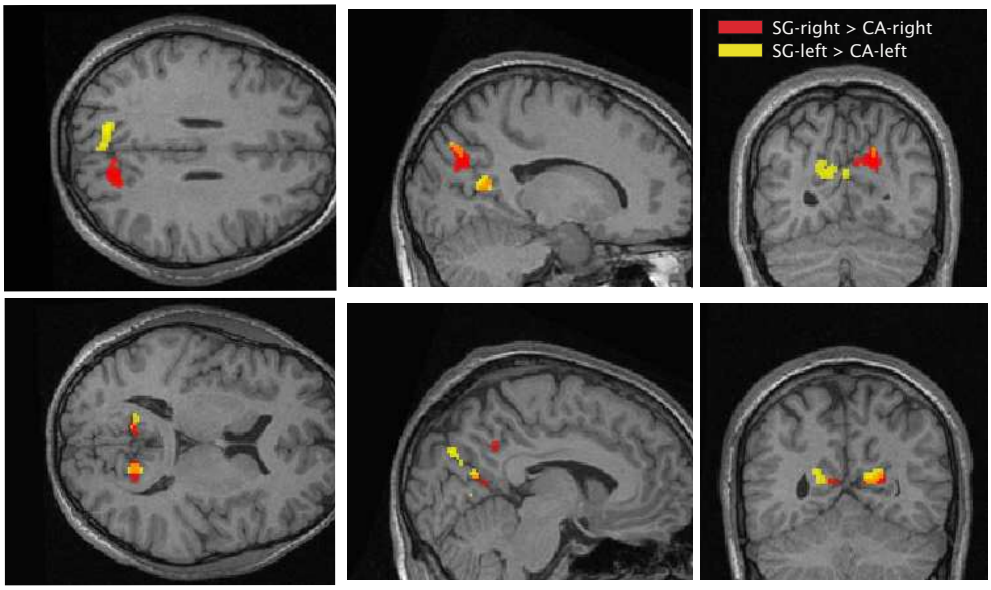

Figure 3.5: SG saccades bilaterally engaged the most anterior part of V1 (upper row) and presented strong lateralized activation clusters in the precuneus (lower row) when compared to CA shifts ($T > 4.5$, $p_{corr} < 0.001$, $k > 5$).

activations (SG-right > CA-right: $T = 4.49$, $p_{corr} < 0.002$; SG-left > CA-left: $T = 4.27$, $p_{corr} < 0.002$) were found during the CA condition. Moreover, the execution of saccades (SG) towards one horizontal direction, elicited stronger activation levels at the lateral parietal cortex (IPS) in the opposite hemisphere (SG-right > CA-right: 6.30, $p_{corr} < 0.0001$; SG-left > CA-left: $T = 6.02$, $p_{corr} < 0.0001$). Covert shifts of attention (CA) did not show any significant lateralization effect in parietal cortex, or in precentral areas (FEF and SEF), even though CA trials (both left and right) engaged more strongly the left lateral intraparietal cortex (LIP). While the most anterior part of the primary visual cortex and the precuneus were active during the execution of self generated saccades in the absolute absence of visual input (Table 3.2 and Figure 3.5), signal changes in these areas did not reach significant levels during the execution of covert shifts of attention.

3.4 Discussion

In general, our results replicate the imaging results on attention reported in previous studies and demonstrate that the execution of saccadic eye movement and the control of visuospatial attention share a common network of functional regions in the parietal and frontal cortex (Astafiev et al., 2003; Corbetta & Shulman, 1998; Nobre et al., 2000; Pierrot-Deseilligny et al., 2004). Because all previous studies used visual stimulation of some type, it was difficult to extract conclusions about the role that occipital areas have beyond their classical function for the processing of visual information. In our experiment, the fixation array is extremely small, very dim and identical in both conditions. The novelty of this study resides on the fact that, because it is the disappearance of the fixation array what triggers the events, self guided saccades and covert shifts of attention were performed in absolute darkness, ruling out that the resulting activities could be triggered by the processing of visual stimulation. Besides, the capability of recording eye movements during the MR measurements, allowed us to have a behavioral control for the correct execution of the task, both during the eye movements and during the covert shifts of attention in which we observe small displacements of the eye positions

towards the direction of the shift (Figure 3.2). These small drifts and microsaccades have been previously found to be strongly correlated with the direction of covert shifts of attention, suggesting that they can be used to map the orientation of spatial visual attention (Engbert & Kliegl, 2003; Hafed & Clark, 2002). Together with the previous training sessions, this drifts served as a confidence measure that made the introduction of catch trials unnecessary, and allowed us to keep the task in its simplest form.

The parietal cortex is a complex integration area that is thought to contain many different spatial representations serving different mechanisms such as attentional, saccadic and reach control (Astafiev et al., 2003). The medial bank of the human IPS has been found to respond during manual reaching, whereas the lateral bank has been found to be involved in visuospatial attention and eye movement control. It is also well known that the majority of neurons in the parietal cortex prefer contralateral stimuli and/or contraversive movements (Blatt, Andersen & Stoner, 1990; Wauschkuhn et al., 1998). Moreover, several recent studies (Schluppeck et al., 2005, 2006; Sereno et al., 2001) have identified up to three cortical areas in human parietal cortex that exhibit some kind of topographical organization during memory guided saccades. By varying the delay period, Schluppeck and colleagues (2006) were able to segregate signals from the memory and motor responses and showed that these responses were lateralized with respect to the direction of the saccade. In our results, we also observed a strong signal differences along the IPS and the precuneus that were associated with the direction of the eye movement but cannot possibly be related to any visual stimulation as, for example, the target-cues used in the delay task used by the authors of the above mentioned experiments. Since we only found this lateralization for the SG events, these signals might reflect the intention to perform a saccade to a certain spatial location rather than to the reallocation of spatial attention, and they are not engaged when gaze is forced to maintain fixation in the center of the display. This behavior resembles that of neurons in the monkey LIP, making human IPS a potential homologous of the intensively explored monkey parietal regions. Activation of the precuneus while performing sequences of saccades in the dark has already been reported (Bodis-Wollner et al., 1997; Petit et al., 1996). In

this area in monkeys (V6A, on the posterior face of the superior parietal gyrus), neurons have been found to encode post-saccadic eye position for arm and eye movements for non-retinotopic coordinates (Nakamura, Chung, Graziano & Gross, 1999), serving space transposition computations after each saccade.

Despite not being correlated with the direction of the shift and, as observed in previous imaging studies on the top-down control of visual attention (Arrington, Carr, Mayer & Rao, 2000; Vallines, En-Ju & Greenlee, unpublised; Weidner, Pollmann, Muller & Cramon, 2002), we found parietal activity during the CA condition to be strongly lateralized to the left hemisphere. Similar laterality effects have also been found in non-spatial attentional tasks involving multidimension monitoring under uncertainty conditions (Weerda, Vallines, Thomas, Rutschmann & Greenlee, 2006). In conflict with our data though, Arrington and colleagues (2000) found this left parietal lateralization when subjects had to attend to an object as compared to attending to a spatial location where the appearance of a visual stimulus was expected. The nature of this lateralization effect remains unclear.

In concordance with the experiment described in Chapter 2, the presentation of color distractors in the periphery has been shown to capture visuospatial attention leading to contralateral BOLD signal increases in regions of the extrastriate visual cortex that represent the distractor locations (Serences, Yantis, Culberson & Awh, 2004; Serences et al., 2005). Moreover, Kastner and colleagues (1999) found an increase of activity in these same extrastriate areas where the subjects covertly directed attention to a peripheral location while expecting the onset of a visual stimulus. In our paradigm, there are neither distractor enhancement effects nor effects of stimulus expectancy, but these response changes could be due to imagery strategies used by the subjects in order to covertly shift attention while deprived of any visual reference. Supporting this idea, Le Bihan and colleagues (1993) published an early fMRI study in which the mere mental representation of a visual stimulus elicited significant signal changes in V1 and in extrastriate area V2. In a more recent study (Klein et al., 2004), imagery has been shown to reliably trigger V1 activity with similar topography than those elicited by a standard visual

perceptual task designed to retinotopically map the primary visual cortex. In this and the previous experiment of this dissertation (Chapter 2), we observe V1 activity only during the execution of saccades, and not during the sustained effort needed to shift and maintain the locus of visuospatial attention in the CA condition. Whether the activity changes triggered by mental recall of spatially extended visual stimuli is due to imagery or to retrieving visuo-spatial information from the coordinate maps that V1 presumably contains, cannot be determined based on our results. V1 is significantly active during the execution of saccades, but this activity cannot be related to nonexistent visual input. Moreover, lesions in monkey V1 seem to impair the spatial accuracy of saccades (Segraves & Goldberg, 1987), and the ablation of the SC completely eliminates the possibility of eliciting saccadic eye movement after microstimulation of V1, V2 and LIP neurons in monkeys (Schiller & Tehovnik, 2005) demonstrating that visual areas reach the brainstem nuclei that control the eye muscles via the SC. In addition, SC is topographically organized, involved in the metrics of the saccadic system (C. Lee et al., 1988), and according to a large body of previous studies and supported by our results, is probably supplied by V1 with the coordinate information needed to prepare saccade even in the absence of visual stimulation.

Furthermore, significant V2 direction specific activity has been observed in both, the SG and the CA conditions but was significantly stronger during the execution of self guided saccades, ruling out any relation with the central cue which remains identical in both experimental conditions. Several electrode-recording studies in the monkey (Khayat et al., 2004; Reynolds et al., 2000; Roelfsema & Spekreijse, 2001) and Event-Related Potential (ERP) studies in humans (Di Russo et al., 2003; Martinez et al., 2001) suggest that enhancement effects in striate cortex are actually the result of delayed feedback signals to V1 from higher extrastriate areas. In our data, the weaker signal amplitude registered in extrastriate areas during the CA condition could have such a small effect in V1 that the signal enhancement, if any, was undetectable.

In summary, visual input seems to be a prerequisite for attentional enhancement in V1 and shifting of attention alone does not appear to engage the primary visual cortex which,

as shown by our results, seems to be controlled mainly by parietal cortices. This evidence rules out that the V1 perisaccadic activity found in the previous experiment could be the result of visuospatial attentional effects rather than being intrinsically related to the production of a saccade.

4 Measuring V1 BOLD Responses to brief visual stimuli

Summary

What is the shortest stimulus duration capable of eliciting a measurable BOLD signal change in V1? The dynamic application of retinotopy in fMRI experiments requires that the visual stimuli are presented during the brief fixational periods in which the retinae are static. By using eye-tracking techniques during the imaging sessions, the position of the retina can be estimated and the cortical areas retinotopically encoding the stimuli can be determined. In this study we demonstrate that it is possible to measure BOLD responses to Gabor stimuli[1] presented during 8 ms, which is the shortest presentation time that can achieved with high performance Digital Direct Drive Image Light Amplifier (D-ILA) projectors[2]. Such a short stimulus duration allows to visually stimulate V1 during fixational periods, while the corresponding cortical encoding locations can be accurately localized with retinotopical procedures.

[1] Gabor stimuli are luminance contrast patches defined by y sinusodial grating multiplied by a two-dimensional Gaussian window.

[2] Direct Drive Image Light Amplifier is a Hughes/JVC technology that uses a reflective Liquid Crystal Display (LCD) to create an image. A xeon light source is then reflected off the reflective LCD and is directed through a lens to the screen.

4.1 Introduction

The recent development of fast event-related fMRI has made possible the implementation of more sophisticated and precise experiments by allowing a closer match between stimulation and measured brain activity (Friston, Fletcher et al., 1998; Friston, Josephs et al., 1998). Event-related designs greatly increase the flexibility of fMRI allowing for trials of different types to occur in unpredictable random sequences, for the responses to rare events to be selectively extracted, and for post-hoc trial-sorting based for example on subject performance, stimulus onset asynchrony or response times. An important limitation of event related-designs is that brief stimuli are able to elicit only a fraction of the signal changes that trains of stimulus trigger in designs where many trials of the same condition are blocked. As already mentioned in Section 1.5, the first problem we face when dealing with BOLD signal is its sluggishness, which is mainly due to its vascular linkage. At the same time, using very brief stimulus presentations, as in ERP studies, can be very advantageous. In most experiments today, subjects are not just passively presented with certain stimuli but instead, they are trained to interact with them providing a much more realistic setting. These interactions are per se events that can be co-modeled in the experimental design. Eye movements, blinks, key presses, etc. are brief events but nevertheless, are known to elicit traceable brain activity (Ogawa et al., 2000). Being able to segregate the different sources of neural activity that lead to measurable BOLD signal changes provides a better ground for the interpretation of fMRI results.

4.1.1 The slow dynamics of the BOLD signal

The main limitation for presenting multiple events in fast sequence is that the BOLD signal is delayed in onset and evolves over an extended time period of about 12 s even for brief neuronal events (Blamire et al., 1992). During this period, it is generally assumed that the signal change resulting from the presentation of two identical stimuli sums in a roughly linear way by following the principles of additivity and superposition (Huettel et al., 2004). On the other hand, responses from two events happening very close in time

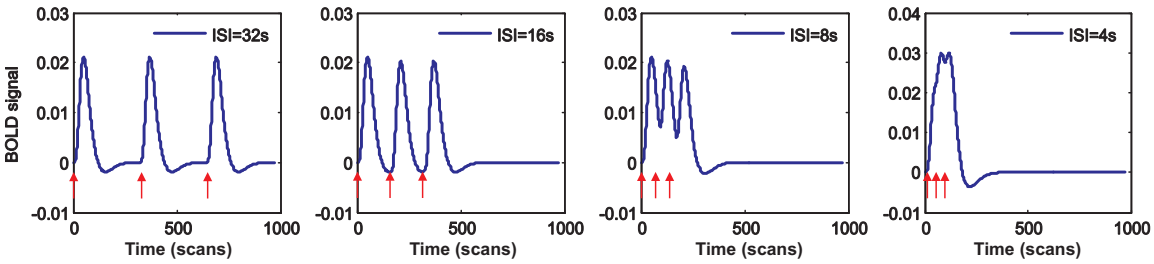

Figure 4.1: Modeled canonical hemodynamic response for a train of three events with different ISIs of 32, 16, 8 and 4 s. Individual signal amplitude-estimation for single events becomes impossible somewhere between 8 and 4 s, where the signal changes triggered by the three stimuli start adding incrementing the combined amplitude of the response, as in block designs.

greatly overlap and it has been shown that they interact in a non linear manner (Friston, Mechelli, Turner & Price, 2000). In these cases, the first stimulus seems to trigger a refractory period during which the the response to the second stimulus is delayed and attenuated, recovering to approximately 90% of normal amplitude when presented 6 s after the first stimulus onset (Huettel & McCarthy, 2000). Deconvolution of responses to short concatenated stimuli can be achieved by previously measuring a deconvolution filter in a short stimulus paradigm. Although this method has been shown to be successful at diminishing the hemodynamically imposed temporal blurring, is only effective when the stimuli are separated by at least 4 s (Glover, 1999).

4.1.2 Eye movements and retinotopy

When the eyes move relative to a stable world, the projection of the stationary world on the retina changes its position. At the same time, every eye movement produces a shift in the cortical retinotopical location that encodes the visual input projected on the retina. Recent developments (Kimmig et al., 1999) have incorporated the possibility of recording eye movements, along with other classical behavioral and physiological responses within the strong magnetic field of a modern MR scanner (Figure 1.5). At the same time, mapping the representation of the retina on the cortex is one of the most successful applications of fMRI in the study of the visual system (DeYoe et al., 1996; Huk,

Dougherty & Heeger, 2002; Tootell et al., 1998; Warnking et al., 2002). In most of these retinotopic studies, stimulation consisted on rotating high contrast flickering dartboard wedges or expanding dartboard rings (Warnking et al., 2002). Goodyear and Menon (1998) studied the effect of luminance contrast on BOLD fMRI responses in human primary visual areas and demonstrated that while extrastriate areas remain unaffected, V1 is especially sensitive to abrupt changes in luminance, such as the onset of a bright dot on a homogeneous background.

4.1.3 Gabor stimuli

Gabor stimuli are luminance contrast patches defined by y sinusodial grating multiplied by a two-dimensional Gaussian window. Apart from its theoretical advantages, this stimulus form minimizes a certain measure of uncertainty of stimulus localization simultaneously in two domains: spatial frequency and visual space (Gabor, 1946). The general expression for a Gaussian-windowed one dimensional sinusoidal luminance grating is

$$L\left(x,y,t\right)=L_m\left\{1+C_p\cos\left[2\pi x f_c+\theta_c(t)\right]\times\exp\left[-\tfrac{1}{2}\left(\tfrac{x}{\sigma_x}\right)^2-\tfrac{1}{2}\left(\tfrac{y}{\sigma_y}\right)^2\right]\right\}$$

where L_m is the mean luminance of the display, C_p is the peak contrast of the Gabor, f_c is the grating spatial frequency, and σ_x and σ_y are standard deviation of the spatial Gaussian window (Fredericksen, Bex & Verstraten, 1997). Manipulation of these parameters allows for changes in many different dimensions. For example changing the phase of the sinusoidal carrier introduces drift-like motion and changing its amplitude increases luminance contrast. Furthermore, it has been proposed that the spatial profile of Gabor stimuli represents well the receptive field structure of simple cells in V1 (Field & Tolhurst, 1986). Because the mean luminance of a Gabor patch is equal to the background luminance, its brief presentation does not introduce abrupt global luminance changes thereby minimizing retinal persistence and afterimage effects.

4.1.4 Purpose of this study

Classical experiments involving retinotopy are constructed under the premise that fixation is accurately maintained. In contrast, during more complex event-related designs (Amaro & Barker, 2006) where subjects cannot be asked to constantly maintain fixation[3], the only way to retinotopically localize a certain presented stimulus is by combining recorded eye position information and very brief stimulus presentation times that ensure that the stimulus is presented during the very short fixation periods in between saccades, which are normally no longer than a few hundred milliseconds. Only if the retinal position is known, the encoding cortical location can be retinotopically determined. How short in time these stimuli can be, is the question we address in this study.

More specifically, we tested whether a luminance-defined stimulus presented for a duration of 8 ms[4] can elicit significant BOLD signal changes in V1. Our hypothesis is that this should be possible by using fine timing, a jittered parametric event-related design (Amaro & Barker, 2006), and across trial averaging on signals extracted from previously localized ROIs.

4.2 Methods

4.2.1 Subjects

Five previously trained subjects (3 male, age 23-28) with normal vision participated in the experiment. They were selected from a larger group based on their excellent oculomotor performance. The experimental protocol was designed and implemented in accordance with the ethical standards of the 1964 Declaration of Helsinki (Rickham, 1964). Subjects participated in several training session and four fMRI measurements and received a monetary compensation after successful completion of all sessions.

[3] Such as during the free viewing of natural scenes or in eye movement experiments.
[4] Which is the shortest duration that a stimulus can be presented by using high performance D-ILA projectors.

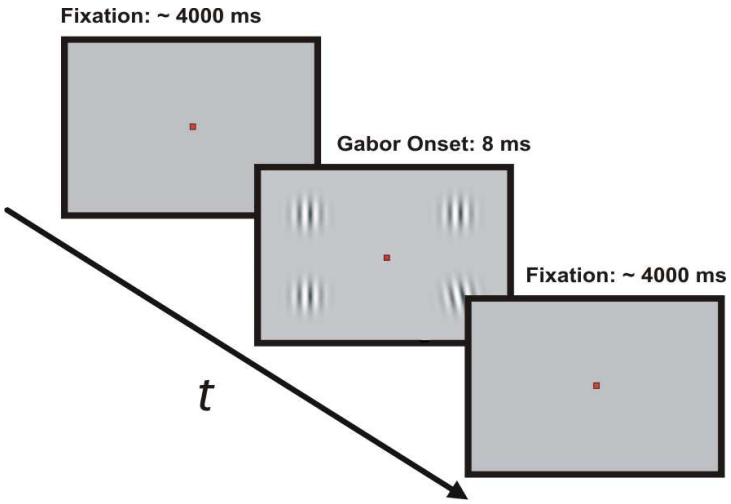

Figure 4.2: On each trial, subjects had to mantain fixation on a central dot and discriminate the orientation of four Gabor stimuli presented during 8 ms. The ISI was randomly varied to increase the sampling resolution.

4.2.2 Stimulation and task

Subjects performed an orientation discrimination task where four Gabors (spatial frequency = 1 cycle/°, luminance contrast = 100%, perceived size = 5° of visual angle) presented extrafoveally at ±10 and ±5° of eccentricity from the vertical and horizontal meridian respectively, were simultaneously presented for 8 ms with a jittered ISI of about 8 s (Figure 4.2). The four Gabors were oriented either all vertically (90° of rotation) or all horizontally (0°), in some random trials only one of the four Gabors was slightly rotated away from the orientation axis of the other three (the direction of the rotation was also randomized, Figure 4.2). Subjects had to press a key indicating whether all the Gabors had the same orientation or not. Rotation values were individually set to yield a percentage correct level of 70% by using a standard staircase procedure. The difficulty level of the task was set relatively high to profit from BOLD signal increases triggered by attentional effects (Gandhi et al., 1999).

During the whole experiment, subjects were asked to maintain fixation on a red dot centered on a homogeneous gray background. Fixation was monitored by using a limbus reflection based MR compatible eye tracker (Cambridge Research Systems, Rochester, England). Visual stimulation was created on a VSG2/5 graphics board with frame con-

trol and independent CPU. Eye movement position was also sampled on-board at 1 kHz and stored along with stimulus onsets and MR triggers to ensure time accuracy. Software written in Delphi-Pascal was specially developed for this experiment to control the graphics CPU independently from the experimental computer, collect behavioral responses, digitalize and store eye movement data and control and record the triggering system. Stimulus presentation was rear-projected by a D-ILA G15U JVC projector (Victor company of Japan) at a spatial resolution of 1024×768 pixels running at native mode with a refresh rate of 78 Hz. While alternating single frame presentations, a photovoltaic cell designed for Cathode Ray Tube (CRT) calibration was used to measure delay, build up and decay times in image formation. These were found to be constant and were accounted for when calculating the onset times for the experimental design-matrix (Figures 5.3 and 4.4). Manual responses within the MR scanner were registered by using a Lumitouch optical response keypad (Photon Control, Burnaby, Canada), which is made entirely out of plastic and produces no interference with the imaging system.

4.2.3 Imaging methods

Imaging was performed on a 1.5 T Siemens Sonata Maestro, equipped with 40 mT/m gradients and an high resolution eight channel head coil (MRI devices). A localizer sequence consisting of seven sagittal images was used to carefully position 8 slices along the calcarine fissure with an effective isovoxel resolution of 3 mm. For each BOLD imaging session, 400 such volumes where acquired using a Maxwell-corrected EPI sequence (TR = 1.32 s, TE = 73 ms, flip angle = 90°, field of view = 190 mm).

In a previous scanning session, the exact retinotopic representation of each of the four Gabors, was determined by presenting one 8 Hz-flickering dartboard during 13.2 s (10 volumes) at each of the four positions where the Gabors were to be subsequently presented in a blocked fashion (Figure 4.3) alternating each position during 10 volumes (400 volumes in total). After retinotopically localizing the stimuli, each subject went through three of 400-volume sessions completing a total of ~ 210 trials on the orientation discrimination task. A high resolution (voxel size = 1 mm^3) MPRAGE sequence was used

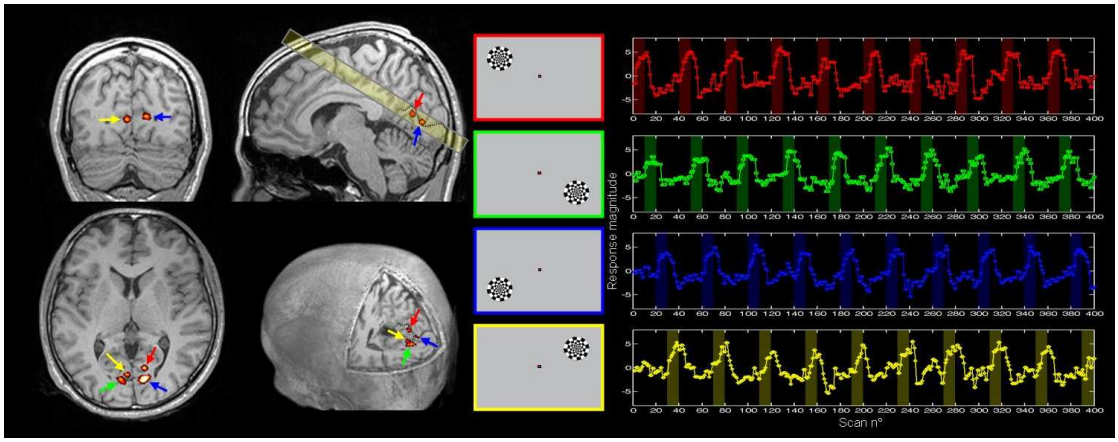

Figure 4.3: BOLD responses at the encoding locations of the four Gabor stimuli were retinotopically localized in primary visual cortex by using a flickering dartboard presented alternatively at each of the same four positions where the Gabor stimuli were later briefly presented. The acquisition volume was carefully positioned along the calcarine sulcus (depicted by the yellow rectangle). Each stimulus position (color coded) revealed its corresponding encoding cluster in V1 ($p_{\mathrm{corr}} < 0.0001$, $\mathrm{k} = 5$). On the left, MR signal changes extracted from the four resulting ROIs plotted against time (in scans). Statistical analysis of BOLD signals in the main experiment was restricted to time series obtained from these clusters.

to obtain an anatomical image from each subject.

Localized hemodynamic response was estimated by using a Bayesian estimation procedure implemented in SPM (Friston et al., 2002), but analysis performed with the resulting kernel did not improve results obtained by using the standard canonical HRF, probably due to signal temporal-overlapping effects. Functional images were preprocessed and analyzed using MATLAB and SPM2 (Section 1.7) running on a high-performance Linux workstation. Raw time series containing the BOLD information were high-pass filtered by removing low-frequency components modeled by a discrete cosine set (cutoff = 90 s), time corrected to the central slice, realigned to the first image and unwarped, to correct for movement-originated susceptibility artifacts. After being co-registered to the anatomical image, both were normalized to the MNI152 T_1 template (from the Montreal Institute of Neurology). Finally, the functional data were smoothed by using a Gaussian kernel with a FWHM of 4 mm. For the statistical analysis, the General Linear Model was used to estimate the parameters of a predictor constructed by convolving the stimulus onset vector with a canonical HRF (Section 1.7) and its corresponding temporal and dispersion derivatives. After localizing the encoding locations of the four Gabors (Figure 4.3), their activation clusters were defined as regions of interest by using the MARSBAR toolbox (http://marsbar.source.net/, Brett et al., 2002) and Region Of Interest (ROI) analysis was performed only on the averaged signals extracted from those clusters during the part of the experiment in which only Gabors were briefly presented.

4.3 Results

One single run of flickering dartboard presentations proved to be an extremely efficient method to accurately localize the areas in visual cortex where Gabors were to be subsequently encoded, as seen in the left peri-stimulus time histogram of Figure 4.6. Clusters used for the region of interest time-course extraction were thresholded to significance levels above $p = 0.0001$ and cluster sizes bigger that 10 voxels. As a result, in four of the five subjects, one cluster was successfully localized for each of the quadrant positions (Figure

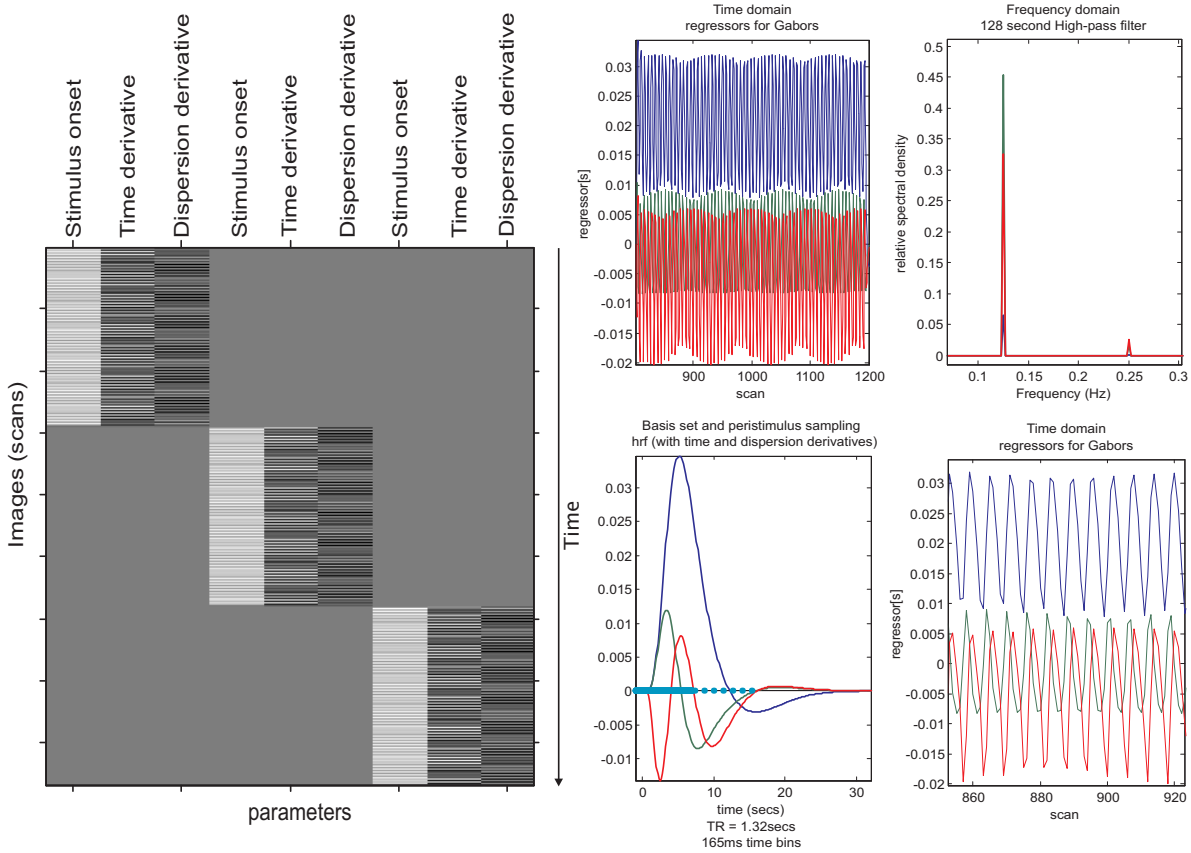

Figure 4.4: fMRI event-related design. Each subject underwent three measurements (left panel) in which BOLD signal changes were recorded for a total of $\sim$ 210 events (four Gabor patches presented simultaneously during 8 ms). Signals extracted from the corresponding encoding clusters in V1 were tested against a regressor that was built on the basis of a canonical hemodynamic response function and its corresponding time and dispersion derivatives (right panel, upper-left plot. HR in blue, derivatives in green an red). A closer inspection of this resulting regressor (right panel, lower-right plot) shows how signal peaks from single events can be safely characterized with inter-stimulus intervals of about 8 s (jittered by a random fraction of TR). Accordingly, on the upper right plot, a discrete fourier transformation of the regression vectors reveals a spectral density peak around 0.12 Hz, reflecting the event frequency.

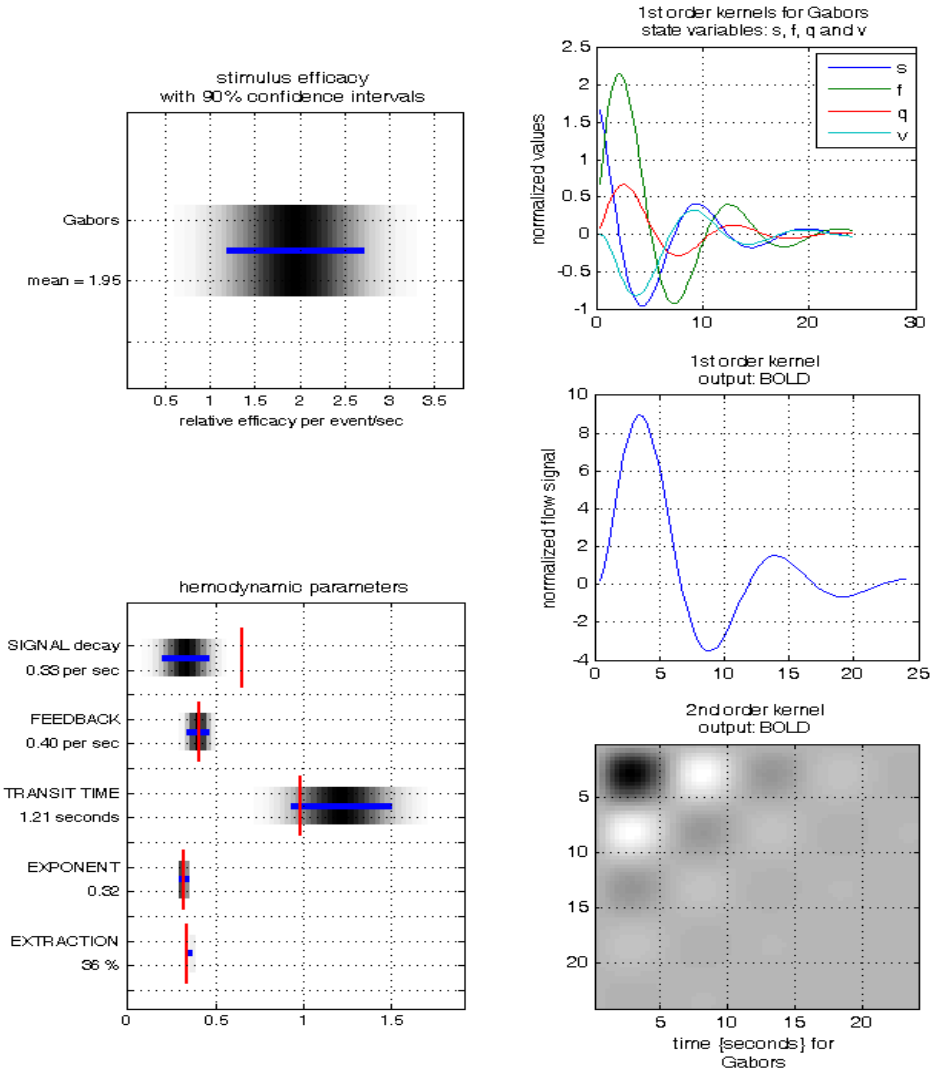

Figure 4.5: BOLD response was estimated by using a Bayesian estimation procedure implemented in SPM (Friston et al., 2002). The top right panel shows the first-order kernels for the state variables (s, signal; f, inflow; q, deoxyhemoglobin content; v, volume). The bottom right panel shows the resulting first- and second-order output kernels for the BOLD response. The left panels show the conditional or posterior distributions. Stimulus efficacy is plotted on the top-left graph and the five biophysical parameters in the bottom-left panel, where gray shading represents the probability density, and the bars the 90% confidence intervals.

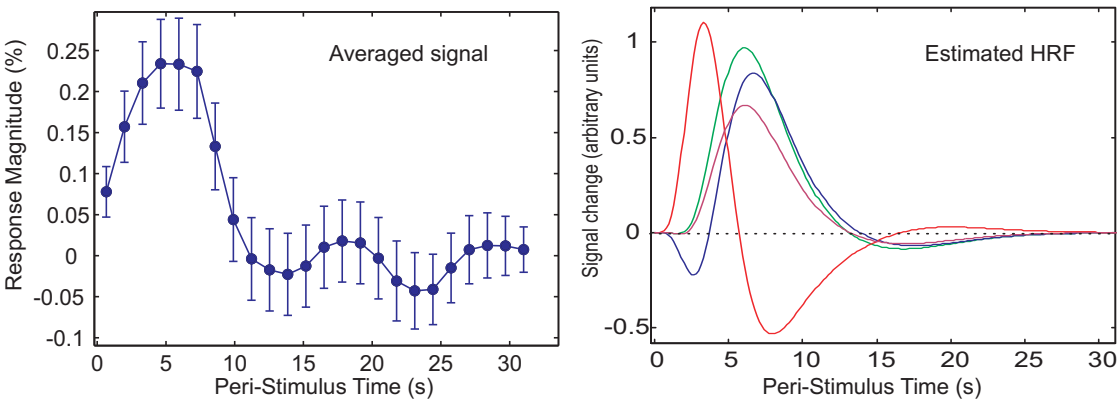

Figure 4.6: After retinotopically localizing the Gabors, three fMRI sessions were conducted to confirm the detectability of such short stimuli in V1 (blue). During these sessions, Gabors were repeatedly presented for 8 ms at intervals of about 8 s ($\pm$ a random fraction of TR) while maintaining fixation. Depicted to the left is an event related peristimulus-time histogram obtained from one subject by averaging the event-locked time-series extracted from the four regions of interest. It can be appreciated how BOLD signal significantly increases when the Gabors were presented (bars represent the standard error). Plotted on the right are the fitted HRFs to the averaged time series extracted from the ROIS for the four subjects after the parameter estimation (each colour represents one subject). The introduction of the time and dispersion derivatives can be observed as a strong deviation from the shape of the canonical HRF and the different peak times, adapting to individual local hemodynamics.

4.3). Presenting the four Gabors for only 8 ms was sufficient to trigger measurable BOLD responses in each of the three runs for the four data sets that could be analyzed (Figure 4.6 right, Table 4.1). For one subject, we failed to precisely localize the encoding clusters in V1. this subject was, therefore, excluded from the analysis. Each of these data sets contained over 200 events, and consistent and significant changes in MR signal occurred time-locked to the onset of the stimulus at the previously retinotopically localized regions of interest (Figure 4.3).

Table 4.1: Retinotopically-localized clusters encoding the Gabor stimuli.

	S1				**S2**				**S3**				**S4**			
	x	y	z	$F_{(1,1158)}$	x	y	z	$F_{(1,1158)}$	x	y	z	$F_{(1,1158)}$	x	y	z	$F_{(1,1158)}$
Lower left Gabor	6	-84	8	43.67	8	-88	0	22.69	12	-80	6	21.55	10	-84	4	64.33
Upper left Gabor	16	-70	14	57.23	4	-76	-6	12.33	14	-74	8	11.65	4	-78	4	64.62
Lower right Gabor	-10	-82	12	48.97	-8	-90	4	19.92	-6	-82	2	35.17	-18	-78	6	76.24
Upper right Gabor	-10	-70	14	60.51	-6	-66	4	25.91	-2	-76	10	32.33	-10	-78	12	71.21

MNI coordinates for encoding clusters ($p < 0.001$).

4.4 Discussion

In this experiment we demonstrate that it is possible to measure BOLD changes produced by a visual stimulus presented for a period as short as 8 ms, which is the shortest achievable onset duration with today's D-ILA projector technology, widely used in experimental fMRI setups. Gabor stimuli were chosen for this experiment because they are thought to be the stimuli that best match the receptive fields in V1 and their properties (mean luminance equal to background luminance and lack of edges) minimize afterimage effects and retinal persistence during brief presentations while maintaining maximal contrast (Section 4.1.3). Gabor's relatively low spatial frequency and its extrafoveal arrangement were intended to engage mostly the much faster magnocellular pathway (Schiller, Logothetis & Charles, 1990), which is extremely sensitive to the onset of a stimulus. Orthogonal Gabor base orientations were chosen based on the work of Furmansky and Engel (2000), who showed how vertical and horizontal gratings elicit stronger V1 responses than oblique orientations, while their magnitudes remain equivalent. The discrimination task was introduced in order to ensure that subjects were transiently attending to the stimuli,

which has been shown to increase the amplitude of BOLD responses in V1 (Liu, Pestilli & Carrasco, 2005).

Time resolution in fMRI is mostly determined by MR physics (spin relaxation times) and hemodynamic delays, nevertheless, shorter stimulation onsets are crucial to be able to successfully assign input (stimulation) to output (MR signal) in order to establish a relation between both. BOLD changes associated to very short stimuli are of a much smaller magnitude than those produced by longer stimulation periods and can easily get lost in noise. On the other hand, smaller magnitude BOLD changes have shorter decay times and can be therefore better segregated from other events. By averaging the hemodynamic responses from many trials, the functional signal-to-noise ratio of fMRI data can be significantly increased. As the number of trials in the sample increases, the precision with which the mean of a sample can be estimated increases with the square root of the number of trials (Huettel & McCarthy, 2001). Huettel and McCarthy (2001) have studied the variability of BOLD responses depending on the number of averaged events showing that between 25 and 36 trials are required to be able to accurately estimate response amplitude from signals extracted from previously identified regions. In our experiment, despite of the extremely short duration and special characteristics of the stimulus used, single runs consisting of ~ 70 events were sufficient to reach signal changes with high statistical significant levels ($p < 0.0001$), and the amplitude of the signal was stable across the three intrasubject sessions.

Three important methodological aspects underlie the successful measurement of these stimuli. First, the use of a calibrated projection system without frame-skipping behavior, together with a VSG card that is able to achieve real-time stimulus presentation, provides the required temporal precision to generate accurate onset vectors for the regression analysis. Second, a great portion of the noise inherent to the MR signal is eliminated by averaging across trials (events) and across voxels within the retinotopically localized clusters. For this purpose, accurate fixation control is required, because the location of the encoding clusters in V1 is fully determined by the position of the stimuli on the retina that, in turn, depends on the position of the eyes. The third important aspect is the use

of multichannel MR high-resolution head-coils, which are arranged as surface receivers and increase the SNR while using parallel imaging techniques to accelerate the acquisition of functional data to measure, as in our experiment, over 32000 voxels at different brain locations per second. This yields, for our TR value of 1.32 s, an effective sampling resolution of 0.76 Hz and increases the accuracy of the HRF parameter estimation.

Being able to detect extremely short stimuli of this kind provides the ground for a multitude of new fMRI paradigms, as the one that constitutes the last study of this dissertation work (Chapter 5). In free viewing conditions, for example, our eyes scan a scene as sequences of short fixations that rarely exceed a couple of hundred milliseconds. It is only during these short times when objects in the visual field can be uniquely assigned to retinotopic locations on the visual cortex. Brief changes in any of these objects during fixational periods can be relevant enough to attract attentional resources and trigger the execution of a new saccade for further foveal exploration. Investigating the cortical processing of these brief changes can help us understand the functioning of spatial visual attention that guides the oculomotor system. Finally, proving that these brief stimuli can be measured with fMRI has great methodological relevance, as the temporal scale of the phenomena that can be approached with any method depends on its ability to measure signals at that same temporal scale.

5 Saccadic Suppression of retinotopically localized stimuli in V1

Summary

Saccadic eye movements are responsible for bringing relevant parts of the visual field onto the fovea for detailed analysis. Since the retina is physiologically unable to deliver sharp images at very high transsaccadic speeds, the visual system minimizes the repercussion of the blurry images we would otherwise perceive during transsaccadic vision by reducing general visual sensitivity and increasing the detection threshold for visual stimuli. Ruling out a pure retinal origin, the effects of saccadic suppression can already be observed some 75 ms before the onset of a saccadic eye movement and are maximal at the onset of motion. The perception of a briefly presented stimulus immediately before the onset of any retinal motion is thus impaired despite the fact that this stimulus is projected onto the stationary retina and is, therefore, physically identical to that presented when no saccadic programming is in course. In this fMRI event-related study, we flashed Gabor patches at different times before the onset of a horizontal saccade and measured BOLD responses at their encoding regions in primary visual cortex (V1) while subjects judged the relative orientation of the stimuli. Closely matching the significant reduction in behavioral performance, the amplitude of the responses in V1 consistently decreased as the stimuli were presented closer to the saccadic onset. These results demonstrate that the neural processes underlying saccade programming transiently modulate cortical responses to briefly presented visual stimuli in areas as early as V1, providing further evidence for the existence of an active saccadic suppression mechanism in humans.

5.1 Introduction

A mirror can be used to conduct a very simple experiment: we cannot see our own eye movements even though they can be seen by other people. An average person makes 3 to 4 saccadic eye movements per second, blurring vision each time for about 30 ms (depending on the amplitude of the movement). Considering a 16-hour waking day, it has been estimated that this blurred vision sums up to about 90 min (Irwing & Carlson-Radvansky, 1996). Apart from that, another striking fact goes unnoticed during our visually active life: we make an average of 12-15 spontaneous blinks every minute, blocking the pupil for some 40-200 ms (Volkmann, Riggs & Moore, 1980). In a normal day, this amounts to somewhere between 10-40 min. Ignoring other sources of distortion, people spend roughly two hours each day effectively blind (Skoyles, 1997).

These observations suggest that vision must involve a close interplay between sensory and oculomotor control systems in the brain in order to integrate the sensory information obtained during a series of sequential fixations while discarding signals delivered during retinal motion and blinks. Visuospatial attention and saccadic eye movements work together to bring relevant parts of the visual scene onto the dense mosaic of photoreceptors located on the fovea for fine scrutiny. Many different perceptual distortions are associated to saccadic activity, from space compression in the direction of movement (Ross, Morrone & Burr, 1997) and stimuli mislocalization (Honda, 1989), to compression of perceived time between two saccades (Morrone, Ross & Burr, 2005). As mentioned at the beginning of this dissertation, saccades are characterized by very high peak velocities that are proportional to the amplitude of the movement. At these very high speeds, a static image projected on the retina shifts very quickly over the receptors hindering sharp signal transduction. The visual system seems to inhibit visual perception during these periods to eliminate disturbing blurs between fixations by means of a mechanism known as saccadic suppression.

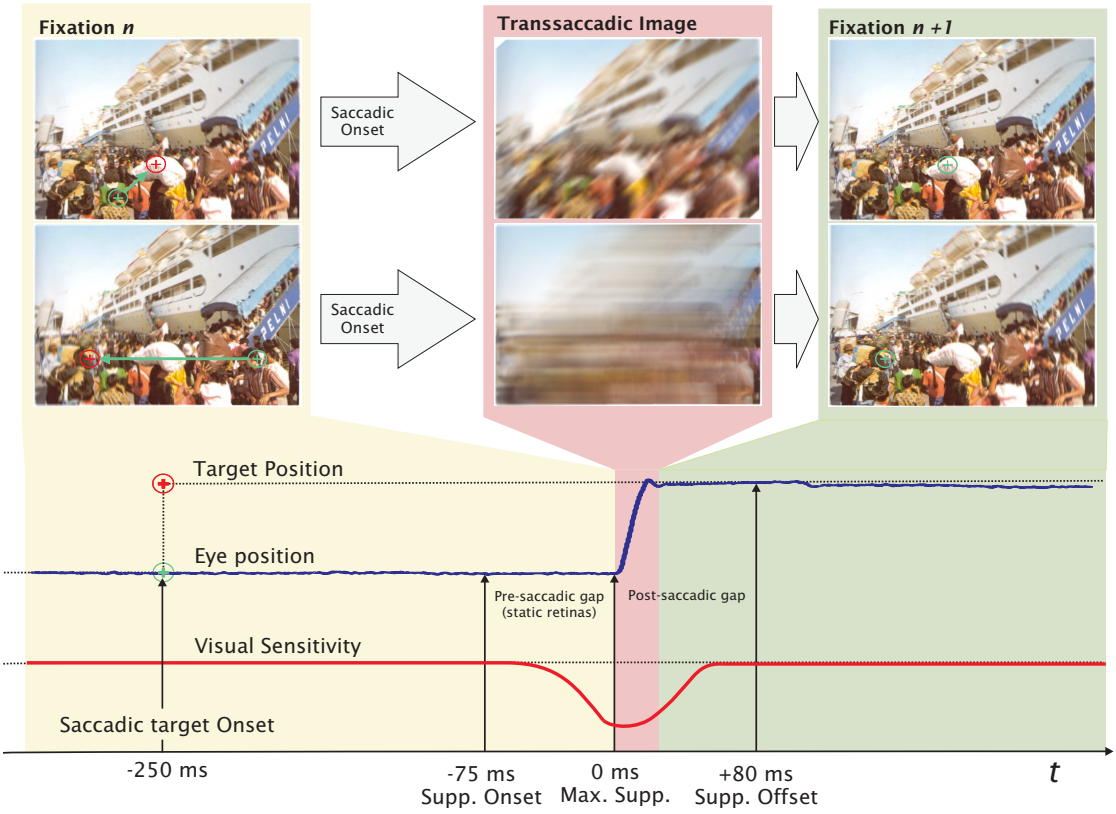

Figure 5.1: On the top-row pictures, two examples of a small (upper row) and a large (lower row) saccades are illustrated. During a fixation period n (yellow block) the part of the visual space falling on the retina (green cross) is explored while a new target from the scene is selected for detail exploration (red cross). During the saccade, the retina moves very fast at a velocity that is proportional to the amplitude of the movement (cyan block), before the new target is brought to the fovea (green block). Saccadic suppression eliminates the blurry images we would otherwise perceive during fast saccades. On the lower part of the figure, the time course of saccadic suppression is schematically presented. A decrease in visual sensitivity (plotted in red) can be measured approximately 75 ms before the onset of an eye movement (plotted in blue), is maximal at motion onset and outlasts the offset of the saccade by about 50 ms.

5.1.1 Evidence for an active suppression mechanism

The mere existence of an active saccadic suppression mechanism and its putative extraretinal origin has been the subject of intense debate (Castet, Jeanjean & Masson, 2001; Garcia-Perez & Peli, 2001; Ross, Morrone, Goldberg & Burr, 2001). Most of the disagreement lies on whether the perceptual impairment occurring around the time of saccades is triggered by an active suppression mechanism or just an epiphenomenon produced by a combination of mechanical shearing forces of the eyeball movement and the low-pass frequency characteristic that filters out fast temporal oscillations in the mammal's visual system. Although an image moving within the range of speeds for saccades but with a stable eye might also contribute to such inhibitory effect due to metacontrast masking (MacKay, 1970; Matin, Clymer & Matin, 1972), this seems to be ruled out by other studies, suggesting the existence of a central inhibitory system. Riggs and colleagues (1974) demonstrated suppression of electrically elicited phosphenes produced during saccades executed in total darkness, and some years later Burr and colleagues (1994) demonstrated that extrafoveally presented low spatial-frequency luminance-defined stimuli are selectively affected by saccadic suppression compared to isoluminant chromatically defined stimuli. Their results imply that saccadic suppression actively suppresses the fast magnocelullar pathway while the sensitivity of the much slower parvocellular system remains unaffected.

5.1.2 Previous studies of saccadic suppression

While previous imaging studies have reported a decrease of activity in primary visual cortex related to saccade frequency (Paus et al., 1995; Wenzel et al., 2000), first attempts to study saccadic suppression by including oculomotor measurements during event-related fMRI failed to make effective use of saccade timing with respect to signal changes exhibited during the perisaccadic period (Kleiser, Seitz & Krekelberg, 2004). Recent work (Thilo, Santoro, Walsh & Blakemore, 2004) has shown how saccades impair the perception of phosphenes elicited at the retinal level, but not of those elicited directly at the occipital cortex, suggesting that retinal signals are suppressed prior to arriving at the visual cortex.

Classical psychophysical research has shown that saccadic suppression provokes a decrease in sensitivity that begins approximately 75 ms before the onset of the actual eye movement, is maximal at motion onset and outlasts the saccadic offset by about 50 ms (Diamond, Ross & Morrone, 2000; Latour, 1962; Riggs, Volkmann, Moore & Ellicott, 1982; Volkmann, Schick & Riggs, 1968; Zuber & Stark, 1966). The perception of a briefly presented stimulus during this pre-saccadic interval (Figures 5.1 and 5.4) is impaired despite the fact that it is projected onto the stationary retina, and its proximal stimulus is therefore identical to the one produced by the same stimulus when no saccadic programming is in course. Right until the moment in which the eyes start to move, retinotopic correspondence is maintained and the encoding location of the visual stimulus can be accurately localized in primary visual cortex (area V1) (DeYoe et al., 1996; Engel et al., 1997; Tootell et al., 1998).

5.1.3 Purpose of this study

In this study, we measured Blood Oxygen Level Dependent (BOLD) responses to four retinotopically localized (Figures 4.3 and 5.2) low spatial-frequency Gabor stimuli. The stimuli were flashed for 8 ms at variable times immediately before the onset of a horizontal eye movement to a visual target. Eye movements were recorded using a limbus-reflection based MR-compatible eye tracker, and an on-line algorithm was used to detect the onset of the saccadic eye movements and to predict the optimal onset-time for the Gabors based on the latency distribution obtained from previous trials during the ongoing fMRI measurements. This procedure significantly increased the probability of successfully presenting the stimuli immediately before the onset of a saccadic eye movement: the precise moment in which both retinas are stationary, the encoding location of the stimuli in V1 is known, and saccadic suppression is thought to be maximal (Figure 5.4, left). If saccadic suppression acts before signals coming from the retina reach primary visual cortex, we would expect BOLD responses elicited by these stimuli to be modulated by the proximity to the saccadic onset, the same way performance drops in detection and discrimination tasks (Latour, 1962; Zuber & Stark, 1966; Volkmann et al., 1968; Riggs et al., 1974; Diamond et al., 2000).

5.2 Methods: Psychophysics part

Before attempting to implement the experimental design in an MR environment, 12 subjects went through intensive psychophysical testing (six sessions each, amounting to $\sim$ 6000 trials in total) during which the stimulus parameters were tuned to maximize the behavioral effect, orientation discrimination thresholds were obtained and the spatial arrangement of the stimulation was optimized. For this purpose, a 24 inch Sony FW900 FD CRT monitor running at 100 Hz and IRIS limbus tracker (Skalar Medical, Delft The Netherlands) were used. Otherwise, the task, angular distances, and the software and hardware implementation were identical to what is described in the following section. In the first two sessions, psychometric functions for the orientation discrimination task were obtained for each subject by using a standard constant stimulus procedure with a rotation value of 1, 2, 3, 6, 12, 24 or 48°. In order to avoid floor and ceiling effects, rotation values delivering correct responses in 90% of the trials were used in the main experiment (described below) .

5.3 Methods: Imaging part

5.3.1 Subjects

Each of the four right-handed naive participants (three male, age range: 23-26 years) gave informed consent and participated in two training sessions outside of the MRI scanner, during which they became acquainted with the task, the eye movement quality was assessed and a psychometric function for the orientation discrimination was acquired. Subjects were chosen based on excellent oculomotor performance and a few other parameters as described in Section 1.6. During the first fMRI session, four measurements were performed to retinotopically localize the encoding location of the four Gabors in V1, and to ensure the detectability of changes in BOLD signal elicited by briefly flashed (8 ms) Gabor stimuli (same as in previous study, Figure 4.6). For the main experiment, in order to obtain a sufficient number of events for the analysis, 12 fMRI measurements distributed over several scanning sessions were conducted for each subject. The experi-

Table 5.1: Normalized MNI coordinates of the clusters encoding the Gabor stimuli for each participant (see Figure 5.2).

	BE			**MU**			**MK**			**MT**		
	x	y	z	x	y	z	x	y	z	x	y	z
Upper left Gabor	8	-88	0	12	-80	6	8	-88	14	10	-84	4
Upper right Gabor	4	-76	-6	12	-70	6	4	-82	8	6	-76	2
Lower left Gabor	-8	-90	4	-6	-82	4	-8	-94	4	-16	-80	8
Lower Right Gabor	-6	-66	4	-4	-76	6	-4	-78	6	-6	-74	12

mental protocol was designed and implemented in accordance with the ethical standards of the 1964 Declaration of Helsinki (Rickham, 1964) and subjects received a monetary compensation after successful completion of all sessions.

5.3.2 Retinotopic localization of the stimuli in V1

Brain clusters encoding the Gabor stimuli used in this experiment were retinotopically localized by presenting one flickering dartboard (as in Secction 4.1.3: 6° of visual angle in size, maximum contrast, 8 Hz flicker rate; Figure 5.2) in each of the four locations where Gabors were subsequently presented in the main experiment. Each single position was presented ten times for a period of 13.2 s (EPI sequence parameters and pre-processing identical as in the main experiment) in a block design such that alternating hemispheres were stimulated in the following order: upper-left, lower-right, lower-left and upper right (Figure 5.2).

The onset vector for each dartboard on each of the four positions was convolved with a canonical hemodynamic response function (HRF) to set up four regressors for the SPM analysis. T-test contrast vectors were defined for each regressor against all other three to detect voxels that significantly responded to one position but not the others. Clusters exceeding 5 voxels in size and with false discovery rate corrected p values smaller than 0.00001 ($T > 7$; $k > 5$) were defined as regions of interest (ROIs; Figure 5.2). Each subject completed three additional fMRI sessions in which the detectability of BOLD changes elicited by the 8 ms flashed Gabors (Figure 4.6) in the time series extracted from the localized ROIs was confirmed (Figure 5.2).

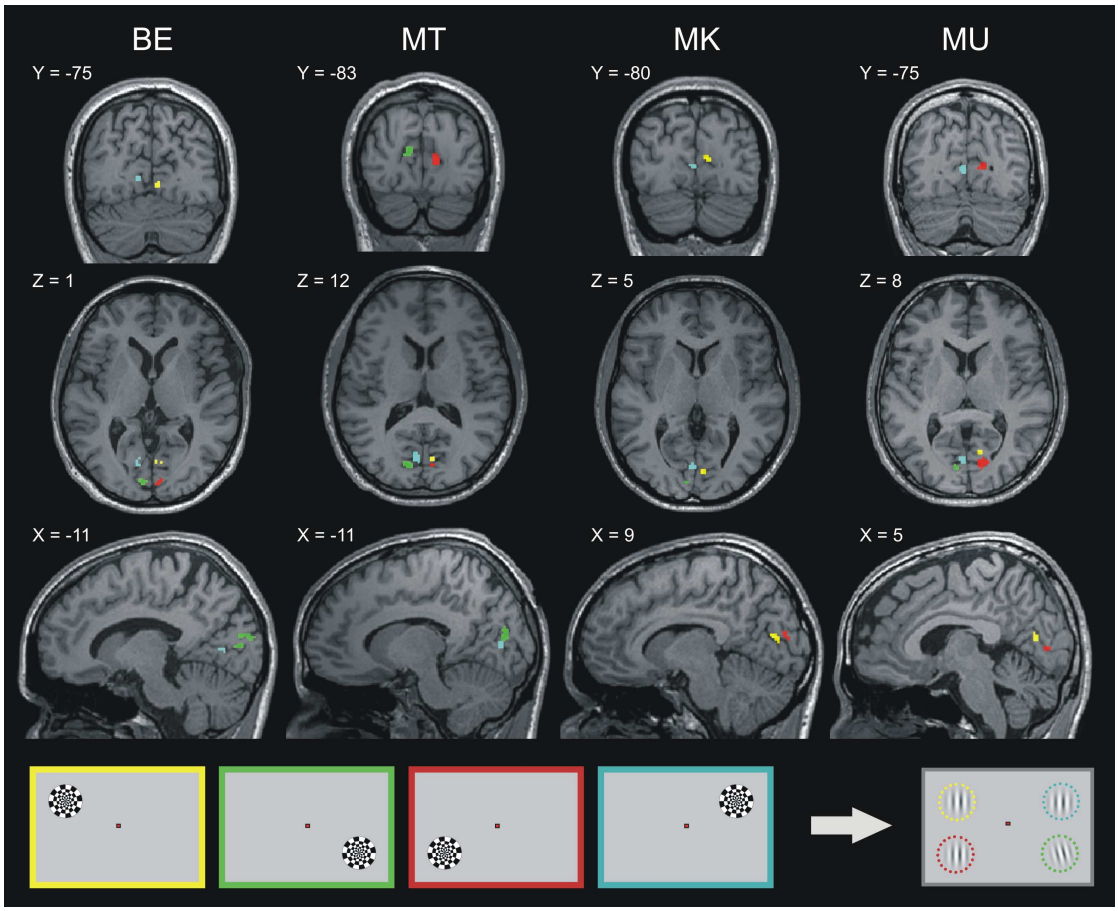

Figure 5.2: Clusters encoding the four Gabor stimuli in V1 were retinotopically localized for each subject (Section 5.3.2). These clusters were defined as regions of interest, restricting the analysis to signals extracted from their respective voxels. A very high threshold was used to eliminate activation in higher visual areas ($T > 7$; $p_{corr} > 0.0001$; $k > 5$). The labels indicate the corresponding MNI coordinate of each plane (see Table 5.1 for the exact cluster coordinates).

5.3.3 Stimuli and Procedure

In an event-related fMRI design, four experimental conditions were randomly interleaved: at variable inter-trial intervals of $\sim 9\,s$, subjects were trained either to maintain fixation (F, $\sim 10\%$ of the trials), to rapidly execute a saccadic eye movement to an eccentrically appearing target (S, $\sim 10\%$), to perform a suprathreshold orientation discrimination of four flashed Gabor stimuli while maintaining fixation (G, $\sim 10\%$), or to perform a saccade and discriminate the orientation of the flashed stimuli which were presented after the target onset but immediately before the saccadic onset (G+S, $\sim 70\%$; Figure 5.4, right). Button responses to the G+S trials resulted from two concurrent judgments: a detection task in which participants were requested to press one of two buttons to signal whether they detected the flashed Gabors (condition F and S were identical to G and G+S except in that no Gabors were presented), and an orientation discrimination task in which the presence of one slightly tilted Gabor among the four was reported by pressing the right button (oddball present), or left button (no oddball present). A small (0.2°) red dot was used as the saccadic target and was randomly presented along the horizontal meridian 10° to the left or to the right the fixation dot. Luminance-defined (maximum contrast) Gabor stimuli were 6° in diameter (full-width-half-maximum of the Gaussian envelope), had a spatial frequency of $1\,\text{cycle}/^\circ$ and were located in each of the four visual field quadrants 20° apart horizontally and 12° apart vertically. Retinal persistence was minimized by the edgeless structure of Gabor stimuli, whose mean luminance is identical to background luminance. Since horizontally and vertically oriented gratings have been shown to elicit equally strong BOLD responses in V1 (Furmanski & Engel, 2000), Gabor stimuli in conditions G and G+S were randomly presented with base orientations of either 0° or 90°. Orientation differences in the discrimination task were individually set during a previous session for each of the participants to reach accuracy levels of 80% in the G condition (90% in the psychophysics part, see Figure 5.6). Rotation values obtained for the different participants were randomly added or subtracted to the base orientation in the main experiment whenever a deviant Gabor was presented. Button responses within the MR scanner were registered by using a Lumitouch optical response keypad.

5.3.4 Eye movement recording and stimulus presentation

Visual stimulation was created on a VSG2/5 visual stimulus generator equipped with full frame control and a real-time dedicated CPU (Cambridge Research Systems, Rochester, England). Horizontal eye movements were recorded using a limbus-reflection based MR-compatible eye tracker (Cambridge Research Systems), digitized on-board at 1 kHz and stored along with stimulus onsets and MR triggers to ensure timing accuracy. Stimulus presentation was rear-projected through a waveguide by a gamma-corrected D-ILA G15U JVC projector (Victor Company of Japan, Yokohama, Japan) positioned outside the RF-shielded scanner room, at a spatial resolution of 1024×768 pixels and a non-interlaced refresh rate of 78 Hz. A fast photovoltaic transducer was used to measure onset-delay, build-up and decay times in image formation directly on the projection screen. With respect to the full width at half the maximum (FWHM) of the temporal luminance profile, we measured a constant effective-onset delay of 17 ms and a stimulus duration of 8 ms (Figure 5.3). These values were used to calculate Stimulus Onset Asynchronys (SOAs) by applying them to presentation times marked by digital triggers delivered by the Visual Stimulus Generator (VSG).

An on-line algorithm built into the presentation software was used to detected the onset of the saccadic eye movement immediately after the end of each trial by selectively back-reading the recorded eye traces and applying a simple amplitude-velocity thresholding procedure that was optimized for each measurement. A new distribution of the saccadic latencies from previous trials was created during each fixation period, and the optimal Gabor onset-time was obtained by taking the modal value of the current binned distribution minus half the duration of the pre-motoric saccadic suppression reported in the literature (75 ms). This method considerably improved the probability of the Gabor stimuli to be presented immediately before the onset of the saccadic eye movement (Figure 5.4, left bar plot). Only trials in which Gabors were presented immediately before the saccadic onset (in the absence of retinal motion) were included in the analysis. Stimulus presentation, eye tracker calibration and eye movement recordings, trigger management, button-response acquisition and the on-line saccadic detection algorithm used to predict

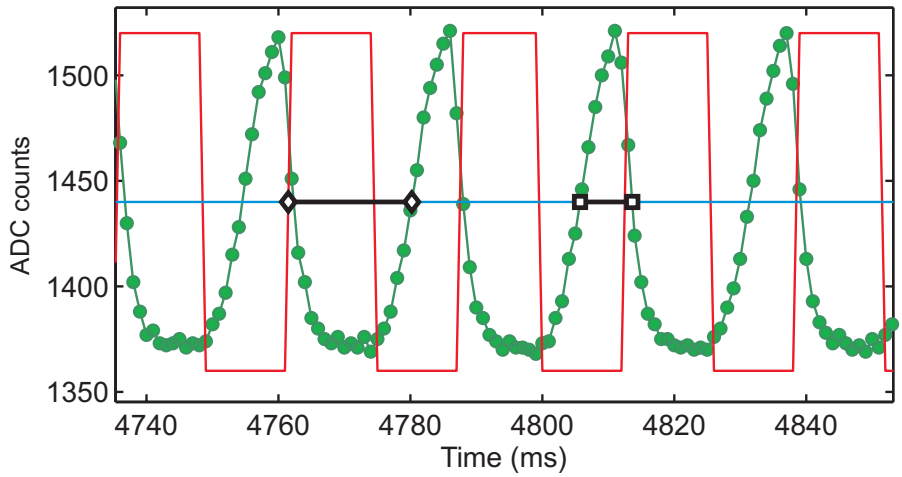

Figure 5.3: To account for presentation delays, we recorded the digital output of the stimulus generator (red) together with the actual projector's luminance output (green) measured on the screen with a fast photovoltaic cell. Image formation started systematically one frame after actual signal delivery. Discounting rise and decay times (taking the FWHM, in blue), we estimated an constant onset delay of 17 ms (diamond-flanked line) and an effective onset stimulus duration of 8 ms (square-flanked line). These values were used to precisely calculate SOAs and make sure stimuli included in the analysis were presented before the onset of the saccade (Figure 5.5).

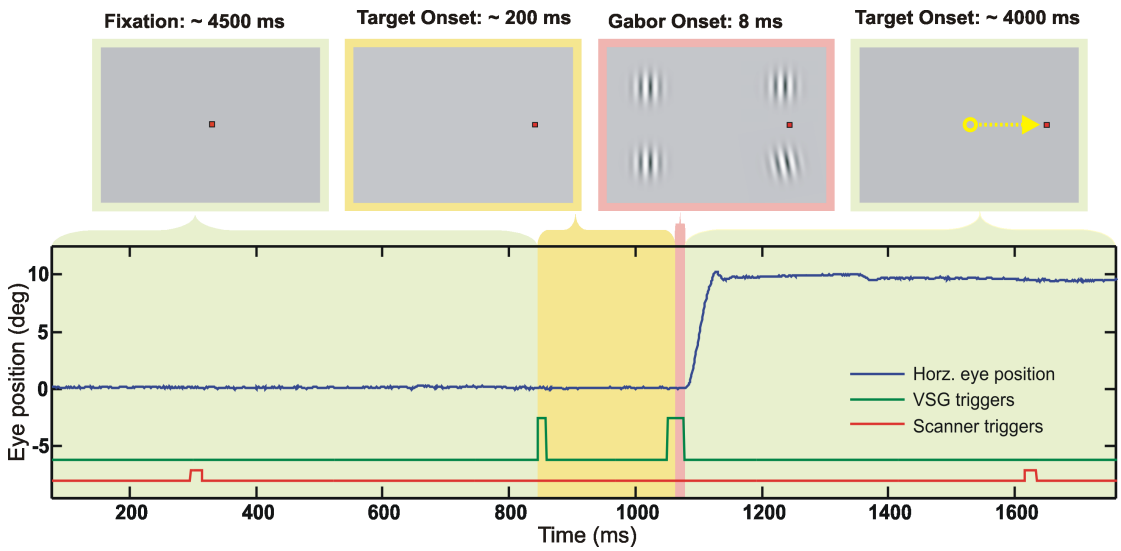

Figure 5.4: Schematic illustration of the time course of an individual trial for the condition GS (saccade and flashed Gabors). At the start of each trial the participants fixed their gaze on a central fixation dot. In a step procedure, the central fixation was extinguished and the saccadic target appeared on the periphery. Immediately prior to saccadic onset, four Gabor stimuli were simultaneously flashed. The lower left panel presents an actual eye-movement trace. Time marks designate triggers to the scanner acquisition onsets (red) and stimulus onset triggers coming from the visual stimulus generator (green), to which fixed image-formation delays were applied.

the stimulus onset were all implemented in software especially developed for this study (Section 1.6). The code was written in Delphi-Pascal by using the VSG v6 software library.

5.3.5 Imaging methods

Imaging was performed on a 1.5 T Siemens Sonata Maestro (Siemens Erlangen, Germany), equipped with 40 mT/m gradients and a high resolution eight-channel head coil (MRI Devices. Gainesville, Florida, USA). Before each measurement, a multi-slab localizer sequence with seven sagittal slices was used to carefully place 8 transversally oriented slices (voxel size = 3x3x3 mm, no gap) along the calcarine fissure of each subject. Each fMRI measurement consisted of 400 such volumes acquired with a Maxwell-corrected EPI sequence running integrated Paralell Acquisition technique (iPAT)[1] with TR = 1320 ms, TE = 77 ms, flip angle = 90°, field of view = 192 mm, matrix size = 64×64 bins, and interleaved acquisition. A high spatial resolution (with 1 mm^3 isotropic voxels) T_1 weighted MPRAGE scan was acquired after each scan session mainly for anatomical co-registration purposes.

5.3.6 Data Analysis

Saccadic onsets were re-calculated offline by using a set of scripts written in MATLAB (Mathworks Inc.) that contained a more sensitive algorithm that included information about the slope of the main sequence obtained from each run, as described by

$$peak\ velocity = V_{max}(1 - e^{-Amplitude/C})$$

where V_{max} is the asymptotic peak velocity and C is a constant. For purposes of quality control, all detected saccadic onsets from all trials were visually inspected by plotting them recursively over the trial period ranging from 100 ms before and after the detected onset point (Figure 5.5). Saccadic target and Gabor onset vectors were calculated from the Visual Stimulus Generator (VSG) digital channels by adding 17 ms to their raising

[1] A method for increasing the image acquisition speed by decreasing the number of phase-encoding imaging steps without reducing image resolution. This is achieved by using several receiver coils with different spatial sensitivity profiles whose signals are combined and reconstructed at a later stage.

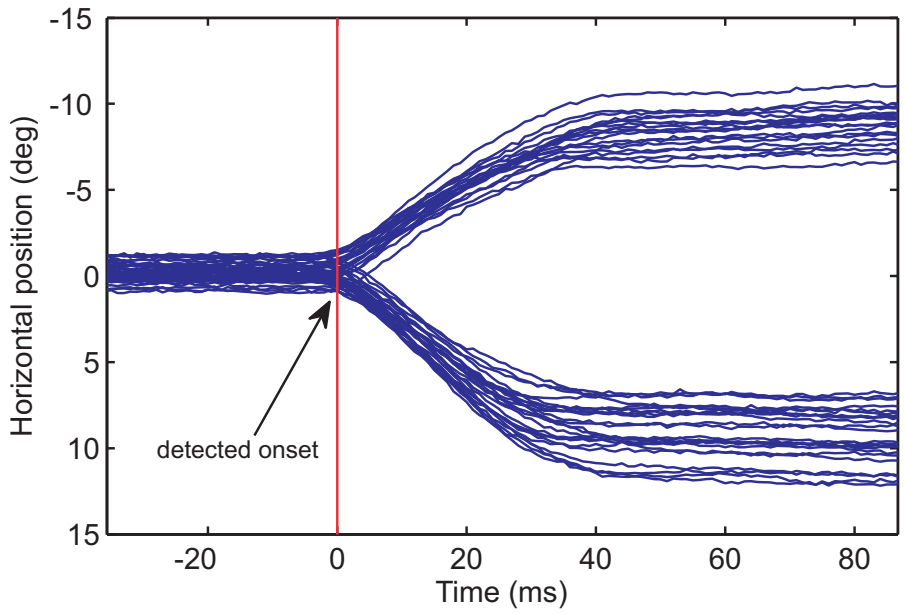

Figure 5.5: The efficacy of the detection algorithm was visually inspected by plotting the horizontal traces from all trials aligned to their automatically-detected saccadic onsets, as presenting the stimuli before the onset of the saccade is crucial for guaranteeing that their retinotopic correspondence is mantained.

edges to adjust for the delays introduced by the digital signal transformation within the projector. Gabor onset vector was shifted by 8 ms to account for their effective onset duration. Stimulus Onset Asynchrony (SOA) was then calculated by subtracting the saccadic onset from the corrected offset of the Gabor stimuli, so that in trials with negative SOAs the stimuli were always flashed before the onset of the eye movement. Only these presaccadic trials were included in the analysis (Figure 5.8, shaded area).

Functional images were time and motion corrected, unwarped, co-registered against a high resolution (1 mm^3 voxel-size) MPRAGE T_1 image, and normalized to a standard template from the Montreal Institute of Neurology (MNI152 T_1). Since regions of interest had been precisely localized for each subject, no Gaussian spatial smoothing was applied. Instead, voxel values extracted from the four clusters retinotopically encoding the Gabors were averaged into a single time course. Data analysis was computed on a high-performance Linux workstation at single subject level and based on the General Linear Model (GLM) as implemented in the statistical parametric mapping (Friston,

Frith et al., 1995; Friston, Holmes et al., 1995) package SPM2 (running under MATLAB, Section 1.7) and used by the region of interest toolbox (Brett et al., 2002) MARSBAR (http://marsbar.sourceforge.net/). Data were global-mean centered, high-pass filtered (cut-off: 0.0078 Hz) to remove slow signal drifts, and corrected for intrinsic serial auto-correlations. The four regressors introduced in the design were set up by convolving the onset vectors for Gabor-only condition (G), Saccade-only condition (S), G+S trials and return saccades with a canonical HRF together with their respective time and dispersion derivatives. In the G+S condition, SOAs were introduced as a non-linear parametric modulator to allow the amplitude of the hemodynamic response function fitted to the data to change as a function of the temporal distance between the presentation of the Gabors and the onset of the saccade. The influence of the parametric modulator was modeled by a second-order polynomial function, and a T-test was used to assess whether its introduction significantly explained additional variance. The significance of the variance explained by the G+S regressor modulated by SOA, relative to error (goodness of the regression) was estimated by using F statistics (Buchel, Wise, Mummery, Poline & Friston, 1996; Buchel, Holmes, Rees & Friston, 1998).

5.4 Results

5.4.1 Psychophysics data

The psychophysics sessions served to test the stimulation and assure a behavioral effect that could be matched to the changes in BOLD response elicited by the Gabor stimuli (Figure 4.6). Psychometric functions reflecting each subject's sensitivity to the presence of a deviant (oddball) Gabor yielded rotation values leading to 80% correct responses ranging between 6.6° and 13.7° for the different subjects (Mean = 9.78; SD = 3.37) (Figure 5.6). Modal values for the saccadic latencies ranged between 170 and 223 ms among the different subjects (global mean = 258, SD = 94). Reaction times obtained from the manual responses show a cumulated mean value of 798 ms (SD = 192 ms) and show a small but significant negative correlation with SOA (r = -0.09, $p < 0.0001$) (Figure 5.7,

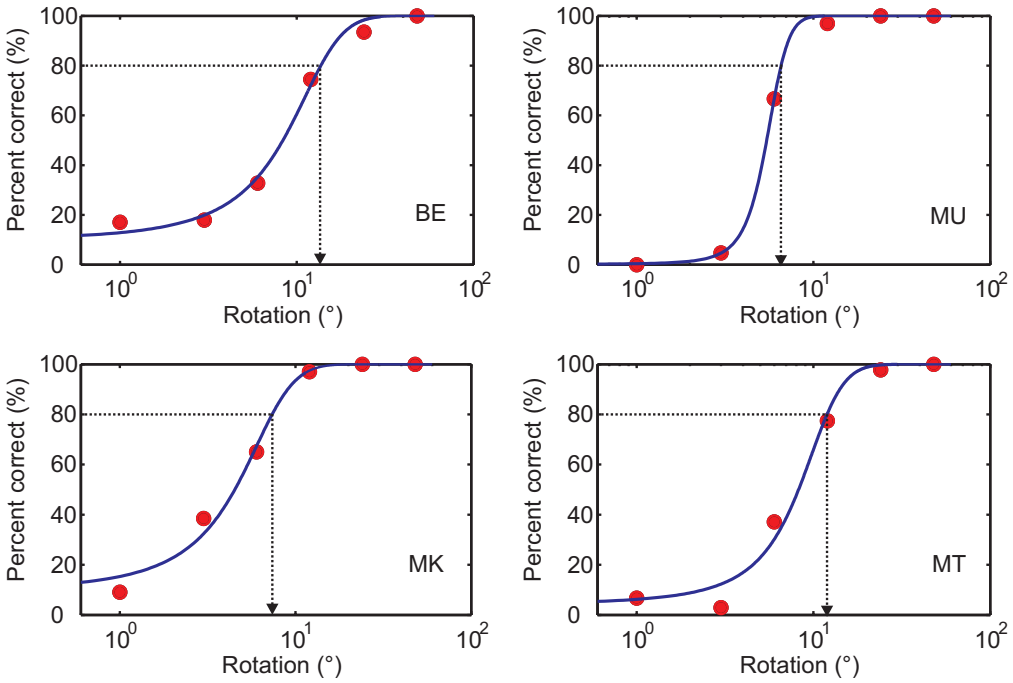

Figure 5.6: Psychometric function (sigmoidal function fitted to the data) for the orientation discrimination task were obtained for each subject by using a standard constant stimulus procedure with rotation values of 1, 2, 3, 6, 12, 24 and 48 degrees. Rotation values delivering correct responses in 80% of the trials were used in the main experiment to avoid floor and ceiling effects. Each graph shows the psychometric function for the orientation discrimination task for one subject.

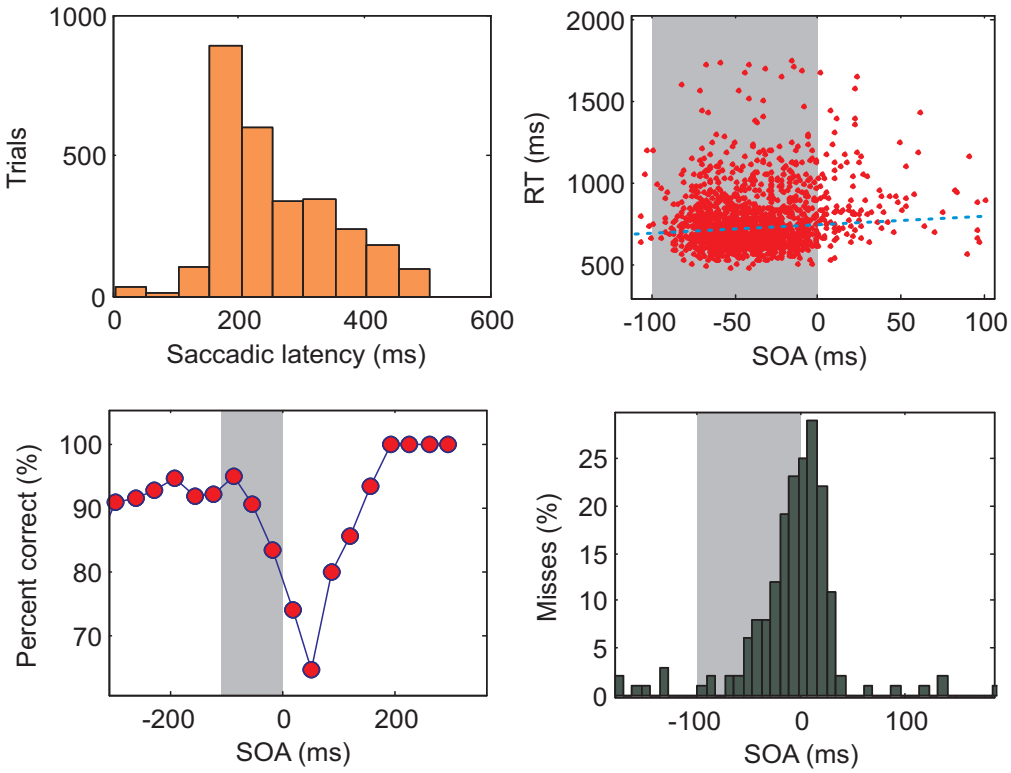

Figure 5.7: Pooled psychophysical results for all participants. On the upper left graph the distribution of the saccadic latencies from the onset of the target can be observed. Modal values for the single subjects ranged from 170 to 223 ms (cumulated mean = 258.63, sd = 94.17). On the right graph RTs (mean = 798, sd = 192) are plotted against SOA values, showing only a small but significant negative correlation (r = -0.09, $p < 0.001$). In the lower left graph, percentage correct in the orientation discrimination task is plotted against SOA. Performance rapidly decreases as the stimuli are presented closer to the saccadic onset, being significantly impaired even when presented immediately before actual movement begins, reaching values close to chance level when presented intrasacadically. On the lower left histogram, the amount of misses is plotted against SOA, showing that in up to 20% of the presaccadic trials, subjects did not detect the stimuli and accordingly, made no button response.

upper-right plot).

The on-line algorithm used proved its efficacy at presenting the Gabor with SOA values between -100 ms and 0 (immediately before the saccadic onset), as depicted in Figure 5.7 (upper right) where single-trial RTs are plotted against SOA values. Performance at the orientation discrimination tasks drops from 90% to about 70% before the eyes start to move, reaching 63% when stimuli are presented intrasaccadically (Figure 5.4, left plot). At the same time, and almost mirroring the performance drop, the amount of misses (trials in which stimuli were presented and no response was given) increases as the Gabors were presented closer to the saccadic onset, amounting to 20% of the GS presaccadic trials and up to 30% of the trials were the stimulation was presented intrasaccadically (Figure 5.7, lower-left plot).

5.4.2 Imaging data

By using the saccadic latency information collected from previous trials, 47.3% of the Gabor stimuli were presented immediately before the saccadic onset (Figure 5.8, bar plot) during the fMRI sessions. Behavioral data collected during the scanning sessions show that even before any retinal motion had begun, subjects failed to detect the stimuli on up to 30% of the trials in which Gabors were presented immediately before the saccadic onset (i.e. with short negative SOA, as can be seen in the right plot of Figure 5.8), mistaking a trial G+S for a trial S and therefore giving no button response. Performance in the orientation discrimination task for trials in which Gabor stimuli were detected immediately before the saccadic onset, dropped from 82% to around 65%, reaching chance levels (50%) when presented intrasaccadically (Figure 5.9, right plot). False alarms (defined by a button press on S trials) happened only rarely, in less that 1% of the trials. The time courses of the BOLD signals were extracted from the ROI in V1 and hemodynamic response functions (HRF) were fitted to the event-related data obtained from the flashed Gabor condition (G), and from the saccade only (S) condition (Figure 5.9, right plot). The combined condition (GS) triggered a BOLD response that approximately corresponds to the linear summation of the response amplitude elicited

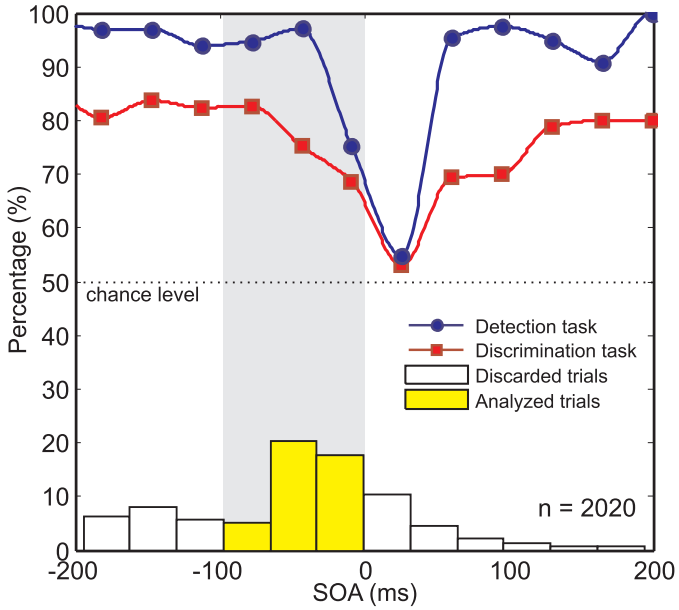

Figure 5.8: Behavioral cumulated data from all participants collected during the MR measurements are shown on the right plot. In the lower part (yellow) a histogram shows the percentage of the total number of GS trials (n = 2030) sorted according to their measured SOA, showing how, as a result of the adaptive algorithm used, most of the trials the Gabors were flashed during the pre-motoric time window prior to saccadic onset. Only trials in which Gabors were inmediately presented before the onset of the saccade were included in the analysis (shaded area). The red squares show performance in the orientation discrimination task. Percentage of trials in which subjects did not detect the presence of the Gabor stimuli is shown by the blue circles and indicates that on approximately 25% of the trials the Gabors were not perceived even though they were presented on a stationary retina, a sort of saccadic blindness.

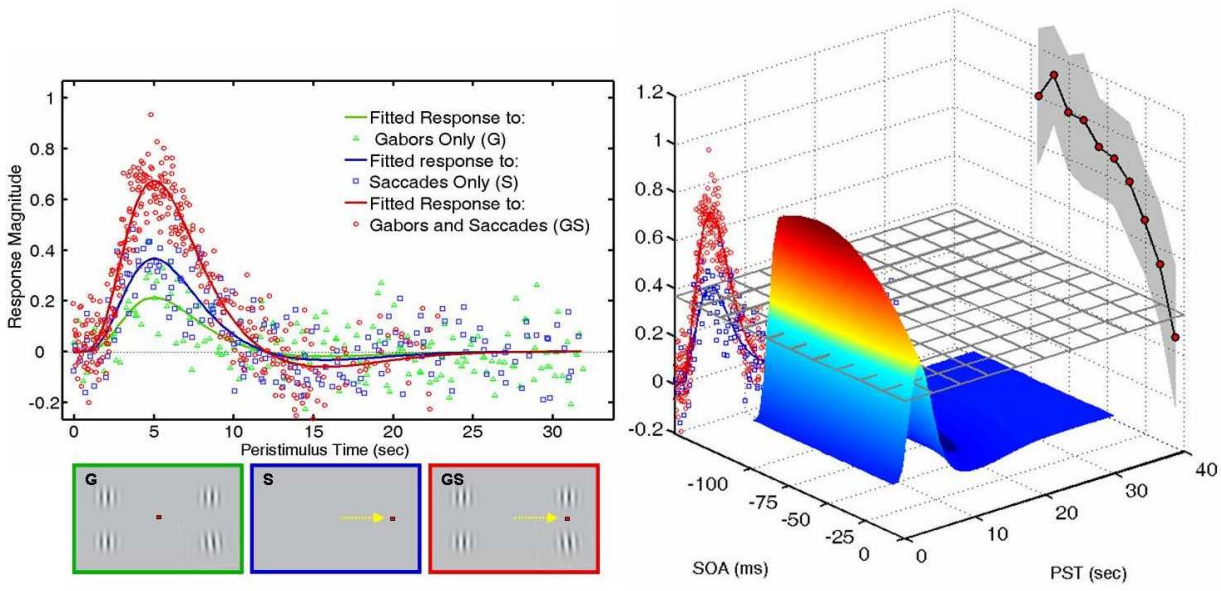

Figure 5.9: Depicted in the left plot is the BOLD response magnitude for the ROI as a function of peristimulus time, where zero corresponds to the event onset. The curves depict fitted HRFs to BOLD measurements from the Gabors-only condition (G, green triangles), the saccade-only condition (S, blue squares) and the Gabor-plus-saccade condition (GS, red circles). Icons under the x axis illustrate the respective conditions. The amplitude of responses in the GS condition roughly corresponds to the summation of the effects from the S and the G control conditions. Each data point depicts the average BOLD response for all voxels within the ROI for each acquired volume. Depicted on the right are the event-related BOLD responses to the GS condition (red) sorted along the z axis according to SOA. The amplitude of an otherwise constant hemodynamic response function is modulated by a 2^{nd}-order polynomial function to improve the fit to the data and estimate the effect of SOA (sorted along the z dimension). In the data from one measurement, it can be observed how the amplitude of the HRF fitted to trials with SOAs close to zero (red = hot colormap) drops to the level (gray grid) of trials in which only saccadic eye movements were performed (blue = cold colormap) indicating that only signals elicited by the Gabor stimuli are actively suppressed. The black line plots the average of all 12 runs for the same subject (MT), where the gray area depicts the standard deviation.

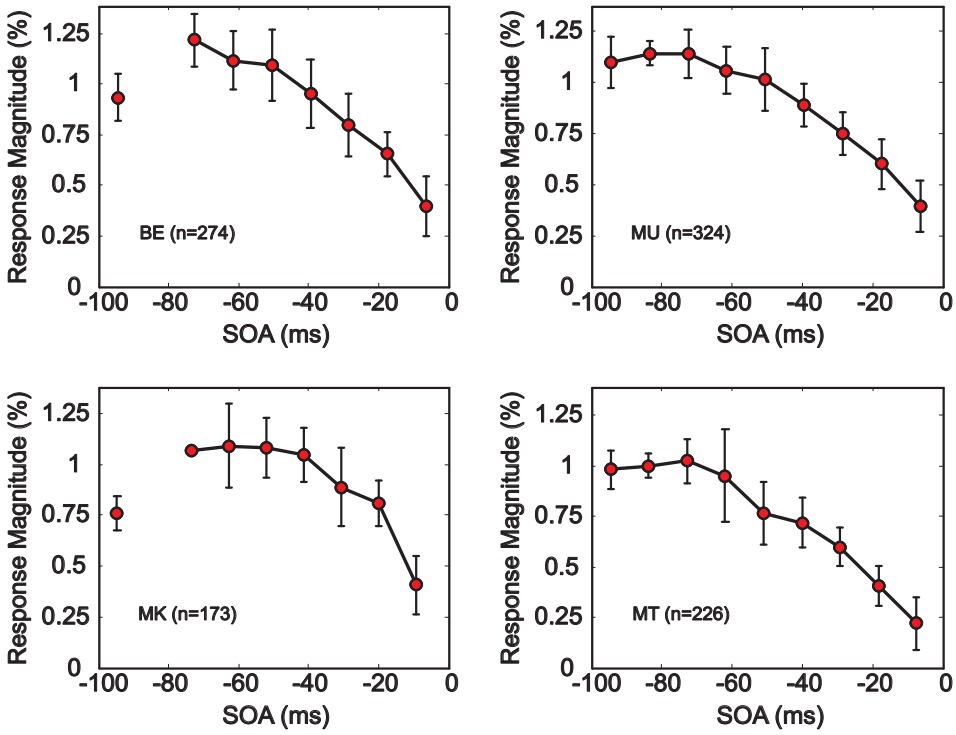

Figure 5.10: BOLD signal changes as a function of SOA for all four subjects obtained by averaging across the 12 measurements obtained for each participant. It can be easily appreciated how the decrease in BOLD signal parallels the decreases in performance observed in the behavioral results shown in Figures 5.7 and 5.8. Bars represent ±1 standard deviation.

by the G and S conditions. After sorting the events according to their SOA, and improving the fit by allowing the amplitude of the HRF to be modulated by a second order polynomial function, we found that response amplitude systematically decreased as the onset of the Gabor stimuli approached the onset of the saccade (Figure 5.9, right graph) reaching trial S levels at SOA values around zero. Comparison between Figure 5.8 and Figure 5.9 (right) shows how this decline in BOLD response matches the decline in detection/discrimination performance observed in the behavioral task, starting up to 75 ms before the onset of any retinal motion. The introduction of a parametric modulator and second-order polynomial expansion successfully explained additional variance in the BOLD signal extracted from the ROIs in all four subjects (subject BE: $T = 2.77$,

$p = 0.002$; subject MK: $T = 5.46$, $p < 0.0001$; subject MT: $T = 3.89$, $p < 0.0001$; subject MU: $T = 4.74$, $p < 0.0001$). BOLD responses elicited by the condition (G+S) on trials with very long SOAs, approximately correspond to the linear summation of the response amplitude elicited by the G and S conditions (Figure 5.9, left) and systematically decreased as the onset of the Gabor stimuli approached the onset of the saccade (Figure 5.10) (BE: $F = 8.61$, df 3,4440, $p < 0.001$; MK: $F = 21.14$, df 3,4440, $p < 0.0001$; MT: $F = 22.62$, df 3,4440, $p < 0.0001$; MU: $F = 28.09$, df 3,4440, $p < 0.0001$). Comparison between Figure 5.8 and the individual plots of Figure 5.10 shows how this decline in BOLD response parallels the decline in detection/discrimination performance observed in the behavioral task, starting up to 75 ms before the onset of any retinal motion.

5.5 Discussion

The behavioral data replicate a finding which is crucial for the interpretation of the imaging results: When presented immediately before the onset of the saccadic eye movement, Gabor stimuli are either not perceived at all, or perceived very poorly (5.8). It is important to emphasize that this impairment occurs in the absence of any retinal motion, implying that the retinotopic correspondence is maintained for all analyzed trials.

Due to the slow temporal dynamics of the BOLD response, it is not possible to segregate the amount of signal change elicited by the Gabor stimuli from the signal produced by the gray background slipping along the retina immediately following the saccadic onset. In order to quantify the contribution from each of these two signal sources, conditions S and G were introduced in the experimental design as sub-components of the G+S condition (S and G, as can be seen in the left plot of Figure 5.9) which can be considered as the sum of both. Worth noting is the fact that, despite the quantitatively smaller cortical responses measured in the G trials, subjects are able to make accurate decisions on the orientation of four spatially distant Gabors while larger responses triggered by saccadic motion on the S trials (Figure 5.9, blue HRF) are perceptually disregarded.

BOLD signals triggered by two stimuli occurring close in time have been shown to

interact in a non-linear fashion (Huettel & McCarthy, 2000), nevertheless, no refractory effect of this kind could be found with inter-stimulus intervals shorter than ∼100 ms, which is the latency of the evoked potential induced by the first of two pulsed stimuli (Ogawa et al., 2000). Thus, the decrease in BOLD signal observed in the encoding clusters when the Gabors were presented immediately before the onset of the saccadic eye movement are not likely to be related to some form of local non-linear summation. Rather, the close temporal correspondence between behavioral and imaging data (Figures 5.4 and 5.10) strongly suggests that the signal decline measured in the visual cortex is truly reflective of saccadic suppression. This decrease in the amplitude of the BOLD response could only have two origins: The first possibility is that feedback signals to V1 coming from higher visual or oculomotor cortical areas (e.g. signals from V4, V5 or the frontal eye fields) are centrally inhibited and that what we observe is actually a decrease in intracortical summation in V1 instead of an intrinsic decrease of V1 activity. These higher visual areas could interrupt feedback signals to V1 while oculomotor areas are engaged in the preparation of a saccade. Such an interruption of feedback processing could lead to a decline in conscious perception of the flashed stimuli, as evidenced by our psychophysical results (Figures 5.7 bottom-left, and 5.4). An alternative explanation could be that saccadic suppression originates at a subcortical level, before retinal signals reach V1. Although both alternatives could account for our results, many recent physiological data converge around the latter.

Animal research has shown that the transmission of an evoked potential, induced by stimulation of the optic chiasm, through the lateral geniculate nucleus (LGN) is reduced up to 60% during saccadic eye movements (Bartlett, Doty, Lee & Sakakura, 1976). In a similar experiment (Zhu & Lo, 1996), microelectrical stimulation of the superior colliculus consistently suppressed the evoked potential in the visual cortex by sending an inhibitory signal to the LGN. Reppas and colleagues (Reppas, Usrey & Reid, 2002) measured the firing behavior of primate LGN neurons at time points before, during and after horizontal saccades and observed a biphasic modulation of their firing rates, with a premotoric inhibition (approximately 50 ms before saccadic onset) followed by a

strong enhancement after the saccadic offset. This effect was greater in neurons belonging to the magnocellular system. Promising attempts to measure the overall modulation of saccade-related activity in human LGN and V1 have been made (Sylvester et al., 2005) reporting a reduction of the overall fMRI signal during saccades in both ROIs. These results, though, are difficult to interpret together with the physiological data, since BOLD signal changes triggered by the multiphasic responses observed by Reppas and colleagues in LGN will sum with unpredictable consequences within a blocked design. In a similar experiment from the same group (Sylvester & Rees, 2006), saccade-induced activation was found in LGN in the absence of visual input, while a suppression of activity was found to be dependent on the luminance level during visual stimulation in V1 for blocks of saccades compared to fixational periods. Since signal enhancement in the dark was also observed in V1 (although not significant), the authors suggest that this positive modulation (extraretinal in nature) could mask the suppressive effect of saccades on visually evoked responses to cerebral stimuli. In our study, the reduction in response magnitude never reaches the baseline level (as determined on the F trials). Although it is not possible to determine whether the suppression mechanism affects more strongly the G or the S signal component, based on the behavioral data, it seems reasonable to assume that at least a large part of this residual signal must be related to retinal motion induced by the saccade. Despite recent disagreement (Price, Ibbotson, Ono & Mustari, 2005), a possible explanation could be that the perceptual effect of saccadic image motion could be canceled at a higher stage by populations of motion-sensitive neurons in Medial Temporal (MT/V5) (Thiele, Henning, Kubischik & Hoffmann, 2002) and Medial Superior Temporal (MST) cortex (Erikson & Their, 1991; Thiele et al., 2002) by selectively remaining silent or reversing its direction tuning during saccadic motion. Based on the above arguments, it seems reasonable to think that saccadic suppression might actually be the result of at least two complementary processes: specific subcortical modulation and high-level motion canceling.

In summary, in this study we combine retinotopic localization, high temporal resolution eye-tracking, event-related fMRI and behavioral measurements to reveal the time course

of saccadic suppression in human V1. Our data show how signals elicited by flashed stimuli are suppressed in primary visual cortex when presented immediately before a saccadic eye movement. Moreover, the present report demonstrates that despite the sluggishness of the BOLD signal, this short-lived modulation, occurring within 100 ms, can be resolved with fMRI. Our evidence indicates that an extra-retinal saccadic suppression mechanism does exist in humans. Signals coming from the retina are suppressed every time a saccadic eye movement is performed, and this study demonstrates for the first time that cortical V1 responses to brief stimuli are greatly suppressed even when presented before the eyes begin to move.

6 General discussion

As earlier noted by Nakamura and colleagues (1999), areas that process space, such as V1, must carry more than just visual information and evidence from primate electrophysiology strongly relates V1 to the execution of saccadic eye movements (reviewed in 1.2, 2.1.1 and 2.4). The non-visual involvement of V1 during the execution of saccadic eye movements is confirmed in our first study in Chapter 2, as demonstrated by the fact that changes in V1 activation can be measured while subjects perform self-paced saccades in the absence of visual stimulation. These signal changes cannot be related to local enhancement effects originated by the redistribution of spatial attention that occurs immediately before the onset of a saccadic eye movement, as evidenced by the second study, in which covert shifts of attention to eccentrical positions in the dark fail to elicit measurable signals changes in primary visual cortex (Chapter 3). At the same time, even the cortical visual representation of the retina (which embraces the traditional conception of V1) is affected by saccadic activity, as demonstrated in Chapter 5.

6.1 The non-retinotopic function of V1

While the exact functional role of non-visual V1 activity cannot be precisely determined with our methods, it is worth considering other non-retinotopical visual phenomena in which V1 also seems to play an important role. For instance, the human visual system is capable of generating non-veridical pictorial representations, such as phosphenes, afterimages, hallucinations, visual imagery and dreams, many of which have been shown to actively engage V1 (Bressloff, Cowan, Golubitsky, Thomas & Wiener, 2001; Burke, 2002; Klein et al., 2004; Le Bihan et al., 1993; Tehovnik et al., 2005). Even a case of

orthographic color-word synesthesia has been reported, in which involuntary visualization of auditorily presented verbal material elicited BOLD signals changes in primary visual cortex in the absence of external visual stimulation (Aleman, Rutten, Sitskoorn, Dautzenberg & Ramsey, 2001). It is also possible to identify hallucinating or dreaming behavior in humans and primates by observing eye movements, as in Rapid Eye Movement (REM) sleep. This intense oculomotor activity during sleep (in the absence of visual stimulation) has also been found to correlate with signal increases in the occipital visual cortex (Igawa et al., 2001; Wehrle et al., 2005). Together with our results, all this evidence strongly suggests that V1 neurons do not only respond to visual stimulation but have a role beyond the topographic representation of the retinal image. What this role could be, might be simpler than is often suggested. Even though other brain areas also show some kind of topographic representation (such as the FEF, the SC, extrastriate, and probably parietal areas), the relatively huge V1 contains the finest spatial representation of the visual field, and is therefore an excellent candidate for providing the accurate spatial information needed for the generation of saccades even in the absence of visual stimulation.

We propose that V1 contains a coordinate map of a portion of the space that is determined by gaze position and changes upon an efference copy[1] after each saccade. That is, a dynamic transformation of the egocentric[2] visual space that changes with every eye movement is represented in the primary visual cortex. In normal circumstances and when visual information is available, LGN projects the retinal information into V1 from where it is fed to secondary visual areas and onto ventral, parietal and frontal areas. Lateral parietal cortices send back modulatory signals through the extrastriate cortex that can be registered at different intensities in our V1 data (Figure 2.12, right). These feedback signals retain spatial specificity and are strongly lateralized (Figures 2.9 and 3.4). We hypothesize that they could activate the circuitry that connects V1 and the SC to pass the spatial information onto the brain stem.

[1] An internal copy of a motor innervation that provides the only extraretinal signal about eye position that is available without delay.

[2] The egocentric frame of reference defines the location of each stimulus relative to the spatial position of the subject.

When V1 is deprived of visual information and because there is no retinal information coming form the LGN, no signal summation process can take place in V1 and only weak feedback signals coming from the extrastriate cortex can be measured (Kastner et al., 1999). In the absence of visual stimulation, V1 activity can be registered only when a saccade does actually take place (Vallines et al., 2002, Chapter 2), but not when attention is covertly shifted (Vallines et al., 2003, Chapter 3). This supports the concept of a soft threshold[3] mechanism that converges in V1, where superior parietal signals controlling the reallocation of attention and saccadic signal from the IPS meet with retinal signals coming form the LGN in V1. Within this context, the suprathreshold summation of these three signals sources could be the origin of conscious visual perception and would activate the V1-SC pathway facilitating the generation of an accurate saccade to the location of the corresponding receptive field. Within this model, saccadic suppression could be explained by a weakened retinal signal modulated by the LGN that fails to trigger feed-forward connections to higher cortical areas, which in turn prevents higher feedback signals from arriving at V1, thus diminishing its perceptual experience during the eye movement and impairing performance as shown in Figures 5.8 and 5.9.

6.2 The gate of visual consciousness

The idea of V1 being the gate of consciousness[4] might certainly sound pretentious at first, but it must be acknowledged that it is at the primary sensory cortical areas where the massive amounts of sensory information first arrive, and that only a small fraction of this information is further passed onto higher order areas. Within this framework there are at least two possibilities: visual conscious perception occurs in V1 itself, or takes place at a higher stage based on signals forwarded by V1. In concordance with our data and the threshold model presented in the previous section, visual consciousness has been proposed to be the result of reverberatory activity in pyramidal cells of the lower layers of the visual cortex involving connections to the thalamus (Crick, 1994). Further-

[3] A smooth probabilistic transition.
[4] Understood as the state of perceptual awareness.

more, converging evidence shows the engagement of V1 in mental imagery and visual recall (Chen et al., 1998; Gulyas, 2001; Klein, Paradis, Poline, Kosslyn & Le Bihan, 2000; Le Bihan et al., 1993) and, while widespread lesions in striate cortex that result in blindness also impede the resolution of cognitive imagery, there are no recorded cases of purely parietal damage which led to a complete loss of conscious vision. Patients with V1 lesions were studied by Goebel and colleagues (2001) who presented colored images of natural objects and found sustained BOLD signal changes in extrastriate areas MT, lateral occipital, and the fusiform gyrus that were not sufficient to generate conscious vision. At the same time, blindsight patients with V1 lesions fail to reach conscious visual awareness but can make behavioral use of stimuli presented within the damaged visual field[5] (Stoerig & Cowey, 1997), probably through indirect subcortical routes that reach extrastriate areas through the LGN and the SC. This suggests that V1 can be necessary for awareness, but not for visually guided behavior, which could be accomplished by signals forwarded by secondary areas. Further developing earlier ideas from Crick and Koch (1995), Vakalopoulos (2005) has suggested that V1 links the ventral and the dorsal visual pathways, and that both must be concurrently active to generate conscious visual awareness. By taking a look at Figures 3.4 and 3.5, it can be observed how concurrent activity of both dorso-parietal and extrastriate areas in the SG condition leads to significant signal changes in V1, while similar (but weaker) extrastriate activity alone[6] during the covert shifts of attention does not. Even though, in the second study participants in the second study (Chapter 3) did not report any visual experience, it is plausible to assume that, under normal circumstances, voluntary oculomotor guidance heavily relies on the conscious perception of visual stimuli and thus both might share a common neural architecture. Moreover, and despite eliciting traceable signals in V1, subjects in the last study failed to detect the onset of four Gabor patches presented immediately before the onset of a saccade. In fact, and as predicted by the threshold model, the detection rate strongly correlated with the measured signal amplitude (Figures 5.8 and 5.9). Even though subthreshold V1 activity remains "invisible" to the subjects, Haynes and Rees

[5] For example by accurate reaching.
[6] Apart from the IPS activity shown in Figure 3.3.

(2005) have shown that multivariate pattern recognition techniques can be used to predict the orientation of undetected masked stimuli in V1. From this evidence, it can be concluded that suprathreshold signal activity in V1 is a requisite for visual awareness. This would explain the effects of attentional enhancement in V1 (Gandhi et al., 1999; T. S. Lee et al., 2002; Liu et al., 2005; Pestilli & Carrasco, 2005) that have been successfully exploited by Ress and colleagues (2000) to predict performance in a visual detection task. Attention would enhance weak V1 retinal signals, bringing them to suprathreshold levels and making them available to conscious perception.

While primary visual cortical responses in humans may start as early as 50 ms after retinal stimulation, peak responses appear some 20-30 ms later and a second peak can be observed after another 50 ms. As noted by Tanaka (2001), these late responses can be the result of feedback signals from higher visual areas, propagation across horizontal connection within V1, or the result of attentional modulation controlled by prefrontal or parietal cortex. TMS studies in humans (Pascual-Leone & Walsh, 2001) show that the perception of a stimulus elicited in V5 can be disrupted by applying a below phosphene-threshold pulse onto V1 some 45 ms after stimulation onset, suggesting that re-entrant feedback signals rather than V1 input alone or horizontal propagation might be the origin of these late responses leading to perceptual awareness. In monkeys (Lamme, Super, Landman, Roelfsema & Spekreijse, 2000; Super, Spekreijse & Lamme, 2001), the intensity of late responses ($>$100 ms) in V1 neurons was correlated with a perceptual decision about the detection of a figure embedded in a patterned background, which was indicated by performing a saccade. Lamme and colleagues argue that the signal cannot be related to the eye movement because the shortest latencies were around 250 ms, but fail to consider that the increased firing rate could be actually subserving the programming of the saccade. In fact, the saccade was performed to the visual quadrant where the stimulus appeared, in a way that the increased neuronal activity could be as well interpreted as encoding the target location of the saccade.

Although we do not argue that conscious visual perception "happens" in V1, we propose that it could represent the first perceptual gate that reflects the sum, or outcome, of top-

down and bottom-up modulation. This idea is supported by the synchronous onset modulation observed in prefrontal cortex and V1, which relates to whether stimuli are perceived or not (Lamme et al., 2000; Lamme & Spekreijse, 2000), and can be relevant for the correct interpretation of the results presented in this dissertation work.

Voluntary eye movements such as saccades, are the result of complex interactions between a distributed network of structures that involves at least the visual, attentional and motor system. For the special case of visually-guided saccades, the movements can be computed based on the information delivered by the retina, which is first cortically encoded in V1, then weighted by top-down attentional processes and are possibly re-entered to V1, where the maximal cortical spatial resolution is restored, to be forwarded to motor areas in charge of orchestrating the motor sequence. The superficial layer of the SC receives afferent connections from V1 layers V and VI and could feedforward these signals directly to the FEF, where the motor commands are programmed (Schall, 1995). It seems logical to think that, in normal circumstances, voluntary saccades are executed to stimuli of which we are aware, or at least to stimuli which are about to enter awareness. Moreover, the degree of awareness must be a factor that facilitates the selection of a stimulus as target for a saccade, as suggested by the differences in activation observed during the execution of self-guided saccades in the absence of visual input (Figure 2.8). In the absence of retinal input, stronger extrastriate feedback signals seem to be needed to reach the suprathreshold V1 activity capable of eliciting an eye movement to a certain spatial position that could be encoded and made available by V1 itself.

6.3 Future directions

Our data demonstrate that V1 is active during saccades in the absence of visual stimulation and that the cortical representation of visual stimuli is affected by saccades, but also leave many questions unanswered. To gain deeper insights in to the role of V1 for the execution of saccades it would be desirable to conduct electrophysiological experiments

recording both from cells in the fixation and the target receptive fields while no visual input is available. Even though it would be difficult to instruct monkeys to execute purely voluntary saccades in the dark, operant conditioning through positive reinforcement to a paired auditory-visual target could be used to train the animals to make a saccade even after the removal of the visual stimulus. Knowing the exact temporal sequence between the increase in firing-rate and the saccadic onset would shed light on the non-visual function of V1, for example by determining whether they could be available in time for computing a saccadic vector.

Acoustically cued saccades could be also used to reveal differences between pure top-down saccadic control and saccades for which spatial information is made externally available by another sensory modality. Also, multivariate neuroimaging approaches as those used by Haynes and Rees (2005), could be applied to recognize V1 patterns leading to saccades.

With regard to the V1 signal intensity changes observed in the cortical representation of visual stimuli immediately preceding a saccade, the role of the LGN should be considered in greater detail. There is strong physiological evidence of the modulating role of the LGN at perisaccadic times (Reppas et al., 2002), and stronger magnetic gradients and better MR-coils have already been used to successfully image the LGN (Chen et al., 1999; Erwin et al., 1999; Haynes, Deichmann & Rees, 2005; Schneider et al., 2004) with enough precision so that saccadic suppression effects could be studied in a similar way as in our last experiment (Chapter 5). This would help to understand the subcortical mechanism that seems to pre-saccadically modulate retinal signals delivered to V1 (Figure 5.10).

Lastly, an interesting application of the sensitivity reduction experienced during saccadic suppression has been tested by Schumacher and colleagues (2004) in the field of computer graphics. They suggested that people who had to spend long hours monitoring computer screens (such as air traffic controllers) could be partially relieved by applying the graphic updates during the course of saccades, while saccadic suppression would minimize the disruptive effect of a large image update. As predicted by our results from Chapter 5, the use of saccade-contingent updates was reported as being much less dis-

turbing than equivalent changes in the absence of saccades (Schumacher et al., 2004). The authors reported difficulties in accurately detecting saccadic onsets with their video-based eye trackers despite the sophistication of the detecting algorithm used, and the limited temporal resolution of the system allowed only for testing with very large saccades. Simple amplitude-velocity based saccade-detecting algorithms like the one used in Chapter 5 together with high temporal resolution tracking techniques, considerably reduce the false alarm rate and increases detection accuracy (Figure 5.5). Alternatively, high temporal resolution imaging methods could be used to identify the brain activity patterns that lead to a saccade, just as electroencephalographic signals have already been successfully used to predict simple motor tasks in humans (Wolpaw, Birbaumer, McFarland, Pfurtscheller & Vaughan, 2002).

6.4 Conclusions

The results of this dissertation provide strong evidence for the close involvement of the primary visual cortex in the generation of saccadic eye movements beyond its classical retinotopic role. Furthermore, they demonstrate that visual input is a requisite for cortical attentional enhancement and suggest that re-entrant signals in V1 coming from higher cortical areas could lead to conscious visual perception, by showing that signal intensity correlates with stimulus awareness.

Functional magnetic resonance imaging has proven to be an excellent tool for the study of brain function. In the experiments described in this work, some of the limitations of this technique have been overcome by implementing innovative designs and further developing software and hardware solutions that allowed to maintain a controlled experimental environment in which behavioral responses could be accurately registered during the imaging sessions.

In light of these data, together with the extensive neuroanatomical, clinical and neurophysiological evidence presented in this work, the functional role of the primary visual cortex must be reconsidered and V1 should be carefully incorporated to the oculomotor network. Despite of the attractiveness of localized functional specialization for modern imaging techniques, only the astute interpretation of converging results from different disciplines can unravel the elusive modus operandi of the human brain.

References

Aleman, A., Rutten, G. J., Sitskoorn, M. M., Dautzenberg, G. & Ramsey, N. F. (2001). Activation of striate cortex in the absence of visual stimulation: an fmri study of synesthesia. *Neuroreport*, *12*(13), 2827-30.

Amador, N., Schlag-Rey, M. & Schlag, J. (2004). Primate antisaccade. ii. supplementary eye field neuronal activity predicts correct performance. *J Neurophysiol*, *91*(4), 1672-89.

Amaro, J., E., & Barker, G. J. (2006). Study design in fmri: basic principles. *Brain Cogn*, *60*(3), 220-32.

Arrington, C. M., Carr, T. H., Mayer, A. R. & Rao, S. M. (2000). Neural mechanisms of visual attention: object-based selection of a region in space. *J Cogn Neurosci*, *12 Suppl 2*, 106-17.

Astafiev, S. V., Shulman, G. L., Stanley, C. M., Snyder, A. Z., Van Essen, D. C. & Corbetta, M. (2003). Functional organization of human intraparietal and frontal cortex for attending, looking, and pointing. *J Neurosci*, *23*(11), 4689-99.

Bartlett, J. R., Doty, R. W., Lee, S., B. B. & Sakakura, H. (1976). Influence of saccadic eye movements on geniculostriate excitability in normal monkeys. *Exp Brain Res*, *25*, 487-509.

Bartz, A. E. (1962). Eye-movement latency, duration, and response time as a function of angular displacement. *J Exp Psychol*, *64*, 318-24.

Beauchamp, M. S., Petit, L., Ellmore, T. M., Ingeholm, J. & Haxby, J. V. (2001). A parametric fmri study of overt and covert shifts of visuospatial attention. *Neuroimage*, *14*(2), 310-21.

Becker, W. (1989). The neurobiology of saccadic eye movements. metrics. *Rev Oculomot Res*, *3*, 13-67.

Becker, W., & Jurgens, R. (1979). An analysis of the saccadic system by means of double step stimuli. *Vision Res*, *19*(9), 967-83.

Berg, J. A., Bradley, D. C., Troyk, P. R., Xu, H., Bak, M., Erickson, R. et al. (2002). Parallel microstimulation of macaque striate visual cortex. *Soc. Neurosci. Abstract.*, *32*, 259.

Bisley, J. W., & Goldberg, M. E. (2003). Neuronal activity in the lateral intraparietal area and spatial attention. *Science*, *299*(5603), 81-6.

Blamire, A. M., Ogawa, S., Ugurbil, K., Rothman, D., McCarthy, G., Ellermann, J. M. et al. (1992). Dynamic mapping of the human visual cortex by high-speed magnetic resonance imaging. *Proc Natl Acad Sci U S A*, *89*(22), 11069-73.

Blatt, G. J., Andersen, R. A. & Stoner, G. R. (1990). Visual receptive field organization and cortico-cortical connections of the lateral intraparietal area (area lip) in the macaque. *J Comp Neurol*, *299*(4), 421-45.

Bodis-Wollner, I., Bucher, S. F. & Seelos, K. C. (1999). Cortical activation patterns during voluntary blinks and voluntary saccades. *Neurology*, *53*(8), 1800-5.

Bodis-Wollner, I., Bucher, S. F., Seelos, K. C., Paulus, W., Reiser, M. & Oertel, W. H. (1997). Functional mri mapping of occipital and frontal cortical activity during voluntary and imagined saccades. *Neurology*, *49*(2), 416-20.

Bodis-Wollner, I., Von Gizycki, H., Avitable, M., Hussain, Z., Javeid, A., Habib, A. et al. (2002). Perisaccadic occipital eeg changes quantified with wavelet analysis. *Ann N Y Acad Sci*, *956*, 464-7.

Bollen, E., Bax, J., Dijk, J. G. van, Koning, M., Bos, J. E., Kramer, C. G. et al. (1993). Variability of the main sequence. *Invest Ophthalmol Vis Sci*, *34*(13), 3700-4.

Bressloff, P. C., Cowan, J. D., Golubitsky, M., Thomas, P. J. & Wiener, M. C. (2001). Geometric visual hallucinations, euclidean symmetry and the functional architecture of striate cortex. *Philos Trans R Soc Lond B Biol Sci*, *356*(1407), 299-330.

Brett, M., Anton, J.-L., Valabregue, R. & Poline, J.-B. (2002). Region of interest analysis

using an spm toolbox. *Neuroimage*, *16*(2), abstract 497.

Bridgeman, B., Heijden, A. H. C. Van der & Velichkovsky, B. M. (1994). A theory of visual stability across saccadic eye movements. *Behavioral and Brain Sciences*, *17*(2), 247-258.

Bruce, C. J., & Goldberg, M. E. (1985). Primate frontal eye fields. i. single neurons discharging before saccades. *J Neurophysiol*, *53*(3), 603-35.

Buchel, C., Holmes, A. P., Rees, G. & Friston, K. J. (1998). Characterizing stimulus-response functions using nonlinear regressors in parametric fmri experiments. *Neuroimage*, *8*(2), 140-8.

Buchel, C., Wise, R. J., Mummery, C. J., Poline, J. B. & Friston, K. J. (1996). Nonlinear regression in parametric activation studies. *Neuroimage*, *4*(1), 60-6.

Burke, W. (2002). The neural basis of charles bonnet hallucinations: a hypothesis. *J Neurol Neurosurg Psychiatry*, *73*(5), 535-41.

Burr, D. C., Morrone, M. C. & Ross, J. (1994). Selective suppression of the magnocellular visual pathway during saccadic eye movements. *Nature*, *371*(6497), 511-3.

Bushnell, M. C., Goldberg, M. E. & Robinson, D. L. (1981). Behavioral enhancement of visual responses in monkey cerebral cortex. i. modulation in posterior parietal cortex related to selective visual attention. *J Neurophysiol*, *46*(4), 755-72.

Castet, E., Jeanjean, S. & Masson, G. S. (2001). 'saccadic suppression'- no need for an active extra-retinal mechanism. *Trends Neurosci*, *24*(6), 316-8.

Chen, W., Kato, T., Zhu, X. H., Ogawa, S., Tank, D. W. & Ugurbil, K. (1998). Human primary visual cortex and lateral geniculate nucleus activation during visual imagery. *Neuroreport*, *9*(16), 3669-74.

Chen, W., Zhu, X. H., Thulborn, K. R. & Ugurbil, K. (1999). Retinotopic mapping of lateral geniculate nucleus in humans using functional magnetic resonance imaging. *Proc Natl Acad Sci U S A*, *96*(5), 2430-4.

Cheng, K., Waggoner, R. A. & Tanaka, K. (2001). Human ocular dominance columns as revealed by high-field functional magnetic resonance imaging. *Neuron*, *32*(2), 359-74.

Colby, C. L., Duhamel, J. R. & Goldberg, M. E. (1996). Visual, presaccadic, and cognitive activation of single neurons in monkey lateral intraparietal area. *J Neurophysiol*, *76*(5), 2841-52.

Connolly, J. D., Goodale, M. A., Goltz, H. C. & Munoz, D. P. (2005). fmri activation in the human frontal eye field is correlated with saccadic reaction time. *J Neurophysiol*, *94*(1), 605-11.

Corbetta, M., Kincade, J. M., Ollinger, J. M., McAvoy, M. P. & Shulman, G. L. (2000). Voluntary orienting is dissociated from target detection in human posterior parietal cortex. *Nat Neurosci*, *3*(3), 292-7.

Corbetta, M., & Shulman, G. L. (1998). Human cortical mechanisms of visual attention during orienting and search. *Philos Trans R Soc Lond B Biol Sci*, *353*(1373), 1353-62.

Crick, F. (1994). *The astonishing hypothesis*. New York: Scribners.

Crick, F., & Koch, C. (1995). Are we aware of neural activity in primary visual cortex? *Nature*, *375*(6527), 121-3.

DeSouza, P. (2000). *Automatic saccadic detection algorithm (asda)*. Carl von Ossietzky University.

Deubel, H., & Schneider, W. X. (1996). Saccade target selection and object recognition: evidence for a common attentional mechanism. *Vision Res*, *36*(12), 1827-37.

DeYoe, E. A., Carman, G. J., Bandettini, P., Glickman, S., Wieser, J., Cox, R. et al. (1996). Mapping striate and extrastriate visual areas in human cerebral cortex. *Proc Natl Acad Sci U S A*, *93*(6), 2382-6.

Diamond, M. R., Ross, J. & Morrone, M. C. (2000). Extraretinal control of saccadic suppression. *J Neurosci*, *20*(9), 3449-55.

Di Russo, F., Martinez, A. & Hillyard, S. A. (2003). Source analysis of event-related cortical activity during visuo-spatial attention. *Cereb Cortex*, *13*(5), 486-99.

Engbert, R., & Kliegl, R. (2003). Microsaccades uncover the orientation of covert attention. *Vision Res*, *43*(9), 1035-45.

Engel, S. A., Glover, G. H. & Wandell, B. A. (1997). Retinotopic organization in human

visual cortex and the spatial precision of functional mri. *Cereb Cortex*, *7*(2), 181-92.

Erikson, R. G., & Their. (1991). A neural correlate of spatial stability during periods of self-induced visual motion. *Exp Brain Res*, *86*, 608-616.

Erwin, E., Baker, F. H., Busen, W. F. & Malpeli, J. G. (1999). Relationship between laminar topology and retinotopy in the rhesus lateral geniculate nucleus: results from a functional atlas. *J Comp Neurol*, *407*(1), 92-102.

Everling, S., & Fischer, B. (1998). The antisaccade: a review of basic research and clinical studies. *Neuropsychologia*, *36*(9), 885-99.

Field, D. J., & Tolhurst, D. J. (1986). The structure and symmetry of simple-cell receptive-field profiles in the cat's visual cortex. *Proc R Soc Lond B Biol Sci*, *228*(1253), 379-400.

Findlay, J. M., & Gilchrist, I. D. (2003). *Active vision : the psychology of looking and seeing.* Oxford ; New York: Oxford University Press.

Findlay, J. M., Walker, R. & Kentridge, R. W. (1995). *Eye movement research : mechanisms, processes and applications.* Amsterdam ; New York: Elsevier.

Fischer, B. (1986). Express saccades in man and monkey. *Prog Brain Res*, *64*, 155-60.

Fischer, B., & Boch, R. (1983). Saccadic eye movements after extremely short reaction times in the monkey. *Brain Res*, *260*(1), 21-6.

Fischer, B., Gezeck, S. & Huber, W. (1995). The three-loop model: a neural network for the generation of saccadic reaction times. *Biol Cybern*, *72*(3), 185-96.

Fitzpatrick, D., Usrey, W. M., Schofield, B. R. & Einstein, G. (1994). The sublaminar organization of corticogeniculate neurons in layer 6 of macaque striate cortex. *Vis Neurosci*, *11*(2), 307-15.

Fredericksen, R. E., Bex, P. J. & Verstraten, F. A. (1997). How big is a gabor patch, and why should we care? *J Opt Soc Am A Opt Image Sci Vis*, *14*(1), 1-12.

Fries, W. (1990). Pontine projection from striate and prestriate visual cortex in the macaque monkey: an anterograde study. *Vis Neurosci*, *4*(3), 205-16.

Friston, K. J., Fletcher, P., Josephs, O., Holmes, A., Rugg, M. D. & Turner, R. (1998). Event-related fmri: characterizing differential responses. *Neuroimage*, *7*(1), 30-40.

Friston, K. J., Frith, C. D., Frackowiak, R. S. & Turner, R. (1995). Characterizing dynamic brain responses with fmri: a multivariate approach. *Neuroimage*, *2*(2), 166-72.

Friston, K. J., Glaser, D. E., Henson, R. N., Kiebel, S., Phillips, C. & Ashburner, J. (2002). Classical and bayesian inference in neuroimaging: applications. *Neuroimage*, *16*(2), 484-512.

Friston, K. J., Holmes, A. P., Poline, J. B., Grasby, P. J., Williams, S. C., Frackowiak, R. S. et al. (1995). Analysis of fmri time-series revisited. *Neuroimage*, *2*(1), 45-53.

Friston, K. J., Josephs, O., Rees, G. & Turner, R. (1998). Nonlinear event-related responses in fmri. *Magn Reson Med*, *39*(1), 41-52.

Friston, K. J., Mechelli, A., Turner, R. & Price, C. J. (2000). Nonlinear responses in fmri: the balloon model, volterra kernels, and other hemodynamics. *Neuroimage*, *12*(4), 466-77.

Fuchs, A. F., & Kornhuber, H. H. (1969). Extraocular muscle afferents to the cerebellum of the cat. *J Physiol*, *200*(3), 713-22.

Fujikado, T., & Noda, H. (1987). Saccadic eye movements evoked by microstimulation of lobule vii of the cerebellar vermis of macaque monkeys. *J Physiol*, *394*, 573-94.

Furmanski, C. S., & Engel, S. A. (2000). An oblique effect in human primary visual cortex. *Nat Neurosci*, *3*(6), 535-6.

Gabor, D. (1946). Theory of comunication. *J Inst Electr Eng*, *24*, 891-910.

Gandhi, S. P., Heeger, D. J. & Boynton, G. M. (1999). Spatial attention affects brain activity in human primary visual cortex. *Proc Natl Acad Sci U S A*, *96*(6), 3314-9.

Garcia-Perez, M. A., & Peli, E. (2001). Intrasaccadic perception. *J Neurosci*, *21*(18), 7313-22.

Gaymard, B., Ploner, C. J., Rivaud, S., Vermersch, A. I. & Pierrot-Deseilligny, C. (1998). Cortical control of saccades. *Exp Brain Res*, *123*(1-2), 159-63.

Gitelman, D. R., Nobre, A. C., Parrish, T. B., LaBar, K. S., Kim, Y. H., Meyer, J. R. et al. (1999). A large-scale distributed network for covert spatial attention: further anatomical delineation based on stringent behavioural and cognitive controls.

Brain, *122 (Pt 6)*, 1093-106.

Glover, G. H. (1999). Deconvolution of impulse response in event-related bold fmri. *Neuroimage*, *9*(4), 416-29.

Goebel, R., Muckli, L., Zanella, F. E., Singer, W. & Stoerig, P. (2001). Sustained extrastriate cortical activation without visual awareness revealed by fmri studies of hemianopic patients. *Vision Res*, *41*(10-11), 1459-74.

Goodyear, B. G., & Menon, R. S. (1998). Effect of luminance contrast on bold fmri response in human primary visual areas. *J Neurophysiol*, *79*(4), 2204-7.

Graham, J. (1982). Some topographical connections of the striate cortex with subcortical structures in macaca fascicularis. *Exp Brain Res*, *47*(1), 1-14.

Grosbras, M. H., Lobel, E., Moortele, P. F. Van de, LeBihan, D. & Berthoz, A. (1999). An anatomical landmark for the supplementary eye fields in human revealed with functional magnetic resonance imaging. *Cereb Cortex*, *9*(7), 705-11.

Gulyas, B. (2001). Neural networks for internal reading and visual imagery of reading: a pet study. *Brain Res Bull*, *54*(3), 319-28.

Gutierrez, C., & Cusick, C. G. (1997). Area v1 in macaque monkeys projects to multiple histochemically defined subdivisions of the inferior pulvinar complex. *Brain Res*, *765*(2), 349-56.

Hafed, Z. M., & Clark, J. J. (2002). Microsaccades as an overt measure of covert attention shifts. *Vision Res*, *42*(22), 2533-45.

Hayakawa, Y., Nakajima, T., Takagi, M., Fukuhara, N. & Abe, H. (2002). Human cerebellar activation in relation to saccadic eye movements: a functional magnetic resonance imaging study. *Ophthalmologica*, *216*(6), 399-405.

Haynes, J. D., Deichmann, R. & Rees, G. (2005). Eye-specific effects of binocular rivalry in the human lateral geniculate nucleus. *Nature*, *438*(7067), 496-9.

Haynes, J. D., & Rees, G. (2005). Predicting the orientation of invisible stimuli from activity in human primary visual cortex. *Nat Neurosci*, *8*(5), 686-91.

Hikosaka, O., & Wurtz, R. H. (1983). Visual and oculomotor functions of monkey substantia nigra pars reticulata. i. relation of visual and auditory responses to

saccades. *J Neurophysiol*, *49*(5), 1230-53.

Honda, H. (1989). Perceptual localization of visual stimuli flashed during saccades. *Percept Psychophys*, *45*(2), 162-74.

Horton, J. C., & Hoyt, W. F. (1991). The representation of the visual field in human striate cortex. a revision of the classic holmes map. *Arch Ophthalmol*, *109*(6), 816-24.

Hubel, D. H., & Wiesel, T. N. (1968). Receptive fields and functional architecture of monkey striate cortex. *J Physiol*, *195*(1), 215-43.

Hubel, D. H., & Wiesel, T. N. (1972). Laminar and columnar distribution of geniculocortical fibers in the macaque monkey. *J Comp Neurol*, *146*(4), 421-50.

Huettel, S. A., & McCarthy, G. (2000). Evidence for a refractory period in the hemodynamic response to visual stimuli as measured by mri. *Neuroimage*, *11*(5 Pt 1), 547-53.

Huettel, S. A., & McCarthy, G. (2001). The effects of single-trial averaging upon the spatial extent of fmri activation. *Neuroreport*, *12*(11), 2411-6.

Huettel, S. A., Song, A. W. & McCarthy, G. (2004). *Functional magnetic resonance imaging*. Sinauer Associates.

Huk, A. C., Dougherty, R. F. & Heeger, D. J. (2002). Retinotopy and functional subdivision of human areas mt and mst. *J Neurosci*, *22*(16), 7195-205.

Huk, A. C., & Heeger, D. J. (2000). Task-related modulation of visual cortex. *J Neurophysiol*, *83*(6), 3525-36.

Igawa, M., Atsumi, Y., Takahashi, K., Shiotsuka, S., Hirasawa, H., Yamamoto, R. et al. (2001). Activation of visual cortex in rem sleep measured by 24-channel nirs imaging. *Psychiatry Clin Neurosci*, *55*(3), 187-8.

Irwing, D., & Carlson-Radvansky, L. A. (1996). Cognitive suppression during saccadic eye movements. *Psychol Sci*, *7*(2), 83.

Isoda, M., & Tanji, J. (2002). Cellular activity in the supplementary eye field during sequential performance of multiple saccades. *J Neurophysiol*, *88*(6), 3541-5.

Itti, L., & Koch, C. (2000). A saliency-based search mechanism for overt and covert

shifts of visual attention. *Vision Res*, *40*(10-12), 1489-506.

Itti, L., & Koch, C. (2001). Computational modelling of visual attention. *Nat Rev Neurosci*, *2*(3), 194-203.

Kastner, S., Pinsk, M. A., De Weerd, P., Desimone, R. & Ungerleider, L. G. (1999). Increased activity in human visual cortex during directed attention in the absence of visual stimulation. *Neuron*, *22*(4), 751-61.

Keating, E. G., & Gooley, S. G. (1988). Saccadic disorders caused by cooling the superior colliculus or the frontal eye field, or from combined lesions of both structures. *Brain Res*, *438*(1-2), 247-55.

Keating, E. G., Gooley, S. G., Pratt, S. E. & Kelsey, J. E. (1983). Removing the superior colliculus silences eye movements normally evoked from stimulation of the parietal and occipital eye fields. *Brain Res*, *269*(1), 145-8.

Khayat, P. S., Spekreijse, H. & Roelfsema, P. R. (2004). Correlates of transsaccadic integration in the primary visual cortex of the monkey. *Proc Natl Acad Sci U S A*, *101*(34), 12712-7.

Kimmig, H., Greenlee, M. W., Gondan, M., Schira, M., Kassubek, J. & Mergner, T. (2001). Relationship between saccadic eye movements and cortical activity as measured by fmri: quantitative and qualitative aspects. *Exp Brain Res*, *141*(2), 184-94.

Kimmig, H., Greenlee, M. W., Huethe, F. & Mergner, T. (1999). Mr-eyetracker: a new method for eye movement recording in functional magnetic resonance imaging. *Exp Brain Res*, *126*(3), 443-9.

Klein, I., Dubois, J., Mangin, J. F., Kherif, F., Flandin, G., Poline, J. B. et al. (2004). Retinotopic organization of visual mental images as revealed by functional magnetic resonance imaging. *Brain Res Cogn Brain Res*, *22*(1), 26-31.

Klein, I., Paradis, A. L., Poline, J. B., Kosslyn, S. M. & Le Bihan, D. (2000). Transient activity in the human calcarine cortex during visual-mental imagery: an event-related fmri study. *J Cogn Neurosci*, *12 Suppl 2*, 15-23.

Kleiser, R., Seitz, R. J. & Krekelberg, B. (2004). Neural correlates of saccadic suppression in humans. *Curr Biol*, *14*(5), 386-90.

Kornhuber, H. H. (1973). Cerebellar control of eye movements. *Adv Otorhinolaryngol*, *19*, 241-53.

Kowler, E., Anderson, E., Dosher, B. & Blaser, E. (1995). The role of attention in the programming of saccades. *Vision Res*, *35*(13), 1897-916.

Lamme, V. A., & Spekreijse, H. (2000). Modulations of primary visual cortex activity representing attentive and conscious scene perception. *Front Biosci*, *5*, D232-43.

Lamme, V. A., Super, H., Landman, R., Roelfsema, P. R. & Spekreijse, H. (2000). The role of primary visual cortex (v1) in visual awareness. *Vision Res*, *40*(10-12), 1507-21.

Latour, P. L. (1962). Visual threshold during eye movements. *Vision Res*(2), 261-262.

Lauterbur, P. C. (1973). Image formation by induced local interactions: Examples employing nuclear magnetic resonance. *Nature*(242), 190-191.

Law, I., Svarer, C., Rostrup, E. & Paulson, O. B. (1998). Parieto-occipital cortex activation during self-generated eye movements in the dark. *Brain*, *121 (Pt 11)*, 2189-200.

Le Bihan, D., Turner, R., Zeffiro, T. A., Cuenod, C. A., Jezzard, P. & Bonnerot, V. (1993). Activation of human primary visual cortex during visual recall: a magnetic resonance imaging study. *Proc Natl Acad Sci U S A*, *90*(24), 11802-5.

Lee, C., Rohrer, W. H. & Sparks, D. L. (1988). Population coding of saccadic eye movements by neurons in the superior colliculus. *Nature*, *332*(6162), 357-60.

Lee, T. S., Yang, C. F., Romero, R. D. & Mumford, D. (2002). Neural activity in early visual cortex reflects behavioral experience and higher-order perceptual saliency. *Nat Neurosci*, *5*(6), 589-97.

Leigh, R. J., & Zee, D. S. (1991). *The neurology of eye movements* (Ed. 2. ed.). Philadelphia: F.A. Davis Co.

Leopold, D. A., & Logothetis, N. K. (1998). Microsaccades differentially modulate neural activity in the striate and extrastriate visual cortex. *Exp Brain Res*, *123*(3), 341-5.

Leung, H. C., Gore, J. C. & Goldman-Rakic, P. S. (2002). Sustained mnemonic response in the human middle frontal gyrus during on-line storage of spatial memoranda. *J*

Cogn Neurosci, *14*(4), 659-71.

Li, C. S., & Lin, S. C. (2002). Inhibition of return in temporal order saccades. *Vision Res*, *42*(17), 2089-93.

Liu, T., Pestilli, F. & Carrasco, M. (2005). Transient attention enhances perceptual performance and fmri response in human visual cortex. *Neuron*, *45*(3), 469-77.

Logothetis, N. K., Pauls, J., Augath, M., Trinath, T. & Oeltermann, A. (2001). Neurophysiological investigation of the basis of the fmri signal. *Nature*, *412*(6843), 150-7.

Luppino, G., Rozzi, S., Calzavara, R. & Matelli, M. (2003). Prefrontal and agranular cingulate projections to the dorsal premotor areas f2 and f7 in the macaque monkey. *Eur J Neurosci*, *17*(3), 559-78.

MacKay, D. M. (1970). Mislocation of test flashes during saccadic image displacements. *Nature*, *227*(5259), 731-3.

Mansfield, P. (1977). Multi-planar image formation using nmr spin echoes. *J Phys*(10), 55-58.

Martinez, A., DiRusso, F., Anllo-Vento, L., Sereno, M. I., Buxton, R. B. & Hillyard, S. A. (2001). Putting spatial attention on the map: timing and localization of stimulus selection processes in striate and extrastriate visual areas. *Vision Res*, *41*(10-11), 1437-57.

Matin, E., Clymer, A. B. & Matin, L. (1972). Metacontrast and saccadic suppression. *Science*, *178*(57), 179-82.

Maunsell, J. H., & Van Essen, D. C. (1983). Functional properties of neurons in middle temporal visual area of the macaque monkey. ii. binocular interactions and sensitivity to binocular disparity. *J Neurophysiol*, *49*(5), 1148-67.

McIlwain, J. T. (1988). Saccadic eye movements evoked by electrical stimulation of the cat's visual cortex. *Vis Neurosci*, *1*(1), 135-43.

Merriam, E. P., Genovese, C. R. & Colby, C. L. (2003). Spatial updating in human parietal cortex. *Neuron*, *39*(2), 361-73.

Moran, J., & Desimone, R. (1985). Selective attention gates visual processing in the

extrastriate cortex. *Science*, *229*(4715), 782-4.

Morrone, M. C., Ross, J. & Burr, D. (2005). Saccadic eye movements cause compression of time as well as space. *Nat Neurosci*, *8*(7), 950-4.

Mort, D. J., Perry, R. J., Mannan, S. K., Hodgson, T. L., Anderson, E., Quest, R. et al. (2003). Differential cortical activation during voluntary and reflexive saccades in man. *Neuroimage*, *18*(2), 231-46.

Moschovakis, A. K., Scudder, C. A. & Highstein, S. M. (1996). The microscopic anatomy and physiology of the mammalian saccadic system. *Prog Neurobiol*, *50*(2-3), 133-254.

Munoz, D. P., Dorris, M. C., Pare, M. & Everling, S. (2000). On your mark, get set: brainstem circuitry underlying saccadic initiation. *Can J Physiol Pharmacol*, *78*(11), 934-44.

Munoz, D. P., & Everling, S. (2004). Look away: the anti-saccade task and the voluntary control of eye movement. *Nat Rev Neurosci*, *5*(3), 218-28.

Munoz, D. P., & Wurtz, R. H. (1995). Saccade-related activity in monkey superior colliculus. ii. spread of activity during saccades. *J Neurophysiol*, *73*(6), 2334-48.

Muri, R. M., Iba-Zizen, M. T., Derosier, C., Cabanis, E. A. & Pierrot-Deseilligny, C. (1996). Location of the human posterior eye field with functional magnetic resonance imaging. *J Neurol Neurosurg Psychiatry*, *60*(4), 445-8.

Nakamura, K., Chung, H. H., Graziano, M. S. & Gross, C. G. (1999). Dynamic representation of eye position in the parieto-occipital sulcus. *J Neurophysiol*, *81*(5), 2374-85.

Nakamura, K., & Colby, C. L. (2002). Updating of the visual representation in monkey striate and extrastriate cortex during saccades. *Proc Natl Acad Sci U S A*, *99*(6), 4026-31.

Nobre, A. C., Cristescu, T., Gough, P. M., Lepsien, J., Morgese, C., O'Reilly, J. et al. (2004). *The cognitive mri revolution.*

Nobre, A. C., Gitelman, D. R., Dias, E. C. & Mesulam, M. M. (2000). Covert visual spatial orienting and saccades: overlapping neural systems. *Neuroimage*, *11*(3),

210-6.

Oezyurt, J., Rutschmann, R. M., Vallines, I. & Greenlee, M. W. (2002). Event-related fmri of saccadic response inhibition. *Perception*, *31 (Suppl.)*, 177.

Oezyurt, J., Rutschmann, R. M., Vallines, I. & Greenlee, M. W. (2004). Event-related fmri during saccadic gap- and overlap-paradigms: Neural correlates of express saccades. *Perception*, *33 (Suppl.)*, 4.

Ogawa, S., Lee, T. M., Kay, A. R. & Tank, D. W. (1990). Brain magnetic resonance imaging with contrast dependent on blood oxygenation. *Proc Natl Acad Sci U S A*, *87*(24), 9868-72.

Ogawa, S., Lee, T. M., Stepnoski, R., Chen, W., Zhu, X. H. & Ugurbil, K. (2000). An approach to probe some neural systems interaction by functional mri at neural time scale down to milliseconds. *Proc Natl Acad Sci U S A*, *97*(20), 11026-31.

Optican, L. M., & Robinson, D. A. (1980). Cerebellar-dependent adaptive control of primate saccadic system. *J Neurophysiol*, *44*(6), 1058-76.

Pare, M., & Wurtz, R. H. (2001). Progression in neuronal processing for saccadic eye movements from parietal cortex area lip to superior colliculus. *J Neurophysiol*, *85*(6), 2545-62.

Pascual-Leone, A., & Walsh, V. (2001). Fast backprojections from the motion to the primary visual area necessary for visual awareness. *Science*, *292*, 510-512.

Pauling, L., & Coryell, C. D. (1936). The magnetic properties and structure of hemoglobin, oxigenated hemoglobin, and carbonmonoxigenated hemoglobin. *Proc Natl Acad Sci USA*(22), 210-216.

Paus, T. (1996). Location and function of the human frontal eye-field: a selective review. *Neuropsychologia*, *34*(6), 475-83.

Paus, T., Marrett, S., Worsley, K. J. & Evans, A. C. (1995). Extraretinal modulation of cerebral blood flow in the human visual cortex: implications for saccadic suppression. *J Neurophysiol*, *74*(5), 2179-83.

Paus, T., Petrides, M., Evans, A. C. & Meyer, E. (1993). Role of the human anterior cingulate cortex in the control of oculomotor, manual, and speech responses: a

positron emission tomography study. *J Neurophysiol*, *70*(2), 453-69.

Penfield, W., & Perot, P. (1963). The brain's record of auditory and visual experience. a final summary and discussion. *Brain*, *86*, 595-696.

Perry, R. J., & Zeki, S. (2000). The neurology of saccades and covert shifts in spatial attention: an event-related fmri study. *Brain*, *123 (Pt 11)*, 2273-88.

Pestilli, F., & Carrasco, M. (2005). Attention enhances contrast sensitivity at cued and impairs it at uncued locations. *Vision Res*, *45*(14), 1867-75.

Petit, L., Clark, V. P., Ingeholm, J. & Haxby, J. V. (1997). Dissociation of saccade-related and pursuit-related activation in human frontal eye fields as revealed by fmri. *J Neurophysiol*, *77*(6), 3386-90.

Petit, L., Orssaud, C., Tzourio, N., Crivello, F., Berthoz, A. & Mazoyer, B. (1996). Functional anatomy of a prelearned sequence of horizontal saccades in humans. *J Neurosci*, *16*(11), 3714-26.

Pierrot-Deseilligny, C., Milea, D. & Muri, R. M. (2004). Eye movement control by the cerebral cortex. *Curr Opin Neurol*, *17*(1), 17-25.

Pierrot-Deseilligny, C., Muri, R. M., Ploner, C. J., Gaymard, B., Demeret, S. & Rivaud-Pechoux, S. (2003). Decisional role of the dorsolateral prefrontal cortex in ocular motor behaviour. *Brain*, *126*(Pt 6), 1460-73.

Posner, M. I. (1980). Orienting of attention. *Q J Exp Psychol*, *32*(1), 3-25.

Price, N. S. C., Ibbotson, M. R., Ono, S. & Mustari, M. J. (2005). Rapid processing of retinal slip during saccades in macaque area mt. *J Neurophysiol*, *94*, 235-246.

Purcell, E. M., Torrey, H. C. & Pound, R. V. (1945). Resonance absorption by nulcear magnetic moments in a solid. *Phys Rev*(69), 37-38.

Quaia, C., Lefevre, P. & Optican, L. M. (1999). Model of the control of saccades by superior colliculus and cerebellum. *J Neurophysiol*, *82*(2), 999-1018.

Regan, D. (1989). *Human brain electrophysiology : evoked potentials and evoked magnetic fields in science and medicine*. New York: Elsevier.

Reppas, J. B., Usrey, W. M. & Reid, R. C. (2002). Saccadic eye movements modulate visual responses in the lateral geniculate nucleus. *Neuron*, *35*(5), 961-74.

Ress, D., Backus, B. T. & Heeger, D. J. (2000). Activity in primary visual cortex predicts performance in a visual detection task. *Nat Neurosci*, *3*(9), 940-5.

Reuter-Lorenz, P. A., Hughes, H. C. & Fendrich, R. (1991). The reduction of saccadic latency by prior offset of the fixation point: an analysis of the gap effect. *Percept Psychophys*, *49*(2), 167-75.

Reynolds, J. H., Pasternak, T. & Desimone, R. (2000). Attention increases sensitivity of v4 neurons. *Neuron*, *26*(3), 703-14.

Rickham, P. P. (1964). Human experimentation. code of ethics of the world medical association. declaration of helsinki. *Br Med J*, *5402*, 177.

Riggs, L. A., Merton, P. A. & Morton, H. B. (1974). Suppression of visual phosphenes during saccadic eye movements. *Vision Res*, *14*(10), 997-1011.

Riggs, L. A., Volkmann, F. C., Moore, R. K. & Ellicott, A. G. (1982). Perception of suprathreshold stimuli during saccadic eye movements. *Vision Res*, *22*(4), 423-8.

Rizzolatti, G., Riggio, L., Dascola, I. & Umilta, C. (1987). Reorienting attention across the horizontal and vertical meridians: evidence in favor of a premotor theory of attention. *Neuropsychologia*, *25*(1A), 31-40.

Robinson, & Fuchs, A. F. (1969). Eye movements evoked by stimulation of frontal eye fields. *J Neurophysiol*, *32*(5), 637-48.

Robinson, D. L., & McClurkin, J. W. (1989). The visual superior colliculus and pulvinar. *Rev Oculomot Res*, *3*, 337-60.

Roelfsema, P. R., & Spekreijse, H. (2001). The representation of erroneously perceived stimuli in the primary visual cortex. *Neuron*, *31*(5), 853-63.

Rosano, C., Krisky, C. M., Welling, J. S., Eddy, W. F., Luna, B., Thulborn, K. R. et al. (2002). Pursuit and saccadic eye movement subregions in human frontal eye field: a high-resolution fmri investigation. *Cereb Cortex*, *12*(2), 107-15.

Ross, J., Morrone, M. C. & Burr, D. C. (1997). Compression of visual space before saccades. *Nature*, *386*(6625), 598-601.

Ross, J., Morrone, M. C., Goldberg, M. E. & Burr, D. C. (2001). Changes in visual perception at the time of saccades. *Trends Neurosci*, *24*(2), 113-21.

Sakai, K., Rowe, J. B. & Passingham, R. E. (2002). Active maintenance in prefrontal area 46 creates distractor-resistant memory. *Nat Neurosci*, *5*(5), 479-84.

Saslow, M. G. (1967). Latency for saccadic eye movement. *J Opt Soc Am*, *57*(8), 1030-3.

Schaefer, E. A. (1888). Experiments on the electrical excitation of the visual area of the cerebral cortex in the monkey. *Brain*, *11*, 1-6.

Schall, J. D. (1995). Neural basis of saccade target selection. *Rev Neurosci*, *6*(1), 63-85.

Schall, J. D. (2004). On the role of frontal eye field in guiding attention and saccades. *Vision Res*, *44*(12), 1453-67.

Schall, J. D., & Thompson, K. G. (1999). Neural selection and control of visually guided eye movements. *Annu Rev Neurosci*, *22*, 241-59.

Schiller, P. H. (1972). The role of the monkey superior colliculus in eye movement and vision. *Invest Ophthalmol*, *11*(6), 451-60.

Schiller, P. H. (1977). The effect of superior colliculus ablation on saccades elicted by cortical stimulation. *Brain Res*, *122*(1), 154-6.

Schiller, P. H., & Chou, I. (2000). The effects of anterior arcuate and dorsomedial frontal cortex lesions on visually guided eye movements in the rhesus monkey: 1. single and sequential targets. *Vision Res*, *40*(10-12), 1609-26.

Schiller, P. H., & Chou, I. H. (1998). The effects of frontal eye field and dorsomedial frontal cortex lesions on visually guided eye movements. *Nat Neurosci*, *1*(3), 248-53.

Schiller, P. H., Finlay, B. L. & Volman, S. F. (1976). Quantitative studies of single-cell properties in monkey striate cortex. i. spatiotemporal organization of receptive fields. *J Neurophysiol*, *39*(6), 1288-319.

Schiller, P. H., Logothetis, N. K. & Charles, E. R. (1990). Role of the color-opponent and broad-band channels in vision. *Vis Neurosci*, *5*(4), 321-46.

Schiller, P. H., Sandell, J. H. & Maunsell, J. H. (1987). The effect of frontal eye field and superior colliculus lesions on saccadic latencies in the rhesus monkey. *J Neurophysiol*, *57*(4), 1033-49.

Schiller, P. H., & Tehovnik, E. J. (2001). Look and see: how the brain moves your eyes about. *Prog Brain Res*, *134*, 127-42.

Schiller, P. H., & Tehovnik, E. J. (2005). Neural mechanisms underlying target selection with saccadic eye movements. *Prog Brain Res*, *149*, 157-71.

Schiller, P. H., True, S. D. & Conway, J. L. (1980). Deficits in eye movements following frontal eye-field and superior colliculus ablations. *J Neurophysiol*, *44*(6), 1175-89.

Schlag, J., & Schlag-Rey, M. (1987). Evidence for a supplementary eye field. *J Neurophysiol*, *57*(1), 179-200.

Schluppeck, D., Curtis, C. E., Glimcher, P. W. & Heeger, D. J. (2006). Sustained activity in topographic areas of human posterior parietal cortex during memory-guided saccades. *J Neurosci*, *26*(19), 5098-108.

Schluppeck, D., Glimcher, P. & Heeger, D. J. (2005). Topographic organization for delayed saccades in human posterior parietal cortex. *J Neurophysiol*, *94*(2), 1372-84.

Schneider, K. A., Richter, M. C. & Kastner, S. (2004). Retinotopic organization and functional subdivisions of the human lateral geniculate nucleus: a high-resolution functional magnetic resonance imaging study. *J Neurosci*, *24*(41), 8975-85.

Schumacher, J., Allison, S., R. & Herpers, R. (2004). Using saccadic suppression to hide graphics updates. In S. Coquillart & M. Goebel (Eds.), *Eurographics symposium on virtual envoronments* (p. 17-24).

Segraves, M. A., & Goldberg, M. E. (1987). Functional properties of corticotectal neurons in the monkey's frontal eye field. *J Neurophysiol*, *58*(6), 1387-419.

Segraves, M. A., Goldberg, M. E., Deng, S. Y., Bruce, C. J., Ungerleider, L. G. & Mishkin, M. (1987). The role of striate cortex in the guidance of eye movements in the monkey. *J Neurosci*, *7*(10), 3040-58.

Serences, J. T., Shomstein, S., Leber, A. B., Golay, X., Egeth, H. E. & Yantis, S. (2005). Coordination of voluntary and stimulus-driven attentional control in human cortex. *Psychol Sci*, *16*(2), 114-22.

Serences, J. T., Yantis, S., Culberson, A. & Awh, E. (2004). Preparatory activity in visual cortex indexes distractor suppression during covert spatial orienting. *J Neurophysiol*, *92*(6), 3538-45.

Sereno, M. I., Pitzalis, S. & Martinez, A. (2001). Mapping of contralateral space in retinotopic coordinates by a parietal cortical area in humans. *Science*, *294*(5545), 1350-4.

Shipp, S., & Zeki, S. (1989). The organization of connections between areas v5 and v1 in macaque monkey visual cortex. *Eur J Neurosci*, *1*(4), 309-332.

Skoyles, J. R. (1997). Another variety of vision. *Trends Neurosci*, *20*(1), 22-3.

Smith, A. T., Singh, K. D. & Greenlee, M. W. (2000). Attentional suppression of activity in the human visual cortex. *Neuroreport*, *11*(2), 271-7.

Somers, D. C., Dale, A. M., Seiffert, A. E. & Tootell, R. B. (1999). Functional mri reveals spatially specific attentional modulation in human primary visual cortex. *Proc Natl Acad Sci U S A*, *96*(4), 1663-8.

Sommer, M. A., & Wurtz, R. H. (2000). Composition and topographic organization of signals sent from the frontal eye field to the superior colliculus. *J Neurophysiol*, *83*(4), 1979-2001.

Sparks, D. L. (1988). Neural cartography: sensory and motor maps in the superior colliculus. *Brain Behav Evol*, *31*(1), 49-56.

Sparks, D. L., Barton, E. J., Gandhi, N. J. & Nelson, J. (2002). Studies of the role of the paramedian pontine reticular formation in the control of head-restrained and head-unrestrained gaze shifts. *Ann N Y Acad Sci*, *956*, 85-98.

Stoerig, P., & Cowey, A. (1997). Blindsight in man and monkey. *Brain*, *120 (Pt 3)*, 535-59.

Super, H., Spekreijse, H. & Lamme, V. A. (2001). Two distinct modes of sensory processing observed in monkey primary visual cortex (v1). *Nat Neurosci*, *4*(3), 304-10.

Suzuki, W., Saleem, K. S. & Tanaka, K. (2000). Divergent backward projections from the anterior part of the inferotemporal cortex (area te) in the macaque. *J Comp Neurol*, *422*(2), 206-28.

Sylvester, R., Haynes, J. D. & Rees, G. (2005). Saccades differentially modulate human lgn and v1 responses in the presence and absence of visual stimulation. *Curr Biol*,

15(1), 37-41.

Sylvester, R., & Rees, G. (2006). Extraretinal saccadic signals in human lgn and early retinotopic cortex. *Neuroimage*, *30*(1), 214-9.

Tanaka, K. (2001). Late responses and perceptual awareness. *Nat Neurosci*, *4*(3), 225-6.

Tehovnik, E. J., Lee, K. & Schiller, P. H. (1994). Stimulation-evoked saccades from the dorsomedial frontal cortex of the rhesus monkey following lesions of the frontal eye fields and superior colliculus. *Exp Brain Res*, *98*(2), 179-90.

Tehovnik, E. J., Slocum, W. M., Carvey, C. E. & Schiller, P. H. (2005). Phosphene induction and the generation of saccadic eye movements by striate cortex. *J Neurophysiol*, *93*(1), 1-19.

Tehovnik, E. J., Slocum, W. M. & Schiller, P. H. (2002). Differential effects of laminar stimulation of v1 cortex on target selection by macaque monkeys. *Eur J Neurosci*, *16*(4), 751-60.

Tehovnik, E. J., Slocum, W. M. & Schiller, P. H. (2003). Saccadic eye movements evoked by microstimulation of striate cortex. *Eur J Neurosci*, *17*(4), 870-8.

Thiele, A., Henning, P., Kubischik, M. & Hoffmann, K. P. (2002). Neural mechanisms of saccadic suppression. *Science*, *295*(5564), 2460-2.

Thilo, K. V., Santoro, L., Walsh, V. & Blakemore, C. (2004). The site of saccadic suppression. *Nat Neurosci*, *7*(1), 13-4.

Tobler, P. N., & Muri, R. M. (2002). Role of human frontal and supplementary eye fields in double step saccades. *Neuroreport*, *13*(2), 253-5.

Tootell, R. B., Hadjikhani, N. K., Vanduffel, W., Liu, A. K., Mendola, J. D., Sereno, M. I. et al. (1998). Functional analysis of primary visual cortex (v1) in humans. *Proc Natl Acad Sci U S A*, *95*(3), 811-7.

Trottier, L., & Pratt, J. (2005). Visual processing of targets can reduce saccadic latencies. *Vision Res*, *45*(11), 1349-54.

Ungerleider, L. G., & Desimone, R. (1986). Cortical connections of visual area mt in the macaque. *J Comp Neurol*, *248*(2), 190-222.

Vakalopoulos, C. (2005). Neural correlates of consciousness: a definition of the dorsal

and ventral streams and their relation to phenomenology. *Med Hypotheses*, *65*(5), 922-31.

Vallines, I., Bodis-Wollner, I., Nagengast, B., Oezyurt, J., Rutschmann, R. M. & Greenlee, M. W. (2002). Saccades in the dark: fmri evidence for separate cortical control of intentional eye movements. *Perception*, *31*(178).

Vallines, I., Bodis-Wollner, I., Oezyurt, J., Rutschmann, R. M. & Greenlee, M. W. (2003). Perisaccadic v1 activity is not due to shifting visuo-spatial attention. *Journal of Vision*, *3*(9), 42.

Vallines, I., En-Ju, L. & Greenlee, M. W. (unpublised). *Cortical control of attentional interference.*

Vallines, I., & Greenlee, M. W. (2004). Modulation of neural activity in human visual cortex during saccade programming. *Washington, DC: Society for Neuroscience, Online.*, *Program No. 302.16.*(2004 Abstract Viewer/Itinerary Planner.).

Vallines, I., & Greenlee, M. W. (2005a). Saccadic suppression of retinotopically localized stimuli in v1: a parametric fmri study. *Perception*, *34*, 52.

Vallines, I., & Greenlee, M. W. (2005b). *Verringerung visueller kortexaktivitaet whaerend sakkadenprogrammierung.* Regensburg: Pabst Science Publishers.

Vallines, I., & Greenlee, M. W. (2006). Saccadic suppression of retinotopically localized blood oxygen level-dependent responses in human primary visual area v1. *J Neurosci*, *26*(22), 5965-9.

Van Essen, D. C., Drury, H. A., Joshi, S. & Miller, M. I. (1998). Functional and structural mapping of human cerebral cortex: solutions are in the surfaces. *Proc Natl Acad Sci U S A*, *95*(3), 788-95.

Van Essen, D. C., Newsome, W. T., Maunsell, J. H. & Bixby, J. L. (1986). The projections from striate cortex (v1) to areas v2 and v3 in the macaque monkey: asymmetries, areal boundaries, and patchy connections. *J Comp Neurol*, *244*(4), 451-80.

Volkmann, F. C., Riggs, L. A. & Moore, R. K. (1980). Eyeblinks and visual suppression. *Science*, *207*(4433), 900-2.

Volkmann, F. C., Schick, A. M. & Riggs, L. A. (1968). Time course of visual inhibition

during voluntary saccades. *J Opt Soc Am*, *58*(4), 562-9.

Wade, N. J., Tatler, B. W. & Heller, D. (2003). Dodge-ing the issue: Dodge, javal, hering, and the measurement of saccades in eye-movement research. *Perception*, *32*(7), 793-804.

Wager, T. D., Vazquez, A., Hernandez, L. & Noll, D. C. (2005). Accounting for nonlinear bold effects in fmri: parameter estimates and a model for prediction in rapid event-related studies. *Neuroimage*, *25*(1), 206-18.

Walker, R., Walker, D. G., Husain, M. & Kennard, C. (2000). Control of voluntary and reflexive saccades. *Exp Brain Res*, *130*(4), 540-4.

Wardak, C., Olivier, E. & Duhamel, J. R. (2002). Saccadic target selection deficits after lateral intraparietal area inactivation in monkeys. *J Neurosci*, *22*(22), 9877-84.

Warnking, J., Dojat, M., Guerin-Dugue, A., Delon-Martin, C., Olympieff, S., Richard, N. et al. (2002). fmri retinotopic mapping–step by step. *Neuroimage*, *17*(4), 1665-83.

Wauschkuhn, B., Verleger, R., Wascher, E., Klostermann, W., Burk, M., Heide, W. et al. (1998). Lateralized human cortical activity for shifting visuospatial attention and initiating saccades. *J Neurophysiol*, *80*(6), 2900-10.

Weerda, R., Vallines, I., Thomas, J. P., Rutschmann, R. M. & Greenlee, M. W. (2006). Effects of nonspatial selective and divided visual attention on fmri bold responses. *Exp Brain Res*.

Wehrle, R., Czisch, M., Kaufmann, C., Wetter, T. C., Holsboer, F., Auer, D. P. et al. (2005). Rapid eye movement-related brain activation in human sleep: a functional magnetic resonance imaging study. *Neuroreport*, *16*(8), 853-7.

Weidner, R., Pollmann, S., Muller, H. J. & Cramon, D. Y. von. (2002). Top-down controlled visual dimension weighting: an event-related fmri study. *Cereb Cortex*, *12*(3), 318-28.

Wenzel, R., Wobst, P., Heekeren, H. H., Kwong, K. K., Brandt, S. A., Kohl, M. et al. (2000). Saccadic suppression induces focal hypooxygenation in the occipital cortex. *J Cereb Blood Flow Metab*, *20*(7), 1103-10.

Wheeless, J., L. L., Boynton, R. M. & Cohen, G. H. (1966). Eye-movement responses to

step and pulse-step stimuli. *J Opt Soc Am*, *56*(7), 956-60.

Wolpaw, J. R., Birbaumer, N., McFarland, D. J., Pfurtscheller, G. & Vaughan, T. M. (2002). Brain-computer interfaces for communication and control. *Clin Neurophysiol*, *113*(6), 767-91.

Wurtz, R. H., & Goldberg, M. E. (1972). The role of the superior colliculus in visually-evoked eye movements. *Bibl Ophthalmol*, *82*, 149-58.

Wurtz, R. H., & Goldberg, M. E. (1989). *The neurobiology of saccadic eye movements.* Amsterdam ; New YorkNew York, NY, USA: Elsevier ;Sole distributors for the USA and Canada, Elsevier Science Publishers Co.

Zhu, J. J., & Lo, F. S. (1996). Time course of inhibition induced by a putative saccadic suppression circuit in the dorsal lateral geniculate nucleus of the rabbit. *Brain Res Bull*, *41*(5), 281-91.

Zuber, B. L., & Stark, L. (1966). Saccadic suppression: elevation of visual threshold associated with saccadic eye movements. *Exp Neurol*, *16*(1), 65-79.

Statutory declaration

Hereby I, Ignacio Vallines García, born on the 8th of October 1974 in Madrid, declare that I wrote this dissertation without any help of third parties and without using any other aids than stated, that this dissertation was neither presented in equal nor in similar form to an other examining board at any other university, and that I cited all sources that were used respecting current academic rules.

Regensburg, February 12, 2007

Acknowledgements

This thesis work would have never been possible without the continuous support of Prof. Mark W. Greenlee, who has been not only an excellent supervisor but also a great mentor throughout all these years. I would also like to acknowledge the generous support of the Deutsche Forschungsgemeinschaft and the Graduate School for Neurosensory Systems at the Carl von Ossietzky University, the Hansa Wissenschaftskolleg, the Volkswagen Stifftung and, of course, the exciting academic environment provided by the University of Regensburg that was home to most of this dissertation work. Special thanks go to Prof. Kollmeier, who supported me during my time at the graduate school, and to my doctoral fellows in Oldenburg, Groningen, and the EDCBS, who lent me their eyes to see the brain from many different perspectives. Thanks to Prof. James P. Thomas for patiently introducing me to psychophysics, to Prof. Bodis-Wollner for teaching me to do good science the hard way, and to Prof. David J. Heeger for hosting me at his lab and providing me with an awesome academic experience. Many thanks to my colleagues in Regensburg, who were not only very supportive, but also great fun to work with. Thanks to my friends, they know who they are and I am proud to say their names would not fit in this page; I am a bit of each of you. Thanks to Natalie, who has given me the strength to write up this thesis and who's lack of patience balances my procrastinating. Finally, many thanks to my family, who has been supporting me since the day I was born.

Thanks to all of you.